Orbital

The Electronic Journal of Chemistry

Oxidação de Metano sobre Pt
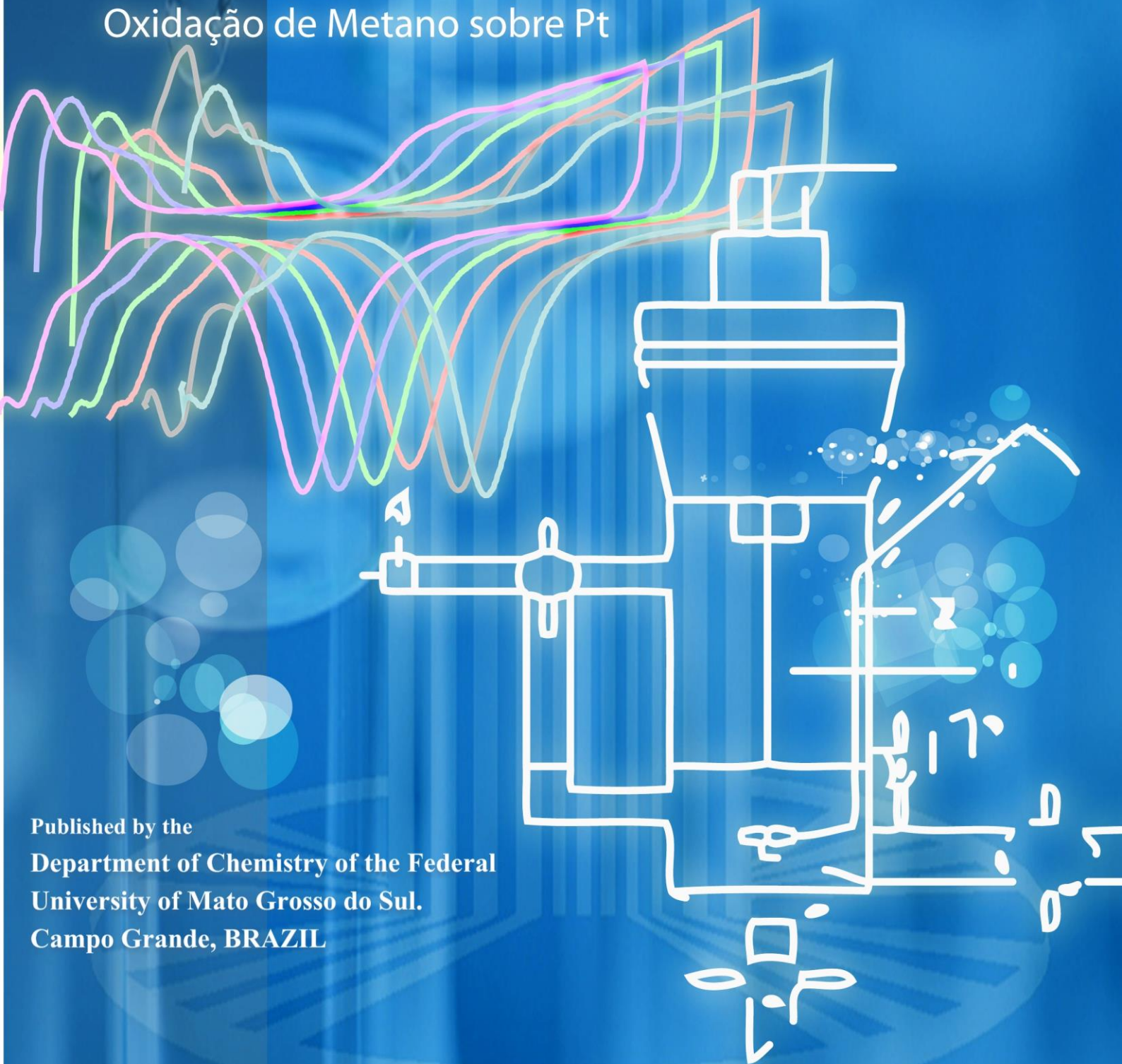
UFMS

Orbital - Vol. 2 No. 3 - July-September 2010

Table of Contents

FULL PAPERS

SHORT COMMUNICATIONS

Full Paper

Stability indicating RP-HPLC method for simultaneous determination of pantoprazole sodium and itopride hydrochloride in bulk and capsule

Krishna R. Gupta*, Rajesh B. Chawla and Sudhir G. Wadodkar

Department of Pharmaceutical Chemistry, S. K. B. College of Pharmacy, New Kamptee 441002, Nagpur (MS) India

ABSTRACT: *A stability indicating reversed-phase HPLC method has been developed and subsequently validated for simultaneous estimation of pantoprazole present as pantoprazole sodium sesquihydrate (PSS), and itopride hydrochloride from their combination product. The proposed RP-HPLC method utilizes a Phenomenex® C18, 5 µm, 250 mm X 4.6 mm i.d. column, mobile phase consisting of phosphate buffer and acetonitrile in the proportion of 55:45 (v/v) with apparent pH adjusted to 5.0, and UV detection at 289.0 nm using a UV detector. PAN, ITH and their combination drug product were exposed to thermal, photolytic, hydrolytic and oxidative stress conditions, and the stressed samples were analyzed by the proposed method. The described method was linear over a range of 4-20 µg/mL for PAN and 15-75 µg/mL for ITH. The mean recoveries were 100.02 and 99.88 for PAN and ITH, respectively. Chromatographic peak purity data of PAN and ITH indicated no co-eluting peaks with the main peaks of drugs which demonstrated the specificity of assay method for their estimation in presence of degradation products. The proposed method can be useful in the quality control of combination drug products.*

Keywords*: stability indicating RP-HPLC; pantoprazole; itopride hydrochloride; UV detector*

Introduction

Pantoprazole sodium sesquihydrate (PSS) [1] (Fig. 1) is sodium sesquihydrate salt of pantoprazole (PAN), which is benimidazole proton pump inhibitor. PAN suppresses gastric acid secretion by inhibiting the gastric H^+, K^+ ATPase at the secretory surface of

---

* Corresponding author. E-mail: *krishnargupta@rediffmail.com*

the gastric parietal cell and blocks the final step of gastric acid secretion. It is used as anti-ulcerative. Itopride hydrochloride (ITH) [2] (Fig. 2) is a gastroprokinetic agent. It increases the release of acetylcholine (Ach) through dopamine D2 receptor antagonistic action and inhibits decomposing of released Ach through its acetylcholinesterase inhibitory action, resulting in enhancement of gastrointestinal motility. It also exerts antiemetic action because of its dopamine D2 receptor antagonistic action at chemoreceptor trigger zone. Combination drug products of PAN and ITH are widely marketed and used in the treatment of acid related disorders eg peptic ulcer, reflux oesophagitis, as gastroprokinetic agent and antiemetic agent.

$3/2\ H_2O$
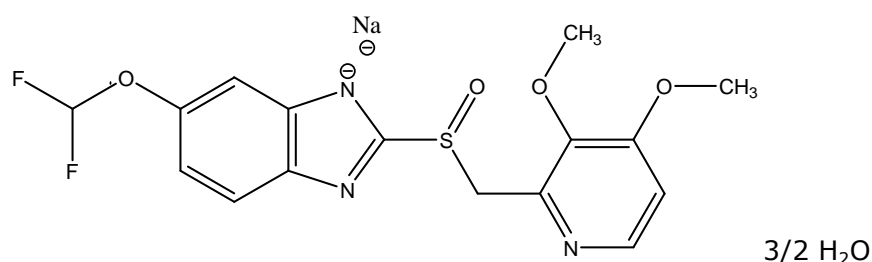
Figure 1. Structure of pantoprazole sodium sesquihydrate
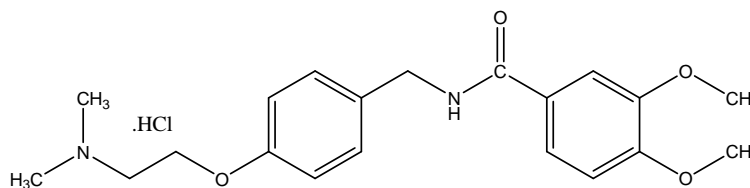
Figure 2. Structure of itopride hydrochloride

Stability testing forms an important part of the process of drug product development. The purpose of stability testing is to provide evidence on how the quality of a drug substance or drug product varies with time under the influence of a variety of environmental factors such as temperature, humidity and light, enabling recommendation of storage conditions, retests periods, and shelf lives to be established. The two main aspects of drug product that play an important role in shelf life determination are assay of active drug, and degradants generated, during the stability study. The assay of drug product in stability test sample needs to be determined using stability indicating method, as recommended by the International Conference on Harmonization (ICH) guidelines [3] and USP (United States Pharmacopoeia) 26 [4]. Although stability indicating methods have been reported for assay of various drugs in drug products, most of them describe assay procedures for drug products containing only one active drug substance. Only few stability indicating methods are reported for assay of combination drug products containing two or more active drug substances. The objective of this work was to develop an analytical LC procedure, which would serve as

210

Orbital Elec. J. Chem., Campo Grande, 2(3): 209-224, 2010

stability indicating assay method for combination drug product of PAN and ITH.

Both the drugs PAN and ITH are not official with USP 30. Detailed survey of literature for PAN revealed several methods based on different techniques, viz. HPLC [5-6], UV spectrophotometry [7-10] for its determination from pharmaceuticals. Similarly, survey of literature for ITH revealed methods based on HPLC [11-13], HPTLC [14], UV spectrophotometry [15] for its determination from pharmaceuticals. Shirore et al. [16] reported an HPLC method for the estimation of PAN in combination with mosapride and Manoj and Anbazhagan [17] reported an HPLC method for the estimation of PAN in combination with domperidone. No stability indicating methods have been reported for determination of PAN and ITH. This manuscript describes the development and subsequent validation of a stability indicating isocratic reversed phase HPLC method for simultaneous determination of PAN and ITH in the presence of their degradants. To establish the stability indicating nature of the method, forced degradation of drug substances and drug product was performed under stress conditions (thermal, photolytic, UV-exposure, acid and basic hydrolytic and oxidative), and stressed samples were analyzed by the proposed method. The proposed LC method was able to separate both drugs from degradants generated during forced degradation studies.

Material and Methods

Chemicals and reagents

PAN and ITH working standards were generous gifts from Relief Lab Pvt. Ltd. (Nagpur, India) and ZIM Lab Ltd. (Nagpur, India), respectively. Combination product of PAN and ITH (Label claim: Pantoprazole 40 mg, as pantoprazole sodium sesquihydrate, and benazepril hydrochloride 150 mg), Itopan and Pantop-IT tablets (Alkem and Unichem Laboratories Ltd.) were purchased from the market. Acetonitrile, methanol, potassium dihydrogen phosphate, potassium hydroxide, sodium hydroxide, hydrochloric acid and hydrogen peroxide were from Qualigens Fine Chemicals (Glaxo Ltd.).

HPLC instrumentation and conditions

The Shimadzu Binary gradient HPLC system consisted of LC 10ATvp/ LC 10ADvp pump, Rheodyne injector and SPD 10 UV detector. The chromatographic separations were performed using Phenomenex C18, 5 µm, 250 mm × 4.6 mm i.d. column, maintained at ambient temperature, eluted with mobile phase at the flow rate of 1.0 mL/min. The mobile phase consisted of 50 mM potassium dihydrogen phosphate buffer–acetonitrile (55:45, v/v), apparent pH adjusted to 5.0 with 0.2 M potassium hydroxide solution, filtered through 0.45 µm nylon filter and degassed in ultrasonic bath prior to use. Measurements were made with injection volume 20 µL and ultraviolet (UV) detection at 289 nm. The output signal was integrated using Spinchrome CFR software (Spincotech

211

Orbital Elec. J. Chem., Campo Grande, 2(3): 209-224, 2010

Ltd.).

Standard and sample preparation

The mix standard stock solution containing 100 µg/mL and 375 µg/mL of PAN and ITH was prepared by dissolving working standards in sufficient proportion of mobile phase and later diluted to desired volume with mobile phase. Standard calibration solutions of PAN and ITH with concentration in the range of 4-20 µg/mL and 15-75 µg/mL, respectively, were prepared by diluting stock solution with mobile phase.

Analysis of dosage form

Twenty tablets were weighed, their mean weight determined, and crushed in mortar. An amount of powdered mass equivalent to 30 mg of ITH was transferred into a 100 mL volumetric flask containing 20 mL of mobile phase, mechanically shaken for 15 min, ultrasonicated for 5 min, and then diluted to volume with mobile phase (sample stock solution). The extract was filtered through Whatman filter paper No. 41 and residue was washed with mobile phase. About 5 mL of sample stock solution diluted to 50 mL with mobile phase (sample solution). A small portion of sample solution was filtered through 0.45 µm nylon filter and used for injection on HPLC.

Procedure for forced degradation study

Forced degradation of each drug substances and the drug product was carried out under thermolytic, photolytic, acid/base hydrolytic and oxidative stress conditions. Thermal and photo-degradation of drug substances and drug product was carried out in solid state. After the degradation these solutions were diluted with mobile phase to achieve a concentration of 20 µg/mL of PAN and 75 µg/mL of ITH (on label claim basis for marketed formulation).

Acid hydrolysis of drug substance and drug product in solution state was conducted by refluxing in 0.5 N hydrochloric acid for 6 h. Base hydrolysis of drug substance and drug product in solution state was conducted by refluxing in 0.5 N sodium hydroxide solution for 6 h. For oxidative stress, sample solutions of drug substance and drug product in 3% hydrogen peroxide were kept at 50 °C for 24 h.

For thermal stress, samples of drug substances and drug product were placed in a controlled-temperature oven at 60 °C for 24 h. For photolytic stress, samples of drug substances and drug product, both in solid state, were irradiated with UV radiation with peak intensities at 254 nm for 24 h. Photochemical exposure (direct sunlight) for 6 h was studied.

For humidity stress, samples drug substance and product were kept in 75% RH for 24 h.

212

Orbital Elec. J. Chem*., Campo Grande,* 2(3): 209-224, 2010

Results and Discussion

Development of validated stability indicating method

To develop a precise, accurate, specific and suitable stability indicating RP-HPLC method for the simultaneous estimation of PAN and ITH, different mobile phases were employed and proposed chromatographic condition was found appropriate for the quantitative determination in the presence of degradation products. The optimal mobile phase consisted of acetonitrile and phosphate buffer (45:55, v/v), apparent pH adjusted to 5±0.1 with 0.2 M potassium hydroxide solution, which was selected because it was found to ideally resolve the peaks of ITH (tR_2.653 min) and PAN (tR_5.753 min), with clear line separation in presence of their degradation products at effluent flow rate of 1.0 mL/min. UV detection wavelength at 289 nm, injection volume of 20 µL, ambient temperature for column and HPLC system were found to be best for analysis.

HPLC studies on stressed solutions

Pantoprazole degraded to more than four degradation products in most of the stress conditions, except in UV and humidity (75% RH) studies while ITH showed slight degradation in most of the stress conditions. Table 1 indicates the percent degradation of PAN and ITH remained under various stress conditions. The retention times (Rt) and relative retention times (RRt) of the PAN and its degradation products as they appear on the chromatogram are given in Table 2 for various stress conditions. The degradation products and drugs carry the numerical notations in accordance with the sequence in which the peaks appeared from left to right on the HPLC chromatogram. HPLC studies of the stressed samples showed the following degradation behavior:

Table 1. Results of analysis of forced degradation samples by proposed method.

Stress condition/duration/state	% Degradation	
	ITH	**PAN**
Alkaline/ 0.5 N NaOH/ 6 h reflux/solution	*0.04*	*85.87*
Acidic/ 0.5 N HCl/ 6 h reflux/ solution	*0.10*	*93.91*
Oxide/ 3% H$_2$O$_2$/24 h/ solution	*2.54*	*75.07*
Thermal/60 °C / 24 h/ solid	*1.88*	*93.64*
Humidity/ 75% RH/ 24 h/ solid	*3.70*	*5.13*
UV/254 nm/24 h/solid	*5.84*	*10.01*
Hotochemical (sunlight)/6 h/solid	*9.71*	*31.87*

Hydrolytic conditions

PAN showed very susceptible behavior towards acid and alkaline stress, showing more than 80% degradation in 0.5 N HCl or 0.5 N NaOH refluxed for 6 h. Pantoprazole

213

Orbital Elec. J. Chem., Campo Grande, 2(3): 209-224, 2010

degraded to five or six degradation products while itopride was found to be slightly degraded in all the hydrolytic stress conditions as minute degradation peaks was seen.

Table 2. Retention times and relative retention times of various peaks of PAN.

Stress condition/ Peaks as on chromatogram	Retention time(Rt)				Relative retention time (RRt)			
	Alkali	Acid	Oxide	Thermal	Alkali	Acid	Oxide	Thermal
1	----	2.853	----	2.630	----	0.525	----	0.473
2	----	3.307	----	3.937	----	0.608	----	0.708
3	2.790	4.687	2.740	4.463	0.487	0.862	0.646	0.802
4	3.327	5.040	3.233	4.970	0.581	0.930	0.762	0.893
5	4.567	5.437P	3.577	5.563P	0.798	1.000	0.843	1.000
6	5.727P	10.227	4.243P	6.323	1.000	1.881	1.000	1.137
7	7.347	11.360	4.467	6.677	1.283	2.089	1.053	1.200
8	8.683	14.113	-----	10. 647	1.516	2.596	1.127	1.914

*P indicates Retention time of PAN as in chromatograms

Oxidative studies

PAN was unstable under the stress and formed more than four degradation products. Not much change in ITH was observed even on exposure of the drug to 3% H_2O_2 for 24 h at 50 °C, showing that it was stable against oxidative stress.

Photolytic studies

Under light for 6 h, PAN showed more than 30% degradation, while ITH degraded to a certain extent without prominent degradation seen in the chromatogram.

Solid state studies

There was significant degradation of solid PAN on exposure to dry heat at 60 °C for 24 h, which indicated that the drug was not stable against thermal stress. Stable behavior of both drugs was observed on exposure of solid drug to the conditions of light (UV), humidity (75% RH) for 24 h.

Singh and Bakshi, in their article on stress testing [18], suggested a target degradation of 20-80% for the establishing stability indicating nature of the assay method, as even inter-mediate degradation products should not interfere with any stage of drug analysis. Though conditions used for forced degradation were attenuated to achieve degradation in the range of 20-80%, this could not be achieved in some cases even after exposure for prolonged duration. PAN showed extensive degradation in acidic and alkaline hydrolysis, oxide and thermal degradation conditions while ITH was found to be stable in all the stress conditions. Fig. 3a-c to 9a-c shows the chromatograms of

214

Orbital Elec. J. Chem*., Campo Grande,* 2(3): 209-224, 2010

forced degraded samples and drug substances.
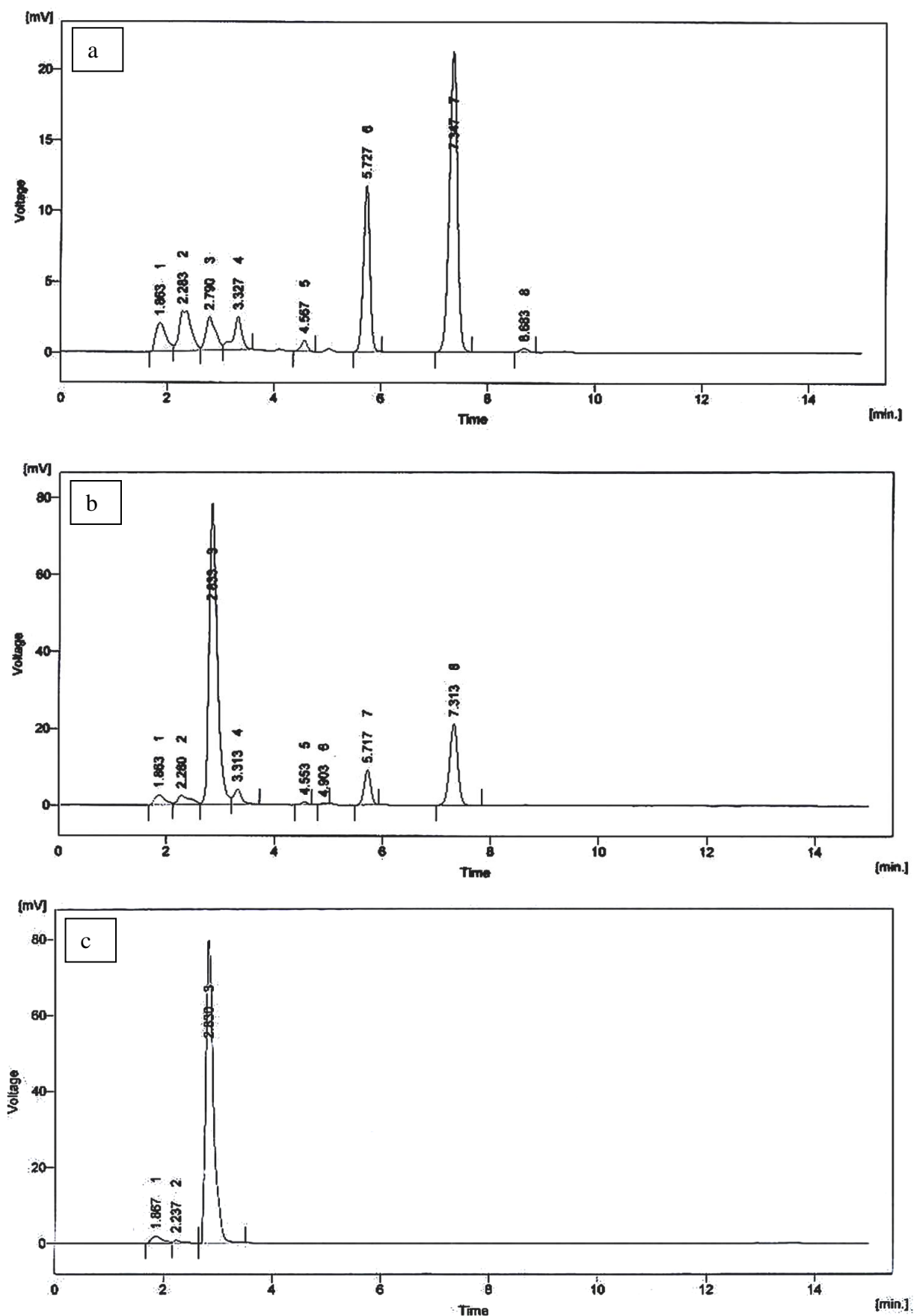
Figure 3. Chromatogram of alkali hydrolysis-degraded- a) PAN, b) capsule c) ITH.

215

Orbital Elec. J. Chem., Campo Grande, 2(3): 209-224, 2010
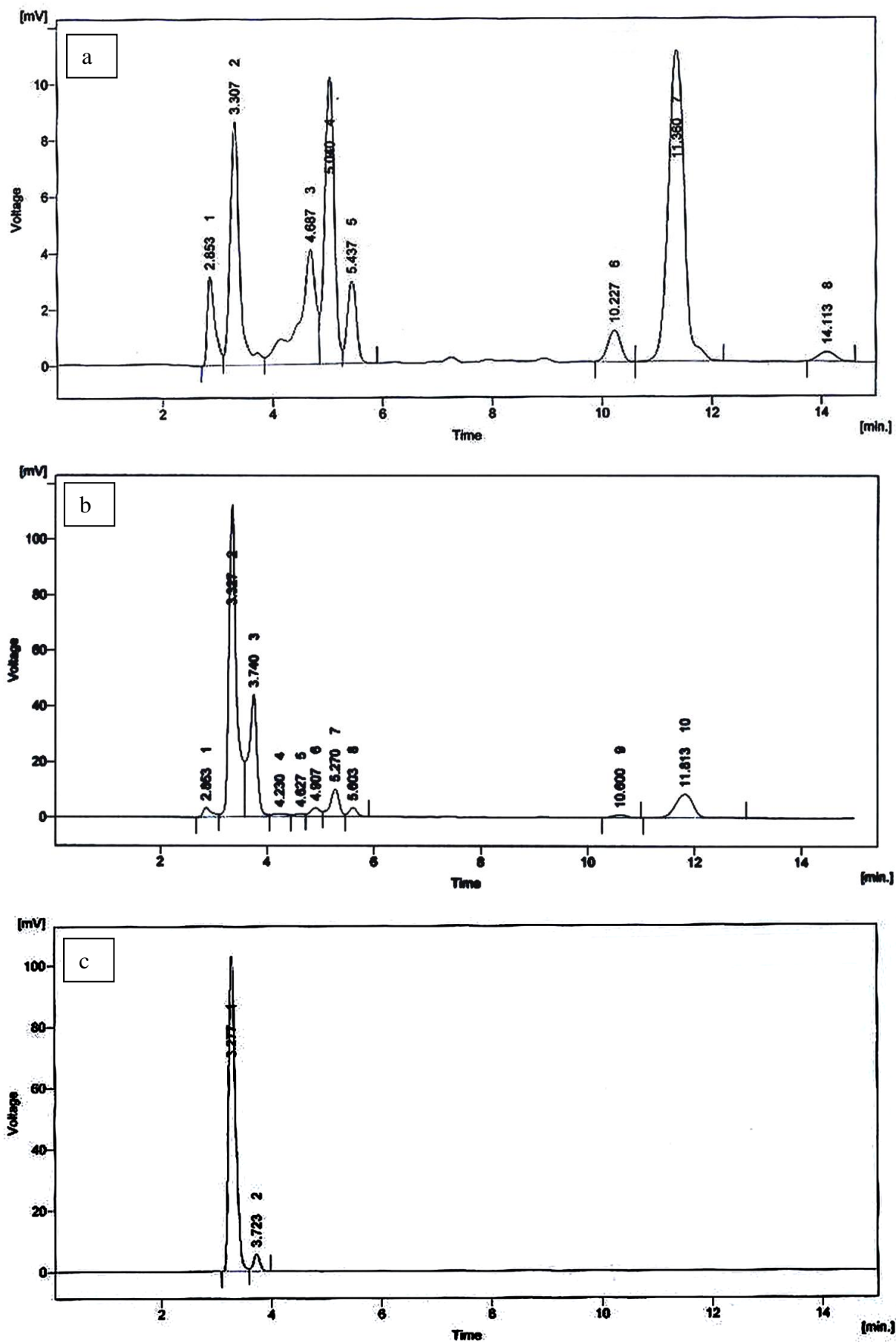
Figure 4. Chromatogram of acid hydrolysis-degraded- a) PAN, b) capsule c) ITH.

216

Orbital Elec. J. Chem., Campo Grande, 2(3): 209-224, 2010
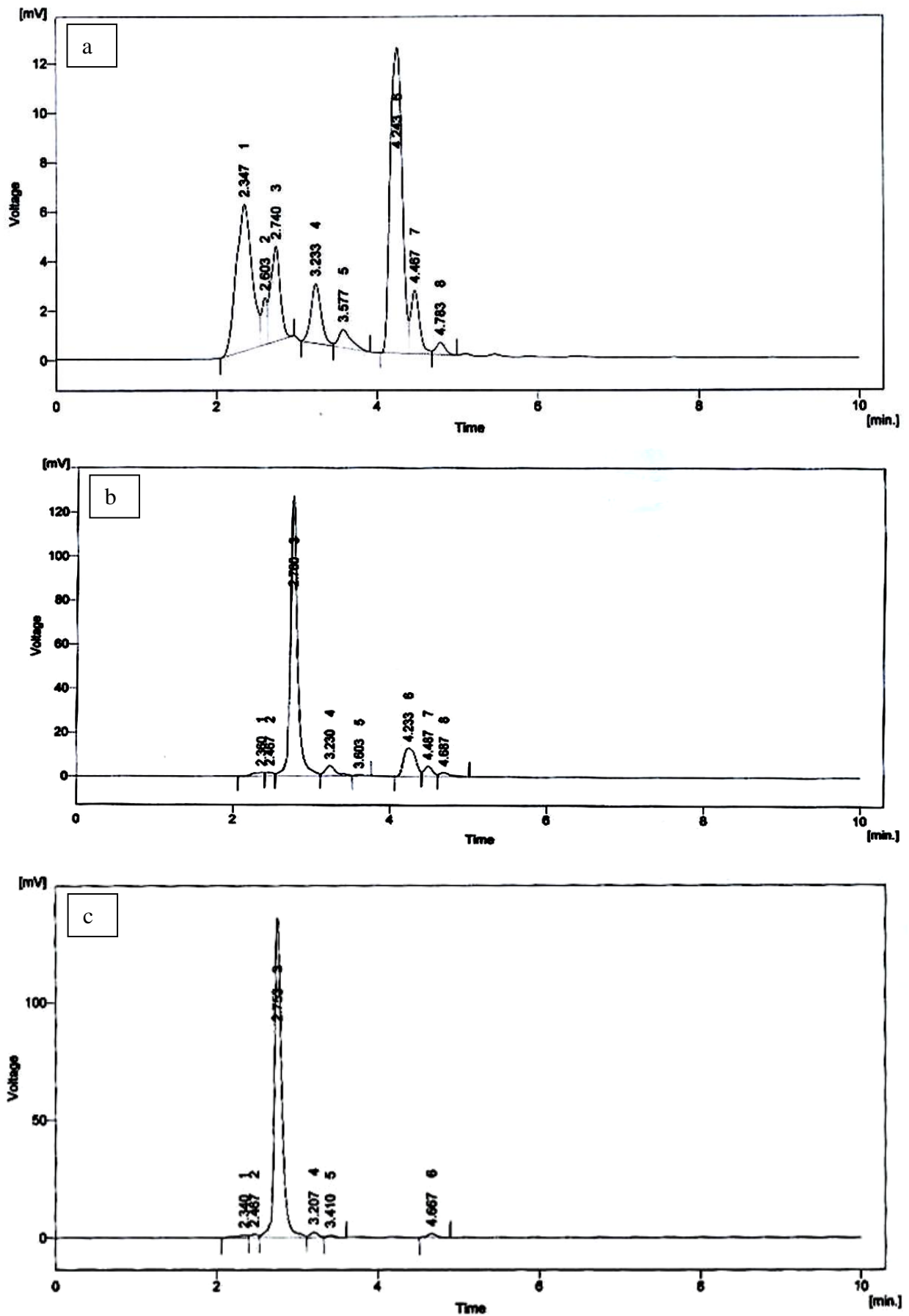
Figure 5. Chromatogram of oxide hydrolysis-degraded- a) PAN, b) capsule c) ITH.

217

Orbital Elec. J. Chem., Campo Grande, 2(3): 209-224, 2010
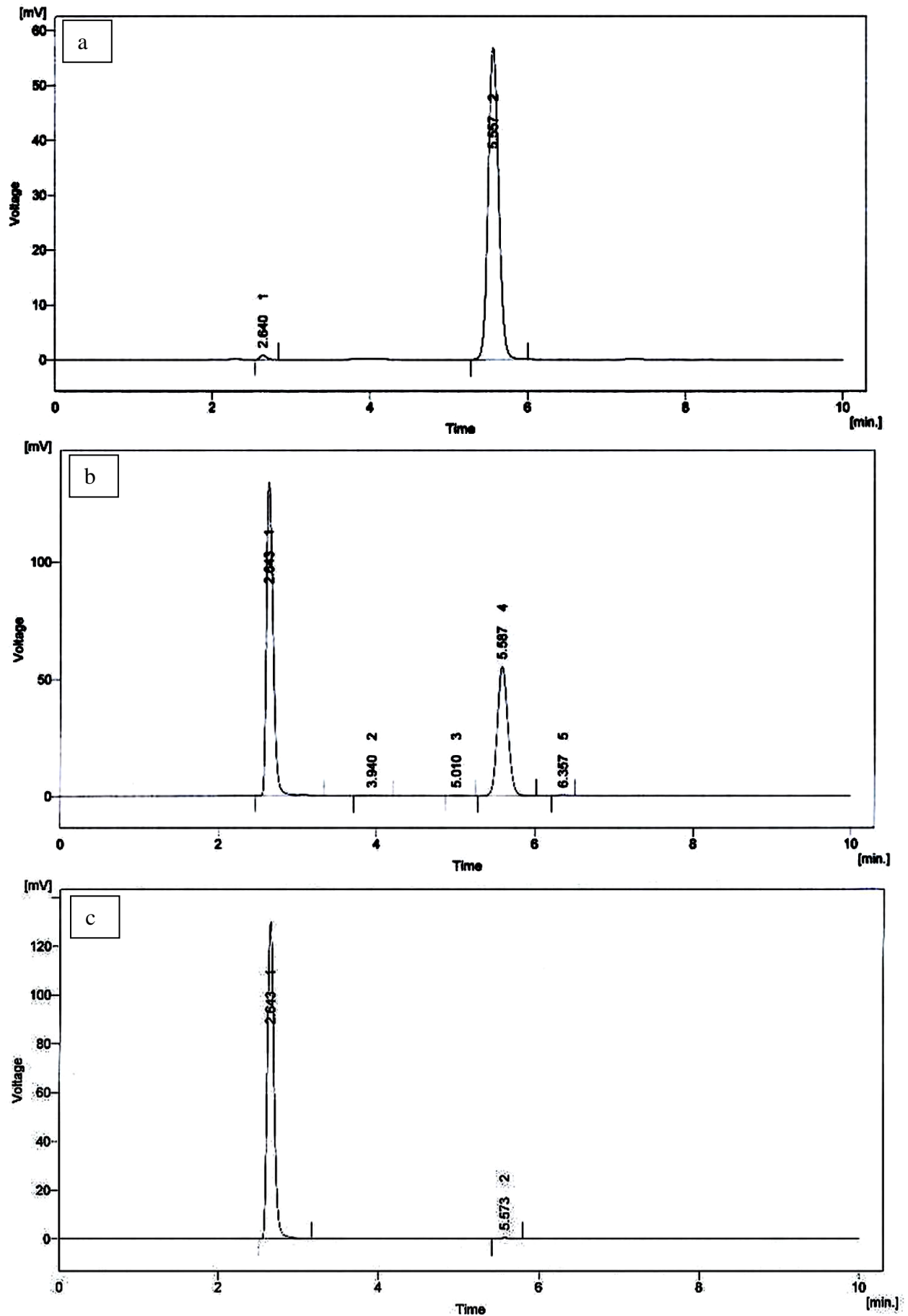
Figure 6. Chromatogram of humidity (75% RH)-degraded- a) PAN, b) capsule c) ITH.

218

Orbital Elec. J. Chem., Campo Grande, 2(3): 209-224, 2010
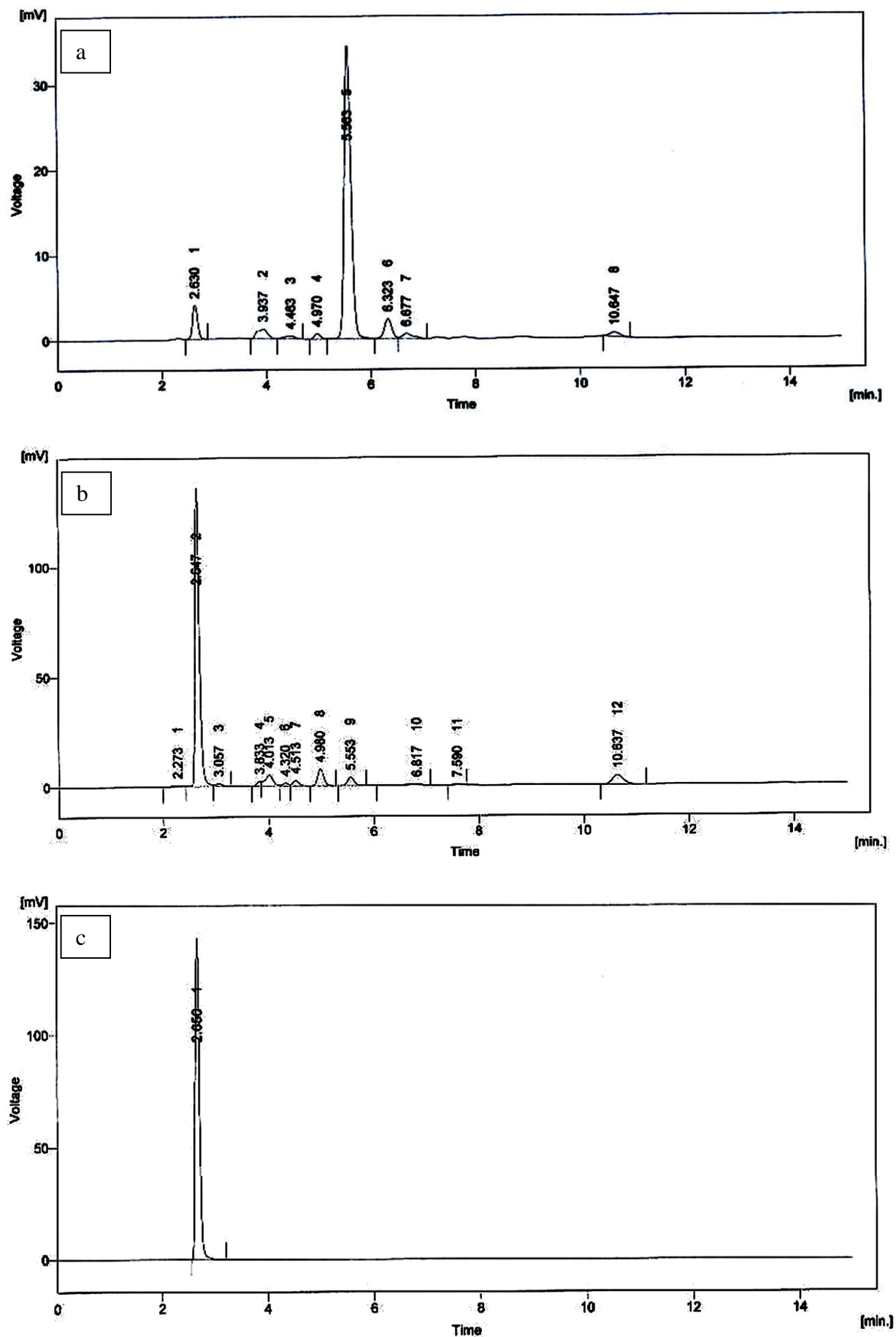
Figure 7. Chromatogram of thermal-degraded- a) PAN, b) capsule c) ITH.

219

Orbital Elec. J. Chem., Campo Grande, 2(3): 209-224, 2010
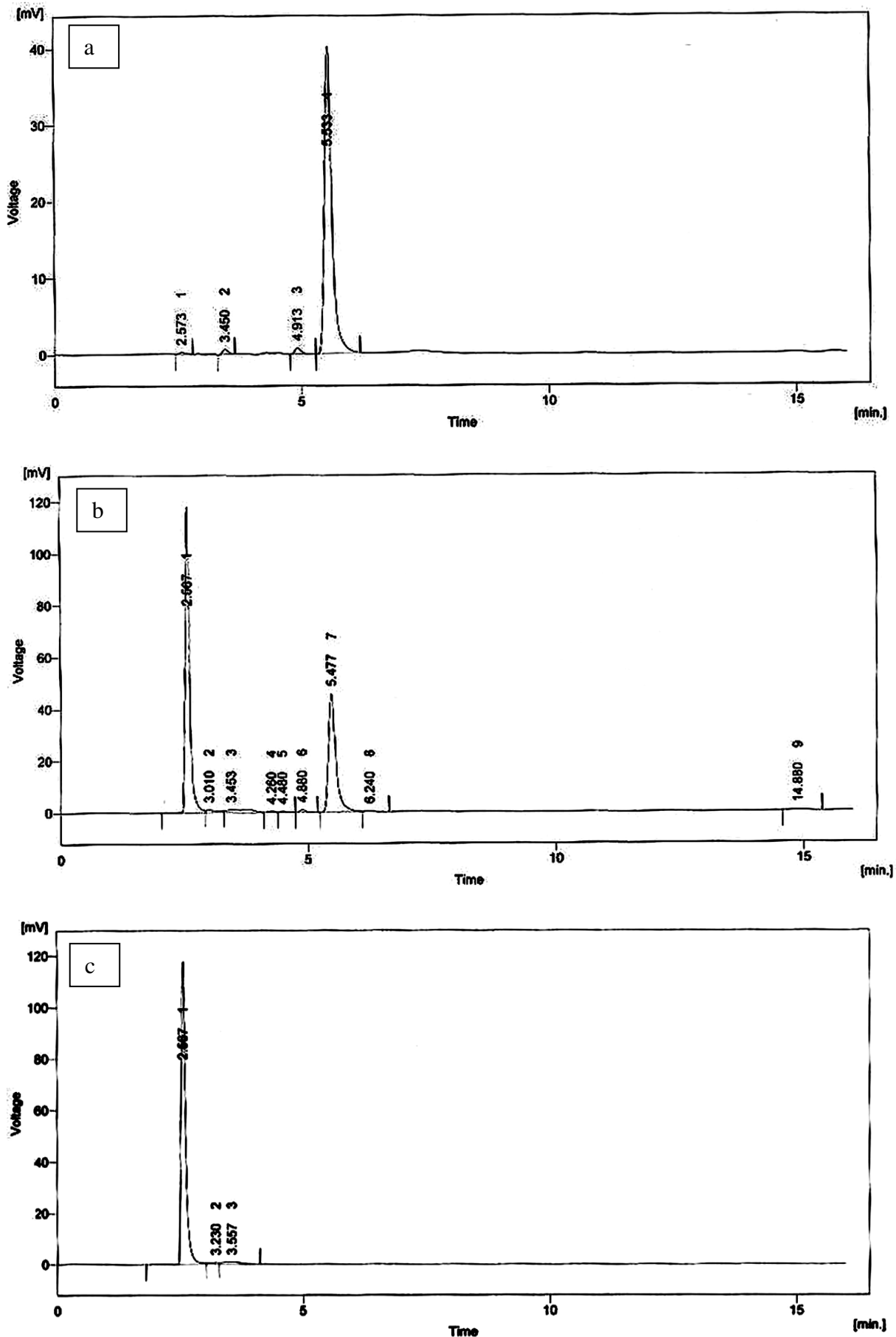
Figure 8. Chromatogram of UV-degraded- a) PAN, b) capsule c) ITH.

220

Orbital Elec. J. Chem*., Campo Grande, 2(3): 209-224, 2010
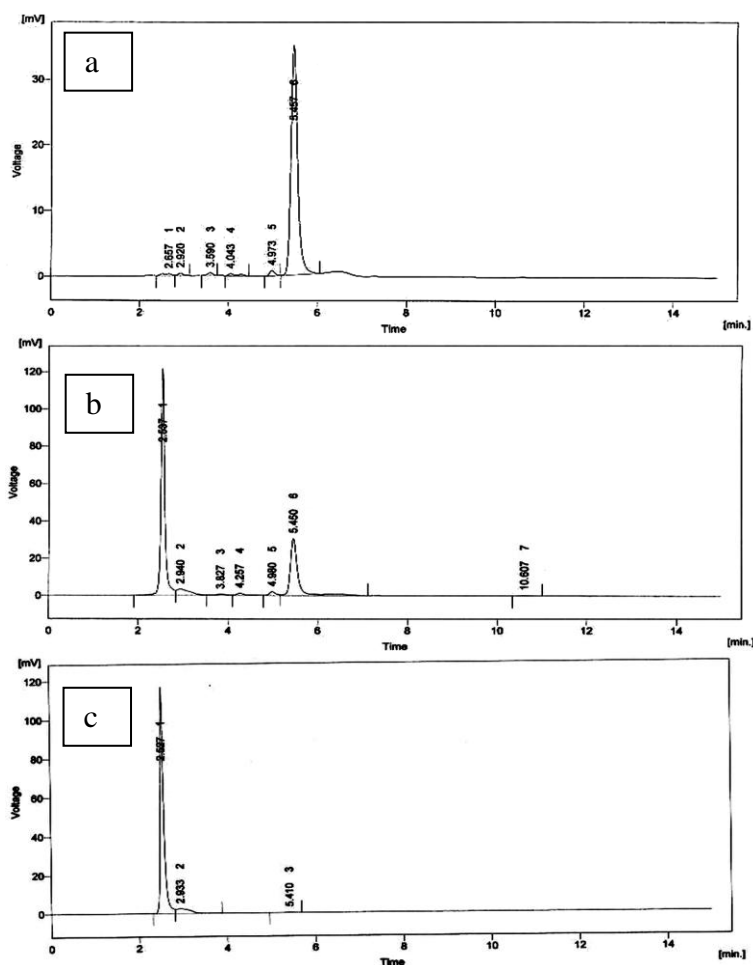
Figure 9. Chromatogram of photochemical-degraded- a) PAN, b) capsule c) ITH.

Method validation

The described method has been validated, apart from specificity, for response function, accuracy, and intermediate precision. The nominal concentrations of standard and test solutions for PAN and ITH were 8 and 30 µg/mL, respectively. Response function was determined by preparing standard solution at five different concentration levels ranging from 4.0 to 20.0 µg/mL for PAN and 15 to 75 µg/mL for ITH. The standard solutions for linearity were prepared five times and slope of regressed line was found to be 1.21 and 0.99% RSD for PAN and ITH, respectively. The correlation coefficients were found to be more than 0.9999 for both the drugs. Repeatability of measurements of peak area was carried out using seven replicates of same concentration (10 and 37.5 µg/mL for PAN and ITH, respectively).

Accuracy of the method was determined by performing the recovery experiment. This experiment was performed at four levels, in which sample stock solutions were spiked with standard drug solution Three replicate samples of each concentration level were prepared and the % recovery at each level and mean % recovery were determined (Table 3a). The mean recovery was 100.02 and 99.88% for PAN and ITH, respectively.

221

Orbital Elec. J. Chem., Campo Grande, 2(3): 209-224, 2010

Precision of estimation of PAN and ITH by proposed method was ascertained by replicate analysis of homogeneous samples of capsule powder. Intermediate precision of the method was studied by intra- and inter-day variation of the method was carried out. The low %RSD values of within a day for PAN and ITH revealed that the proposed method is precise (Table 3b). Day to day variations studies showed that ITH was stable even on 15th day while PAN, on 4th day gave rise to prominent degradation product, which increased to a large extent on 15th day as can be seen on the chromatogram recorded on 15th day as shown in Fig. 10a-d.
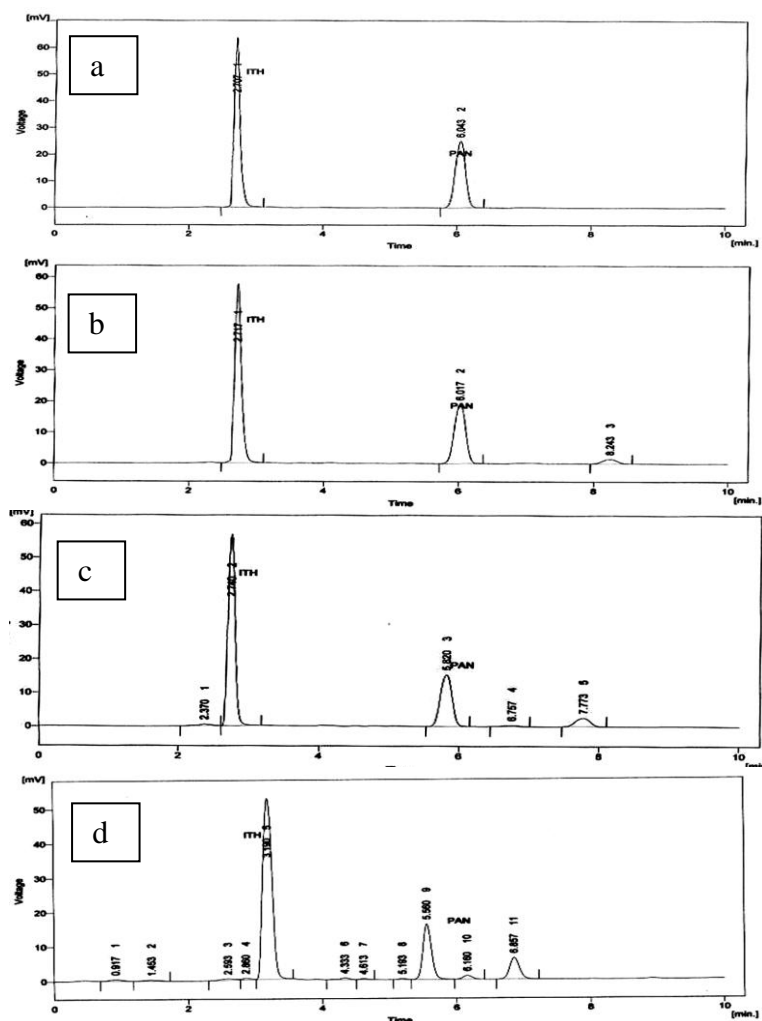
Figure 10. Chromatogram showing degradation product of PAN on a) day 1, b) day 4, c) day 7, d) day 15.

A batch of tablets was analyzed by two different analysts on different days using proposed method, %RSD values were found to be less than 1% indicating ruggedness of the method.

Conclusion

Based on the results obtained from the analysis of forced degraded samples using

222

Orbital Elec. J. Chem*., Campo Grande,* 2(3): 209-224, 2010

described method, it can be concluded that there is no other co-eluting peak with the main peaks and the method is specific for the estimation of PAN and ITH in presence of degradation products and impurities. The method has linear response in stated range and is accurate and precise. Though no attempt was made to identify the degradation products, described method can be used as stability indicating method for assay of PAN and ITH in their combination drug product. The proposed method can also be conveniently adopted for dissolution testing of tablets containing PAN and ITH.

Table 3. Method Validation data for PAN and ITH.

a) Results of accuracy studies using proposed method					
		PAN		**ITH**	
	Taken (mg)	**Recovered (mg)**	**(%) recovery**	**Taken (mg)**	**Recovered (mg)**	**(%) recovery**
Level 1	3.8	3.775	99.34	15.0	15.142	100.94
Level 2	5.7	5.698	99.96	22.5	22.450	99.77
Level 3	7.6	7.641	100.54	30.0	29.862	99.54
Level 4	9.5	9.523	100.24	37.5	37.229	99.28
Mean % recovery			100.02			99.88
% RSD			0.73			0.51

b) Results of intermediate precision for PAN and ITH in capsule formulation				
Intermediate precision		**Percent of label claim ± %RSD**		
	Intraday		**Inter-day**	
	PAN	**ITH**	**PAN**	**ITH**
	98.90±1.37	99.86±0.53	76.40±26.65	100.06±0.66

References and Notes

[1] Reynolds, J. F.; Martindale, The Extra Pharmacopoeia, 35th ed. London: Pharmaceutical Press, p. 1217.

[2] Reynolds, J. F.; Martindale, The Extra Pharmacopoeia, 35th ed. London: Pharmaceutical Press, p. 1229.

[3] International Conference on Harmonization: Draft Revised Guidance on Q1A (R) Stability Resting of New Drug Substances and Products, Federal Register 65, 2000, 21446.

[4] The United States Pharmacopoeia, 26th ed., Rockville, MD: US Pharmacopoeial Convention, 2003, p. 1151.

[5] Cass, Q.; Degani, A.; Cassiano, N.; Pedra, Z. *J. Chromatogr.* **2002**, *766*, 153.

[6] Mansour, A. M.; Sorour, O. M. *Chromatographia* **2001**, *53*, 468.

[7] Mustafa, A. A. M. *J. Pharm. Biomed. Anal.* **2000**, *22*, 45.

[8] Mashru, R. C.; Patel, P. M. *Indian Drugs* **2003**, *40*, 300.

[9] Karlji, K.; Rajic, K.; Novovic, D.; Marinkovic, V.; Agbaba, O. *J. Pharm. Biomed.*

223

Orbital Elec. J. Chem., Campo Grande, 2(3): 209-224, 2010

Anal. **2003**, *32*, 1019.

[10] Abdel, A.; Wahbi, M.; Abdel, R. O.; Gazy, A. A.; Mahagoub, H.; Momeeb, M. S. *J. Pharm. Biomed. Anal.* **2003**, *30*, 1133.

[11] Kaul, N.; Agrawal, H.; Maske, P.; Ramchandra, R. J.; Mahadik, K. R.; Kadam, S. S. *Indian J. Pharm. Sci.* **2005**, 1566.

[12] Dighe, V. V.; Sane, R. T.; Menon, S. N.; Tambe, H.; Inamdar, S.; Pillai, S. *Indian Drugs* **2006**, *43*, 282.

[13] Singh, S. S.; Jain, M.; Sharma, K.; Shah, B.; Vyas, M.; Thakkar, P.; Shah, R.; Singh, S.; Lohray, B. *J. Chromatogr.* **2005**, *818*, 213.

[14] Suganthi, A.; Karthikeyan, R.; Ravi, T. K. *Indian Drugs* **2006**, *43*, 827.

[15] Smitha, G.; Areefulla, H. S.; Swamy, P. V.; Appala, R. S. *Asian J. Chem.* **2007**, *19*, 3445.

[16] Shirore, P. D.; Srirkhedkar, A. A.; Fursule, R. A.; Telele, G. S.; Surana, S. J. *Indian Drugs* **2006**, 43, 315.

[17] Manoj, K.; Anbazhagan, S. *Indian Drugs* **2004**, *41*, 837.

[18] Singh, S.; Bakshi, M. *Pharm. Technol.* **2000**, *26*, 24.

224

Orbital Elec. J. Chem., Campo Grande, 2(3): 209-224, 2010

Full Paper

Degradation dynamics of an oxime carbamate insecticide (methomyl) in aqueous medium of varying pH under laboratory simulated condition

Md. Wasim Aktar[a§], Samsul Alam[b], Dwaipayan Sengupta[c], Ashim Chowdhury[c]*

[a]Pesticide Residue Laboratory, Department of Agricultural Chemicals, Bidhan Chandra Krishi Viswavidyalaya, Mohanpur-741252, Nadia, West Bengal, India
[b]Institute of Pesticide Formulation Technology Sector-20, Udyog Vihar, Opp. Ambience Mall (on NH-8), Gurgaon-122016, Haryana, India
[c]Department of Agricultural Chemistry and Soil Science, Institute of Agricultural Science, University of Calcutta, Kolkata, West Bengal, India
[§]Present address: Residue Section, Laboratory Service, SGS India Pvt. Ltd. Behala Industrial Complex, Phase-II, First Floor, 620, Diamond Harbour Road, Kolkata-700034, W.B., India

ABSTRACT: *Laboratory degradation studies were performed in water at pH 4.0, 7.0 and 9.2 using methomyl (Lannate 12.5 L) formulation at the rates of 1.0 (T_1) and 2.0 (T_2) μgmL^{-1}. Water samples collected on 0 (2 h), 3, 7, 15, 30, 45, 60 and 90 days after treatments were processed for residue analysis of methomyl by HPLC equipped with Photo Diode Array Detector. In 60 days, dissipation was 84-87% at pH 4.0, 71-77% at pH 7.0, and 91-93% at pH 9.2 in both treatments showing very little effect of pH on dissipation. The half-life periods observed were 20.76 and 22.13 days at pH 4.0, 27.87 and 28.67 days at pH 7.0 and 15.84 and 16.54 days at pH 9.2 at T_1 and T_2 doses respectively.*

Keywords: *methomyl; pH; dissipation; kinetics; insecticide*

Introduction

Methomyl S-methyl *N*-[(methylcarbamoyl)oxy]-thioacetimidate [$C_5H_{10}N_2O_2S$] is an insecticide of oxime carbamate group (Fig. 1). The compound was introduced in 1966 as a broad spectrum insecticide. It is mainly used to control the larvae of the diamondback moth, *Plutella xylostella* (L) and its two major parasitoids, *Cotesia plutellae* (Kurdjumov) and *Oomyzus sokolowskii* (Kurdjumov). It is also used as an acaricide to control ticks and

---

* Corresponding author. E-mail: sengupta_d@yahoo.co.in

spiders. It is used for foliar treatment of vegetable, fruit and field crops, cotton, commercial ornamentals, and in and around poultry houses and dairies. It is also used as fly bait. It is effective in two ways: (a) as a "contact insecticide," because it kills target insects upon direct contact, and (b) as a "systemic insecticide" because of its capability to cause overall "systemic" poisoning in target insects, after it is absorbed and transported throughout the pests that feed on treated plants. It is capable of being absorbed by plants without being "phytotoxic" or harmful, to the plant [1-3].
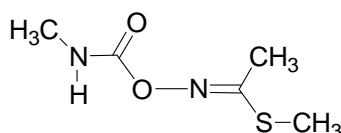
Figure 1. Chemical structure of methomyl.

Methomyl has low persistence in the soil environment and possesses the risk of groundwater contamination because of its high solubility in water [4]. Additionally, it is moderately to highly toxic to fish and highly toxic to aquatic invertebrates [4-6]. Therefore, persistence study of methomyl in soil-solution and pure water system has earned importance in respect of its possible food chain contamination. pH is a prime factor controlling dissipation, transformation and fate of pesticides in soil-water system. The present dissipation study of methomyl in water, has therefore, been carried out at different pH levels. Methomyl residue at different days interval was determined by reversed-phase high-performance liquid chromatography with fluorescence detection after postcolumn derivatization. The separation of carbamates is performed on a C8 column with water-methanol as mobile phase [7, 8].

Material and Methods

Chemicals and reagents

The certified reference standards of methomyl were purchased from Dr. Ehrenstorfer GmbH, Germany, and were of >99% purity. All the solvents were of HPLC grade or equivalent quality. Methomyl formulation (Lannate 12.5 L) was procured from local market. Sodium sulphate was washed repeatedly with distilled acetone and activated at 110 ^{o}C for 2 h before use. Stock solution (100 µgmL^{-1}) was prepared in methanol and working solution was prepared by diluting it.

Preparation of matrices and application of chemical

The pH of water was adjusted using buffer. Buffer capsules of pH 4.0, 7.0 and 9.2 from E. Merck were used for the purpose of preparing buffer solution. One capsule was required for 100 mL of distilled water to maintain the above mentioned pH. In a series of

226

Orbital Elec. J. Chem., Campo Grande, 2(3): 225-234, 2010

Winchester bottles (10 L capacity) 6 L distilled water was kept and sixty capsules were added to each of the bottle. The bottles were then left in room temperature for overnight to homogenize the buffer solutions. For carrying out laboratory experiment, water (6 L) of each pH triplicate was spiked at the rate of 1.0 (T_1) and 2.0 (T_2) µg of a.i. per mL with methomyl formulation and stored in Winchester bottles from October to December, 2009 under room temperature (15-39.5 ^{o}C). Untreated control was also carried out simultaneously. Samples were drawn periodically on 0 (2 h), 3, 7, 15, 30, 45, 60, and 90 days after treatments and analyzed for methomyl residues.

Extraction and clean-up of residues

Representative 200 mL water sample was taken in 1 L separating funnel and 5-10 g sodium chloride was added to it. It was extracted thrice (100, 50, 50 mL) with dichloromethane by liquid-liquid partitioning. Organic phases were combined, passed through over sodium sulphate and concentrated on a rotary vacuum evaporator under reduced pressure at 40 ^{0}C followed by a gas manifold evaporator till near dryness. Final solution was made to 1 mL in methanol and subjected to HPLC analysis. No clearing was required as no interference peaks were observed during analysis.

Estimation of residues

Final analysis of methomyl in water samples were done by HPLC (Shimadzu Model No. SPD M 1O A) equipped with Photo Diode Array Detector. The C-18 reverse phase column (15 cm x 4.6 mm i.d.) along with guard column was used. The mixture of acetonitrile and water (4:6 v/v) was used as mobile phase for the detection of methomyl residue. The other parameters like flow rate, wave length (λ_{max}), retention time were 1 mLmin^{-1}, 240 nm and 3.55±0.2 min, respectively (Fig. 2).
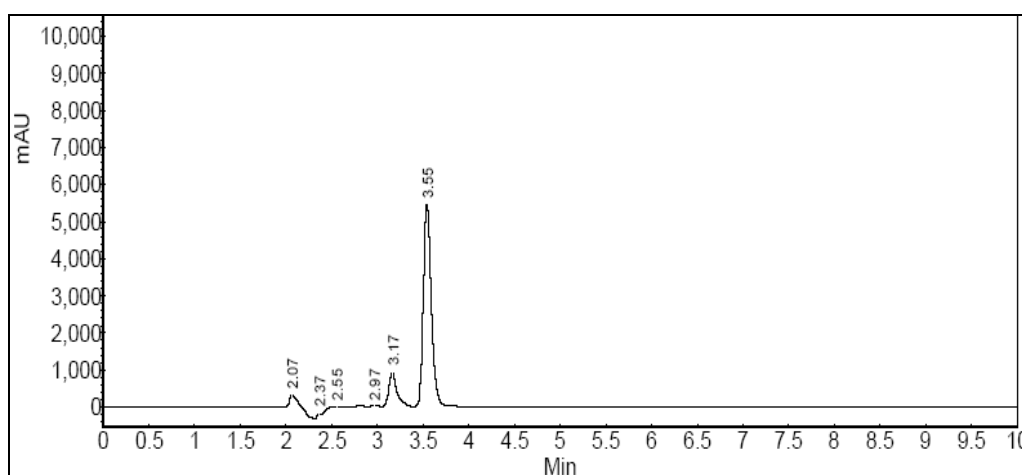
Figure 2. HPLC chromatogram of methomyl in substrate.

Confirmation of the residues by LC-MS/MS

227

Orbital Elec. J. Chem., Campo Grande, 2(3): 225-234, 2010

The substrates were extracted using the above stated method and finally subjected to analysis in LC-MS (Quattro Micro system) coupled with Waters 2695 separation module. Detection as well as confirmation was carried out by Quattro Micro (Tandem mass spectrometry detector) fitted with an electro spray ionization source (ESI). The MS parameters were optimized in direct infusion mode using Mass Lynx Auto tune software program. The Ion Mode, Inter Channel Delay (s), Inter Scan Time (s), Span (Da), Dwell time (s), Cone (V), Collision Energy (eV), Molecular Ion (m/z) and Daughter Ion (m/z) are MRM, ES+, 0.010, 0.010, 0.2, 0.1, 17.00, 7.00, 163.00 and 87.60, respectively (Fig. 3).

Column	:	100 x 2.1 mm; Symmetry ® C_{18}, 5 μ (RPC)
Mobile phase	:	Methanol/water (90:10, v/v) + 5 mM ammonium acetate
Flow rate	:	0.3 mL/min.
Retention time	:	3.39 ± 0.05 min.
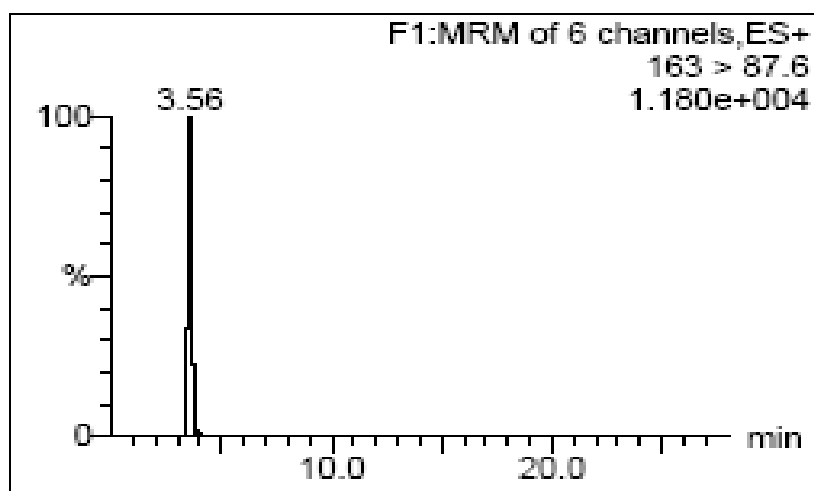
Figure 3. LC-MS/MS MRM transition for methomyl.

Calculation of residues

The residue content was calculated by using the formula

$$\text{Residue (in } \mu g g^{-1}) = \frac{A_1 \times C \times V_1}{A_2 \times W \times V_2} \times R_f$$

Where,

A_1 = Area of methomyl from sample, in chromatogram.

A_2 = Area of methomyl from standard, in chromatogram.

V_1 = Total volume of sample (in mL).

228

Orbital Elec. J. Chem*., Campo Grande, 2(3): 225-234, 2010*

C = Concentration of analytical standard in ppm (µg/ml) x µL injected.

W = Weight of the final working sample drawn from laboratory sample obtained

   from raw sample after quartering technique (in g).

V_2 = Injected volume of sample (in µL).

R_f = Recovery factor.

Linearity was evaluated by linear regression analysis.

The residue data were subjected to regression analysis and the fit of the data to first order kinetics (Ct = $C_o e^{-KI}$) was confirmed by testing the statistical significance of correlation coefficient. The half-life values were calculated from dissipation constant calculated from regression analysis.

The calibration curves for the compounds were obtained by plotting the peak area against the concentration of the corresponding calibration standards. The limit of detection (LOD) of the test compounds was determined by considering a signal-to-noise ratio of 3 with reference to the background noise obtained for the blank sample, whereas the limits of quantification (LOQ) were determined by considering a signal-to-noise ratio of 10.

Results and Discussion

Recovery Study and Method Validation

To work out the extraction efficiency of methods employed for methomyl from aqueous phase of varying pH were spiked in triplicate at three different levels (i.e. at the rate of 0.5, 1.0 and 5.0 µgmL^{-1}) with the above mentioned insecticide. Average recoveries of methomyl from water varied from 86.0-89.6% at pH 4.0, 84.0-88.8% at pH 7.0 and 86.6-92.4% at pH 9.2 (Table 1). The linearity of the calibration curve was the range 0.05–2.00 µgmL^{-1} for methomyl with a correlation coefficient (R^2) of the calibration curve of >0.99. For matrix calibration, the R^2 was also >0.99 for methomyl. The LOD and LOQ of the compound were 0.02 and 0.05 µgmL^{-1}, respectively. The coefficients of variation regarding the repeatability and intermediate precision for methomyl at 0.5 µgmL^{-1} were 2.5% and 6.5%, respectively.

Effect of pH

As evident from the data in Table 2, at pH 4.0, initial residues of 0.96 µgmL^{-1} in treatment T_1 dissipated to 0.86 µg mL^{-1} in 3 days, 0.45 and 0.15 µgmL^{-1} in 30 and 60 days, respectively. Corresponding dissipation were 10.07, 53.47 and 84.03%, respectively. In treatment T_2, initial residues of 1.96 µgmL^{-1} dissipated to 1.72, 0.83 and 0.26 µgmL^{-1} in 3, 30 and 60 days after application with corresponding dissipation of

229

Orbital Elec. J. Chem., Campo Grande, 2(3): 225-234, 2010

12.27, 57.41 and 86.54%, respectively.

Table 1. Recoveries of methomyl from water of different pH (4.0, 7.0 and 9.2)

Fortified samples	Treatment applied (μgmL^{-1})	Amount recovered (μgmL^{-1}) (% recovered)			
		R_1	R_2	R_3	Mean
pH 4.0	5.0	4.50 (90.00)	4.35 (87.00)	4.60 (92.00)	4.48 (89.60)
	1.0	0.88 (88.00)	0.90 (90.00)	0.87 (87.00)	0.88 (88.33)
	0.5	0.40 (80.00)	0.44 (88.00)	0.45 (90.00)	0.43 (86.00)
pH 7.0	5.0	4.38 (87.60)	4.64 (93.80)	4.25 (85.00)	4.42 (88.80)
	1.0	0.90 (90.00)	0.85 (85.00)	0.82 (82.00)	0.86 (85.60)
	0.5	0.42 (84.00)	0.40 (80.00)	0.44 (88.00)	0.42 (84.00)
pH 9.2	5.0	4.67 (93.40)	4.75 (95.00)	4.75 (89.00)	4.72 (92.40)
	1.0	0.89 (89.00)	0.92 (92.00)	0.94 (94.00)	0.92 (91.60)
	0.5	0.44 (88.00)	0.45 (90.00)	0.41 (82.00)	0.43 (86.60)

Table 2. Dissipation of methomyl residues in water at pH 4.0

Time (days)	Residues (μgmL^{-1})									
	1.0 μgmL^{-1}					2.0 μgmL^{-1}				
	R_1	R_2	R_3	Mean ($\pm$ SD)	% loss	R_1	R_2	R_3	Mean ($\pm$ SD)	% loss
0	0.97	0.95	0.96	0.96 ($\pm$0.010)	-	1.96	1.95	1.96	1.96 ($\pm$0.006)	-
3	0.87	0.84	0.88	0.86 ($\pm$0.021)	10.07	1.72	1.70	1.73	1.72 ($\pm$0.015)	12.27
7	0.75	0.79	0.73	0.76 ($\pm$0.031)	21.18	1.58	1.55	1.54	1.56 ($\pm$0.021)	20.44
15	0.68	0.65	0.63	0.65 ($\pm$0.025)	31.94	1.41	1.44	1.42	1.42 ($\pm$0.015)	27.26
30	0.43	0.47	0.44	0.45 ($\pm$0.021)	53.47	0.85	0.83	0.82	0.83 ($\pm$0.015)	57.41
45	0.24	0.2	0.21	0.22 ($\pm$0.021)	77.43	0.53	0.55	0.52	0.53 ($\pm$0.015)	72.74
60	0.12	0.16	0.18	0.15 ($\pm$0.031)	84.03	0.28	0.25	0.26	0.26 ($\pm$0.015)	86.54
90	BDL	BDL	BDL	-	-	BDL	BDL	BDL	-	-

BDL=Below Detectable Limit

At pH 7.0, initial residues of 0.97 μgmL^{-1} in T_1 treatment, dissipated to 0.87, 0.56 and 0.28 μgmL^{-1} in 3, 30 and 60 days after treatment with corresponding dissipation of 10.07, 42.42 and 71.41% respectively, whereas in T_2 initial residues of 1.98 μgmL^{-1} dissipated to 1.80, 0.92 and 0.45 μgmL^{-1} in 3, 30 and 60 days after treatment showing

230

Orbital Elec. J. Chem., Campo Grande, 2(3): 225-234, 2010

dissipation of 9.26, 53.54 and 77.27%, respectively (Table 3).

Table 3. Dissipation of methomyl residues in water at pH 7.0

Time (days)	Residues (μgmL^{-1})									
	1.0 μgmL^{-1}					2.0 μgmL^{-1}				
	R_1	R_2	R_3	Mean (± SD)	% loss	R_1	R_2	R_3	Mean (± SD)	% loss
0	0.98	0.96	0.97	0.97 (±0.010)	-	1.98	1.96	2.00	1.98 (±0.020)	-
3	0.88	0.85	0.89	0.87 (±0.021)	10.07	1.81	1.80	1.78	1.80 (±0.015)	9.26
7	0.76	0.80	0.74	0.76 (±0.031)	21.18	1.64	1.65	1.66	1.65 (±0.010)	16.67
15	0.71	0.68	0.66	0.69 (±0.026)	29.25	1.47	1.50	1.45	1.47 (±0.025)	25.59
30	0.54	0.59	0.55	0.56 (±0.026)	42.42	0.92	0.94	0.90	0.92 (±0.020)	53.54
45	0.43	0.36	0.38	0.39 (±0.037)	59.75	0.61	0.63	0.60	0.61 (±0.015)	69.02
60	0.22	0.29	0.33	0.28 (±0.055)	71.41	0.45	0.48	0.42	0.45 (±0.030)	77.27
90	0.09	0.12	0.09	0.10 (±0.017)	89.69	0.23	0.28	0.25	0.25 (±0.025)	87.21

At pH 9.2, from treatment T_1 initial residues of 0.97 μgmL^{-1} dissipated to 0.69, 0.52 and 0.17 μgmL^{-1} in 3, 15 and 45 days after treatment with corresponding dissipation of 28.77, 46.09 and 82.12%, respectively. In T_2 residues of 1.96 μgmL^{-1} on 0 (2 h) day dissipated to 1.56, 1.14 and 0.30 in 3, 15 and 45 days after treatment and corresponding dissipation was 20.43, 42.69 and 84.52%, respectively (Table 4). The Regression equation, Correlation Co-efficient and half-life for the dissipation of methomyl in water at different pH are presented at Table 5.

It is clear that methomyl residues in water dissipated more than 80% in 60 days at pH levels of 4.0, 7.0 and 9.2 in both treatments under laboratory conditions under temperature ranging from 15 to 39.5 ^{0}C. The degradation was slow during first 3 days followed by relatively faster degradation from 3rd day onward to 45 days after which it became slow (figures 4-6).

Almost identical degradation ranging from 71.41 to 93.03% at all the three pH levels during 60 days study indicate that there was no significant effect of pH on degradation, although dissipation was a little faster at pH 9.2 throughout the studies (Fig. 6). Half-life values at pH levels of 4.0, 7.0 and 9.2 varied from 22.35 to 21.76, 27.87 to 28.67 and 15.84 to 16.54 days, respectively. At all pH levels degradation was observed to be faster in T_1 than T_2. The slow dissipation at higher rate could attribute to inhibition of microbial activity.

231

Orbital Elec. J. Chem., Campo Grande, 2(3): 225-234, 2010
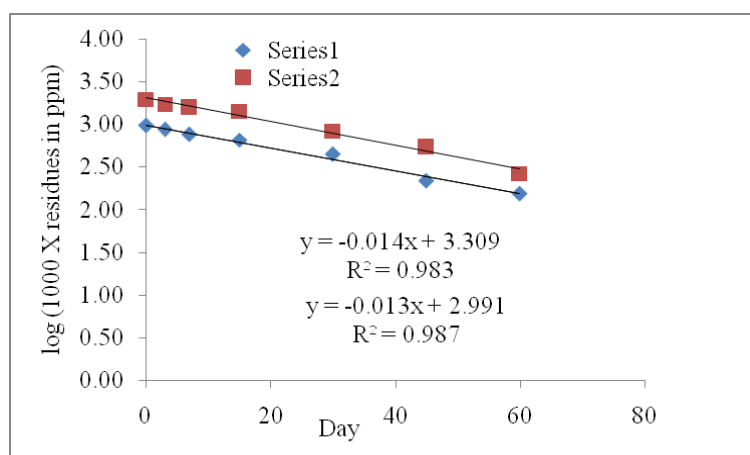
Figure 4. Dissipation of methomyl at pH 4.0 (ppm = μgmL^{-1})

Table 4. Dissipation of methomyl residues in water at pH 9.2

Time (days)	Residues (μgmL^{-1})									
	1.0 μgmL^{-1}					2.0 μgmL^{-1}				
	R_1	R_2	R_3	Mean (± SD)	% loss	R_1	R_2	R_3	Mean (± SD)	% loss
0	0.98	0.96	0.97	0.97 (±0.010)	-	1.96	1.94	1.98	1.96 (±0.020)	-
3	0.70	0.67	0.70	0.69 (±0.017)	28.77	1.54	1.56	1.58	1.56 (±0.020)	20.41
7	0.60	0.63	0.58	0.61 (±0.024)	37.57	1.39	1.42	1.40	1.40 (±0.015)	28.40
15	0.54	0.52	0.50	0.52 (±0.020)	46.09	1.13	1.10	1.14	1.12 (±0.021)	42.69
30	0.34	0.38	0.35	0.36 (±0.017)	63.15	0.59	0.60	0.60	0.60 (±0.006)	69.56
45	0.19	0.16	0.17	0.17 (±0.017)	82.12	0.29	0.32	0.30	0.30 (±0.015)	84.52
60	0.09	0.10	0.08	0.09 (±0.010)	90.70	0.15	0.14	0.12	0.14 (±0.015)	93.03
90	BDL	BDL	BDL	-		BDL	BDL	BDL	-	-

BDL=Below Detectable Limit

Table 5. Regression equation, Correlation Co-efficient and half-life for the dissipation of methomyl in water at different pH

pH	Treatments (μgmL^{-1})	Regression Equation	Correlation co-efficient	Half-life (days)
4.0	1.0	y =2.991-0.013x	0.986	22.35
	2.0	y = 3.308-0.013x	0.983	21.65
7.0	1.0	y = 2.997-0.010x	0.993	27.87
	2.0	y = 3.286-0.010x	0.976	28.67
9.2	1.0	y = 2.942-0.015x	0.979	15.84
	2.0	y = 3.291-0.018x	0.973	16.54

232

Orbital Elec. J. Chem., Campo Grande, 2(3): 225-234, 2010
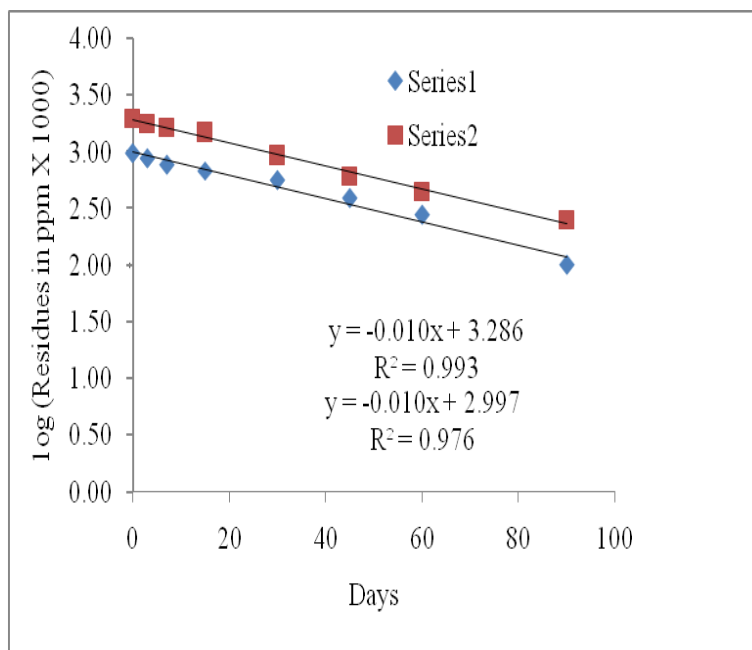
Figure 5. Dissipation of methomyl at pH 7.0 (ppm = μgmL^{-1})
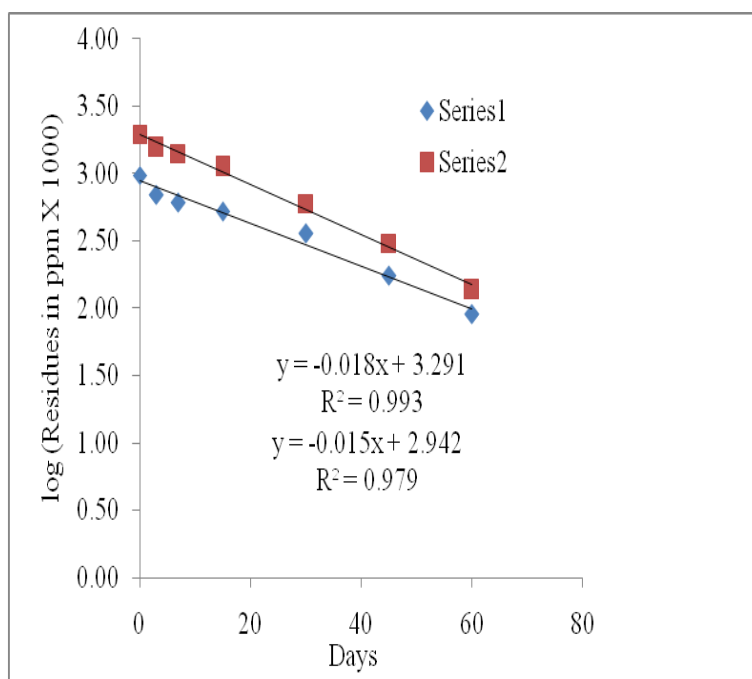
Fig 6. Dissipation of methomyl at pH 9.2 (ppm = μgmL^{-1})

Similar observations have been reported for prchloraz [9] and benthiocarb [10] in water where dissipation was independent of pH and was subject to photodegradation following pseudo first order kinetics. Dissipation of butachlor residues has also been reported [11] following pseudo first order kinetics in river waters. Whereas in another studies decomposition of trifluralin and metribuzin in water as pH and dose dependent, resulted in faster dissipation under alkaline conditions and at low dose of application [12,

Orbital Elec. J. Chem., Campo Grande, 2(3): 225-234, 2010

233

13]. Slightly faster dissipation of methomyl at alkaline pH has been observed in our studies also. Considering rapid dissipation of Methomyl at the tested doses in water system, its much faster degradation can be expected under field condition.

Acknowledgements

References and Notes

[1]   Fukuto, R. T. In: Fate of Pesticides in the Environment, Publication Number 3320. Biggar, J. W.; Silber, J. N., eds. Davis, CA: University of California Agricultural Experiment Station Publications, 1987.

[2]   Ware, G. W. Fundamentals of Pesticides, a Self-Instruction Guide. Fresno, CA: Thompson Publications, 1986.

[3]   Stevens, J. T.; Sumner, D. D., (1991). In: Handbook of Pesticide Toxicology. Hayes, W. J (Jr.).; Laws, E. R (Jr.)., eds. New York, NY: Academic Press, 1991, 3-5.

[4]   Howard, P. H. Handbook of Environmental Fate and Exposure Data for Organic Chemicals: Pesticides. Chelsea, MI: Lewis Publishers, 1991, 3-15.

[5]   Kidd, H.; James, D. R. eds. The Agrochemicals Handbook, Third Edition. Cambridge, UK: Royal Society of Chemistry Information Services (as updated), 1991, 3-11.

[6]   U.S. Environmental Protection Agency. Health Advisory Summary: Methomyl. Office of Drinking Water. Washington, DC 1987, 3-40.

[7]   Sanchez, B. C.; Albero, B.; Tadeo, J. L. *J. Food Protec*. **2004**, *67*, 2565.

[8]   Zhang, J. Q.; Dong Y. H.; An, Q. O.; Liu, X. C. *Acta. Pedo. Sin.* **2006**, *43*, 772.

[9]   Aktar, M. W.; Sengupta, D.; Purkait, S.; Ganguly, M.; Paramasivam, M. *Inter Toxicol.* **2008**, *1*, 203.

[10] Aktar, M.W.; Paramasivam, M.; Bhattacharyya, A. *Int. J. Environ. Res*. **2008**, *2,* 71.

[11] Liu, Y. J.; Lin, C.; Yeh, K. J.; Lee, A. *Bull. Environ. Contam. Toxicol*. **2000**, *64*, 780.

[12] Chang, W. L., (1973). J*. Taiwan Agri Res*. **1973**, *22*, 111.

[13] Prasad, H.; Kumari, B.; Rani, D.; Kathpal, T. S. *Pollution Res.* **2005**, *24*, 535.

234

Orbital Elec. J. Chem*., Campo Grande,* 2(3): 225-234, 2010

Full Paper

Adsorption of methylene blue from aqueous solution on zeolitic material and the improvement as toxicity removal to living organisms

Denise A. Fungaro[a]*, Lucas C. Grosche[a], Alessandro S. Pinheiro[b], Juliana C. Izidoro[a], Sueli I. Borrely[b]

[a]Chemical and Environmental Center, Nuclear and Energy Research Institute, Av. Prof. Lineu Prestes, 2242, CEP 05508-000, São Paulo, Brazil
[b]Radiation Technology Center, Nuclear and Energy Research Institute, Av. Prof. Lineu Prestes, 2242, CEP 05508-000, São Paulo, Brazil

ABSTRACT: *The adsorption of methylene blue (MB) from aqueous solution was carried out using zeolite. This adsorbent material was synthesized from fly ash as a low-cost adsorbent, allowing fly ash to become a recycled residue. Factors that affected adsorption were evaluated: initial dye concentration, contact time and temperature. The equilibrium of adsorption was modeled by Langmuir, Freundlich and Temkin models. The adsorption obtained data were well described by Temkin, the adsorption isotherm model. Thermodynamic calculations suggest that the adsorption of methylene blue on zeolite synthesized from fly ash is a spontaneous and exothermic reaction. Acute toxicity was determined for raw and adsorbed methylene blue solutions, as if it was a real liquid residue. Acute effects were substantially reduced after the adsorption treatment. The values of untreated solution of methylene blue were 16.58 ppm up to 18.64 ppm for Vibrio fischeri bacteria and from 0.16 ppm up to 0.43 ppm for Daphnia similis cladoreca exposed to the dye for 48 hours.*

Keywords: *methylene blue; zeolite; dye adsorption; acute toxicity; D. similis; V. fischeri*

Introduction

Synthetic dyes are used extensively by several industries including the textile dyeing and paper industry. It is estimated that at least 10% of the dyes are lost in the dye effluent during such dyeing processes. The colored wastewater damages the aesthetic nature of water and reduces the light penetration through the water's surface and the photosynthetic activity of aquatic organisms due to the presence of metals,

---

* Corresponding author. E-mail: dfungaro@ipen.br (D.A. Fungaro)

chlorides and other contaminants. Many of the dyes used in these industries may also be carcinogenic and mutagenic [1-4].

Textile industries feature among the eight most important sectors of the industrial activity of Brazil, occupying first place in direct employment and in billing. The discharge of colored wastewater has increased considerably with the development of the textile industry in the Santa Catarina state (Brazil), aggravating the environmental problems [5].

Among several chemical and physical treatment methods, the adsorption has been found to be superior to other techniques for the removal of dyes from aqueous solution in terms of methodology, operational conditions and efficiency. Currently, the most common procedure involves the use of activated carbons as adsorbents due to their higher adsorption capacities. Commercially available activated carbons are usually derived from wood or coal, being considered expensive. This has led to the scientists to use lower-cost adsorbents which are cheaper efficient substitutes [6-7].

Fly ash is formed by combustion of coal in coal-fired power station as a waste product. The generation rate of coal fly ash in Brazil is approximately 4 million tons per year and is predicted to increase. Efficient disposal of coal fly ash is a worldwide issue due to its massive volume and harmful risks to the environment. As a technique for recycling coal fly ash, synthesis of zeolites from coal fly ash has attracted a great deal of attention.

Holler and Wirsching [8] and Henmi [9] were the first to report the modification of fly ash by hydrothermal treatment in alkaline solutions at elevated temperatures and pressures to produce zeolites. Since them, the synthetic approach has been modified to include microwave assisted synthesis [10] and the fusion of ash with base prior to hydrothermal treatment [11]. Zeolitic materials have been widely used as low-cost adsorbents as reviewed by Querol et al. and Rayalu et al. [12-13].

In our group we have been developing zeolites synthesized from Brazilian coal fly ashes from the Figueira power plant to remove metals ions from aqueous effluents and soil [14-16]. The efficiency of zeolitic materials from baghouse filter as adsorbent allowed investigations focused on the removal of dye [17-18].

Methylene blue (MB) is one of the most commonly used basic dyes for printing and textural dyeing for acrylic, nylon, silk, wool and medicinal purposes. Although it's not strongly hazardous, can causes permanent injury to the eyes of human and animals. On inhalation, it can give rise to short periods of difficult breathing, while ingestion through the mouth produces a burning sensation and may cause nausea, vomiting, profuse sweating, mental confusion, painful micturition, and methemoglobinemia [19]. The

Orbital Elec. J. Chem., Campo Grande, 2(3): 235-247, 2010

236

uptake of methylene blue is usually used as an index of adsorption performance for adsorbents.

Regarding to biological aspects few data is available on the efficacy of developing treatment technology on toxicity removal. The importance of ecotoxicological and mutagenic aspects for suitable developing of treatment technologies is a growing understanding. The negative effects of treated dyes and their byproducts is an important way to confirm if the treatment will really imply in a better product for the environment [20].

Part of the study was dedicated to evaluate the capability of zeolite from fly ash for the decoloration of methylene blue and the second objective was addressed to the toxicity of dye and how the treatment will modify this property. To this end, fly ashes from cyclone filter were selected. The zeolite efficacy was evaluated for toxicity reduction using two lived organisms: the crustacean *D. similis* and luminescent bacteria *V. fischeri*. These species are significant for treatment aspects and water quality. Brazilian water monitoring plan is looking to toxicity evaluation for the same organisms and this is partially the reason why they were selected [21].

Material and Methods

Materials

Methylene blue (CI 52015) was obtained from Merck and used as received. A stock solution (3.2 g. L^{-1}) was prepared with deionized water (Millipore Milli-Q) and the solutions for adsorption tests were prepared by diluting. The samples of coal fly ash (CFA) from cyclone filter were obtained from a coal-fired power plant located at Figueira County, in Paraná State, Brazil. A Commercial zeolite 4A from Bayer was also used in the adsorption study for comparing.

Zeolite synthesis

Coal fly ash (20 g) was mixed with 160 mL of 3.5 mol L^{-1} aqueous NaOH solution in a 300 mL Teflon vessel. This mixture was heated to 100 $^{\circ}$C in oven for 24 h. After finishing of the process, the suspension was filtered with 4A quantitative filter paper. The zeolitic material was repeatedly washed with deionized water until the pH of washing water reach ~11 and dried at 100 $^{\circ}$C for 24 h [9]. The zeolite obtained was label as ZM.

Characterization techniques

The physico-chemical characteristics of materials were determined using standard procedures. Bulk density was determined by helium pycnometer (Micromeritics – Accupyc 1330). The surface area was determined by N_2 adsorption isotherm with relationship using NOVA 1200 (Quantachrome Corp.). Before adsorption experiments, the samples

Orbital Elec. J. Chem*., Campo Grande,* 2(3): 235-247, 2010

237

were degassed at 150 ^{o}C for 12 h. The specific surface area was obtained by five points at p/p^0 between 0.05 and 0.20 applying the Brunauer–Emmet–Teller equation to the adsorption data. The phases of the zeolite were determined by X-ray diffraction analyses (XRD) with an automated Rigaku multiflex diffractometer with Cu anode using Co Kα radiation at 40 kV and 20 mA over the range (2θ) of 5–80° with a scan time of 1°/min. The chemical composition of zeolite was determined by a RIX-3000 RIGAKU X-ray fluorescence spectrometer (XRF) equipped with a Rh X-ray tube (operated at 50 kV-60 mA). Scanning Electron micrograph was obtained by using XL-30 Philips scanning electron microscope (SEM). The cation exchange capacity (CEC) value was determined using ammonium solutions. The pH of zeolite was measured as follows: 0.1 g of samples were mixed with 10 ml of distilled water and shaken for 24h. After filtration, the pH of solution was determined by a pH meter.

Adsorption studies

The adsorption was performed by batch experiments. Kinetic experiments were carried out by stirring 100 mL of dye solution of known initial dye concentration with 1 g of zeolite at room temperature (25 ^{o}C) at 120 rpm in different 250 mL PE flasks. At different time intervals, samples have been drawn out and then centrifuged at 2000 rpm for 20 min. The concentration in the supernatant solution was analyzed using a UV spectrophotometer (Cary 1E – Varian) by measuring absorbance at λ_{max} = 650 nm and pH = 5. Adsorption isotherms were carried out by contacting 1 g of zeolite with 100 mL of methylene blue over the concentration ranging from 3.2 to 96 mg L^{-1}. The agitation last 10 min, which is sufficient time to reach equilibrium. The methylene blue adsorption performance of the original coal fly ash was also studied for comparison.

The amount of adsorption at equilibrium (q_e, mg g^{-1}) was calculated by using the following equation:

$$q_e = \frac{V(C_o - C_e)}{W} \quad (1)$$

where C_o and C_e (mg L^{-1}) are the liquid-phase concentrations of dye at initial and equilibrium, respectively, V is the volume of the solution (L) and W is the mass of the adsorbent (g).

Toxicity evaluation

Daphnia similis crustacean and *Vibrio fischeri* luminescent bacteria were the tested-organisms for the evaluation of methylene blue acute toxicity. While the first assay evidences the immobility of the organisms due to the exposure, the second is

238

Orbital Elec. J. Chem*., Campo Grande,* 2(3): 235-247, 2010

based on the light emission reduction caused by the toxicant. Three acute toxicity experiments were performed for MB solutions before and after zeolite adsorption.

Acute toxicity for crustacean assays were performed with *D. similis* exposure for 24 h and 48 h at 20 ^{o}C $\pm$0.5 [22]. The water hardness was adjusted and fixed to 46 mg L^{-1} $CaCO_3$ for the toxicity tests and for the culture of this lived organism. At least five MB solution concentrations were analyzed and MB was diluted at the same water used for the maintenance of test-organisms. The results were expressed as EC_{50} (%, 48 h). Once this parameter is inversely proportional, the values were transformed into Toxic Units (TU = 100 / EC_{50}) to allow an easier comparison.

Acute toxicity for luminescent bacteria was carried out with Microtox® System – model 500 (Azur Environment, USA). The bacterial luminescence was measured after 15 min exposition and the lost sign (luminescence) was related to the effect according to the dye concentration. The assay results were expressed as EC_{50}, which is the effective concentration that causes 50% of light inhibition after 15 min exposure. The assay considered the suitable color correction when required due to hard blue color of the untreated samples. These assays were performed according to ABNT and ISO methods [23]. After obtaining Toxic Units the efficacy of zeolites adsorption was calculated as removal percentage.

The contaminants of *dye-saturated zeolite* were analyzed by means of leaching and solubilization tests [24-26].

Results and Discussion

Characterization of materials

The morphology of the starting material CFA and synthesized product ZM were examined using SEM (Fig. 1). Fig. 1a confirms that CFA particles had the predominance of spherical shapes of different size ranges and smooth surfaces. By contrast, the surface of ZM is rough, indicating that zeolite crystals were deposited on the surface of underlying fly ash particles during the hydrothermal treatment (Fig. 1b).

Table 1 shows some properties of fly ash and zeolitic material. XFR measurement indicates that the original fly ash is a ready source of Al and Si for forming zeolites. According to the American Society for Testing Materials (ASTM C618) [27], fly ashes are defined as Class F produced from the burning of higher rank coals. Vitrinite reflectance analyses indicated a high volatile B/C bituminous coal at the Figueira Power Plant [28]. The chemical composition of zeolitic material synthesized from fly ash is mainly silica, alumina, iron oxide and sodium oxide. A significant amount of Na element is incorporated in the final product due the hydrothermal treatment with NaOH solution. Table 1 also includes data on the specific surface areas of materials and the value of zeolitic product

Orbital Elec. J. Chem*., Campo Grande*, 2(3): 235-247, 2010

239

has increased 5-fold. This surface area increase is related to the crystallization of the many zeolite crystals on the originally smooth ash spheres. The CEC rose from 1.55 meq 100 g^{-1} for the unmodified ash to 137.6 meq 100 g^{-1} for the modified product due to crystal formation of the material-type zeolite.
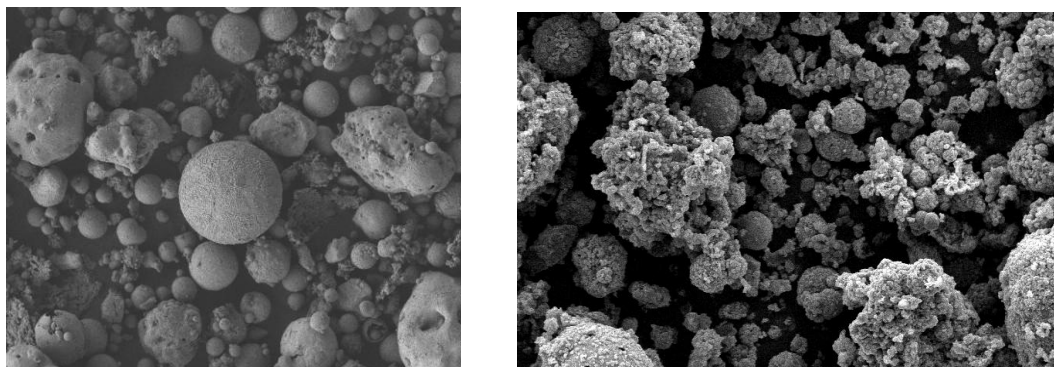

Figure 1. SEM images of (a) CFA (b) ZM.

Table 1. Physicochemical properties of fly ash and zeolitic material

Property	CFA	ZM
SiO_2 (wt%)	40.4	39.5
Al_2O_3 (wt%)	15.2	25.0
Fe_2O_3 (wt%)	10.6	16.6
Na_2O (wt%)	0.988	11.8
CaO (wt%)	1.65	2.68
K_2O (wt%)	2.23	0.480
TiO_2 (wt%)	0.781	1.17
SO_3 (wt%)	0.914	1.05
MgO (wt%)	0.348	1.04
ZnO (wt%)	0.101	0.120
ZrO_2	0.0851	0.16
CEC (meq/100 g)	1.55	137.6
Specific surface area (m^2/g)	7.55	40.0
Bulk density (g/cm^3)	2.40	2.65
pH	8.18	9.23

Figure 2 illustrates the XRD profiles of the original coal fly ash (CFA) and zeolitic product (ZM). The mineralogical composition of fly ash depends on the geological factors related to the formation and deposition of coal and its combustion conditions. XRD profile of CFA is composed mainly of peaks of quartz (JCPDS 001-0649) and mullite (JCPDS 002-0495). Mullite and quartz are produced during the decomposition of clay minerals such as kaolinite [29]. Intensities of these peaks decrease and peaks caused by generation of zeolite increase with treatment of zeolite production. The major phase in zeolitic material was hydroxysodalite (JCPDS-ICDD 00-011-0401) with peaks of quartz and mullite of fly ash that remained after the treatment. The modification process leaded to reductions in the amount of mullite and quartz as indicated by the decrease in the peaks at 26.65. Hydroxysodalite is a condensed phase, and thermodynamically it is the most stable phase formed from the Na_2O–Al_2O_3–SiO_2–H_2O quaternary system [30].

240

Orbital Elec. J. Chem*., Campo Grande,* 2(3): 235-247, 2010
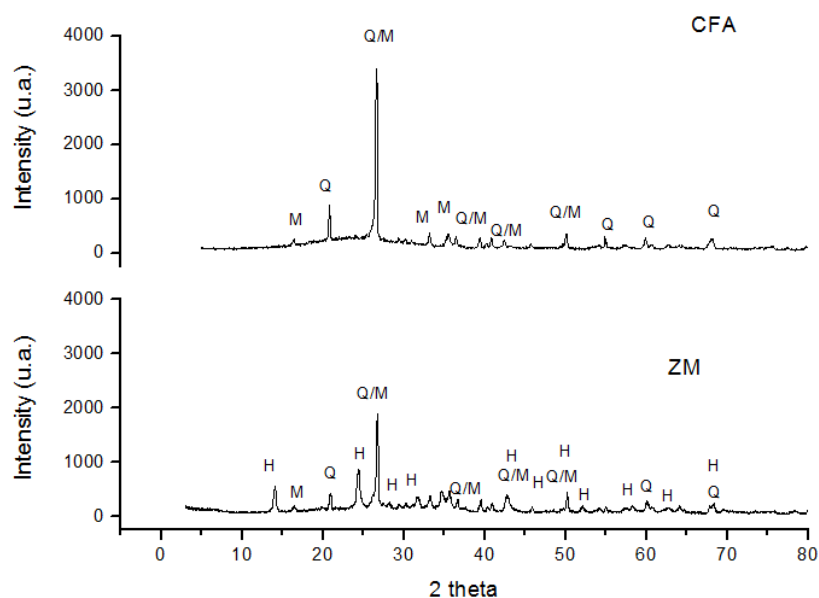
Figure 2. X-ray diffractograms for (a) CFA; (b) ZM. M = mulitte; Q = quartz; H = hydroxysodalite.

Effect of contact time

The effect of contact time on adsorption process was investigated at various initial dye concentrations. It can be seen from Fig. 2 that the adsorption of methylene blue on zeolite occurred very quickly within the first 10 min. after which a maximum value of adsorption capacity was attained. This rapid uptake can be attributed to the concentration gradient created at the start of the adsorption process between solute concentration in solution and that at the zeolite surface. Another factor that contributes to the rapid adsorption rate is that there are only adsorbate and adsorbent interactions with negligible interference from solute– solute interactions [31]. The equilibrium of the adsorption process was attained so fast that the kinetic data could not be modeled.
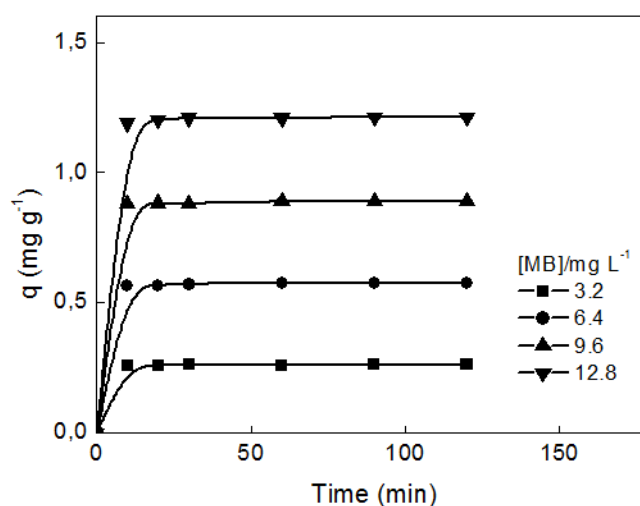
Figure 2. Adsorption kinetics for methylene blue onto zeolite.

Orbital Elec. J. Chem., Campo Grande, 2(3): 235-247, 2010

241

Full Paper

Adsorption isotherms

Equilibrium isotherm is described by an adsorption isotherm, characterized by certain constants whose values express the surface properties and affinity of the adsorbent. The adsorption equilibrium is established when the concentration of adsorbate in the bulk solution is in dynamic balance with that at the adsorbent interface.

In order to quantify the affinity of zeolite for the basic dye studied, three widely used isotherm models (Langmuir, Freundlich and Temkin isotherm models) were used to analyze the data obtained from the adsorption process.

The linear form of the Langmuir expression may be written as:

$$C_e/q_e = 1/bK_L + C_e/K_L \quad (2)$$

where q_e is solid-phase adsorbate concentration at equilibrium (mg g^{-1}), C_e is aqueous-phase adsorbate concentration at equilibrium (mg L^{-1}), K_L (mg g^{-1}) is the maximum amount of adsorbate per unit weight of adsorbent to form a complete monolayer on the surface, and b is the Langmuir isotherm constant (L mg^{-1}), related to the affinity of the adsorption sites. A plot of C_e/q_e versus C_e gives a straight line of slope $1/K_L$ and intercept $1/K_L b$.

The linear form of Freundlich equation is expressed as:

$$\text{Log } q_e = \log K_F + 1/n \ (\log C_e) \quad (3)$$

where K_F (mg/g(L/mg)$^{1/n}$) and n are Freundlich constants related to adsorption capacity and adsorption intensity of adsorbents. The Freundlich constant K_F and n can be calculated from the intercept and slope of plot between log q_e and logC_e.

The linear form of the Temkin isotherm model is:

$$q_e = B_T \ln K_T + B_T \ln C_e \quad (4)$$

where $B_T = RT/b$, *b* is the Temkin constant related to heat of sorption (J mol^{-1});K_T is is the equilibrium binding constant (L g^{-1}) corresponding to the maximum binding energy, *R* the gas constant (8.314 J/mol K) and *T* the absolute temperature (K). A plot of q_e *versus* ln C_e enables the determination of the isotherm constants B_T and K_T from the slope and the intercept, respectively.

Equilibrium data of methylene blue onto zeolite synthesized from fly ash are shown in Fig. 3. The isotherm shapes are largely determined by the adsorption mechanism and can therefore be used to diagnose the nature of the adsorption [32]. The equilibrium isotherm has the shape of L3 type curve and indicates that the second layer of dye can form readily.

The parameters obtained from the isotherms are given in Table 2. Langmuir

Orbital Elec. J. Chem*., Campo Grande,* 2(3): 235-247, 2010

242

constants are not given in Table 2 due this poor fit to experimental data. Negative values for the Langmuir isotherm constants imply that this model is not suitable to explain the adsorption process, since these constants are indicative of the surface binding energy and monolayer coverage. This suggests that some heterogeneity in the surface or pores of the zeolite synthesized from fly ash will play a role in dye adsorption.
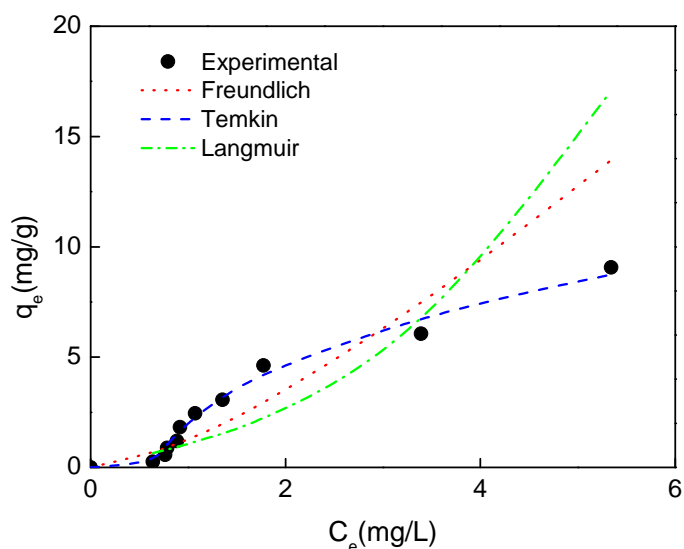
Figure 3. Adsorption isotherm of methylene blue onto zeolite.

Table 2. Equilibrium isotherm constants for methylene blue onto zeolite from fly ash

Adsorbent	Freundlich			Temkin		
	$K_F{}^*$	n	R^2	K_T (L g^{-1})	B_t	R^2
Zeolite	1.28	0.701	0.890	1.61	4.02	0.992
Fly ash **	0.158	1.05	0.966	1.09	0.422	0.940
Zeolite 4A	1.28	1.01	0.765	1.99	2.79	0.876

(*) [(mg g^{-1}) (L mg^{-1})$^{1/n}$]; (**) [AM] = 3.2 – 12.8 mg L^{-1}; t_{equil} = 2 h

The adsorption isotherm can be fitted using Temkin model with correlation coefficient >0.99. A comparison was also made between isotherms plotted in Fig. 3, which shows the experimental data points and the two theoretical isotherms plotted on the same graph. The parameters obtained from the isotherm of methylene blue onto original coal fly ash and onto commercial zeolite type 4A were presented in Table 2 for comparison. The coal fly ash presented lower adsorption capacity for methylene blue than the zeolite. Samples using zeolite required shorter agitation before reaching equilibrium and were able to remove more methylene blue from aqueous solution than

243

Orbital Elec. J. Chem., Campo Grande, 2(3): 235-247, 2010

the fly ash. The adsorption capacity can be correlated with the variation of surface area and porosity of the adsorbent. Higher surface area will generally result in higher adsorption capacity. The surface area value in zeolite increased about 80% compared to raw ash. In addition, conversion of fly ash to zeolite changes the surface properties of solid adsorbents by increasing the cation exchange capacity, which also favours the adsorption of methylene blue on treated fly ashes. It can be seen from Table 2 that adsorption capacity values of commercial zeolite and zeolite from fly ash were the same.

Thermodynamics parameters

To understand better the effect of temperature on the adsorption, it is important to study the thermodynamic parameters such as standard Gibbs free energy change (ΔG°), standard enthalpy (ΔH°) and standard entropy (ΔS°). The Gibbs free energy of adsorption by using equilibrium constant (K_c) is calculated from the following equation:

$$\Delta G^{\circ} = - 2.0303 \, RT \log K_C \quad (5)$$

Standard enthalpy, (ΔH°), and standard entropy, (ΔS°), of adsorption can be estimated from van't Hoff equation given in

$$\text{Log } Kc = \frac{\Delta S^0}{2.303 R} - \frac{\Delta H^0}{2.303 RT} \quad (6)$$

where R is the gas constant, K_c is adsorption equilibrium constant. The K_c value is calculated from the equation [7]

$$K_C = \frac{C_{Ae}}{C_{Se}} \quad (7)$$

where C_{Ae} is the equilibrium concentration of the dye ions on adsorbent (mg L^{-1}) and C_{Se} is the equilibrium concentration of the dye ions in the solution (mg L^{-1}).

The plot of log K_c against $1/T$ (in Kelvin) should be linear. The slope of the van't Hoff plot is equal to $-\Delta H^{\circ}/2.303$ R, and its intercept is equal to $\Delta S^{\circ}/2.303$ R. The van't Hoff plot for the adsorption of MB onto zeolite synthesized from fly ash is given in Fig. 4. Thermodynamic parameters obtained are given in Table 3.

As shown in Table 3, the negative values of ΔG° at different temperatures indicate the spontaneous nature of the adsorption process. Positive ΔH° reveals endothermic adsorption. The positive value of ΔS° suggests the increased randomness at the solid/solution interface during the adsorption of the dye onto zeolite synthesized from fly ash. A similar trend has been reported for the adsorption of methylene blue onto synthetic zeolite MCM-22 [33].

Orbital Elec. J. Chem., Campo Grande, 2(3): 235-247, 2010

244
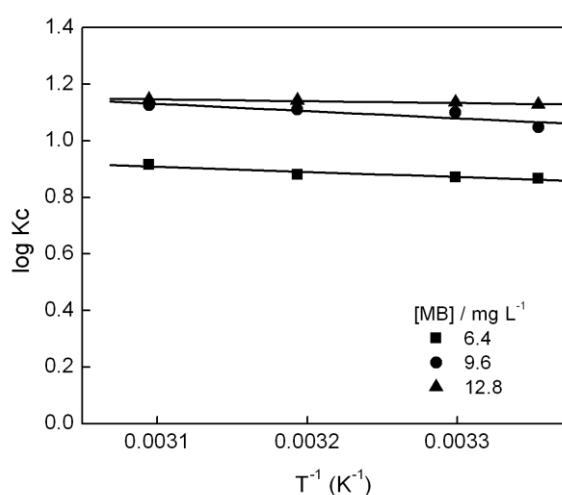
Figure 4. Van´t Hoff plot of methylene blue adsorption onto zeolite.

Table 3. Thermodynamic parameters for the adsorption of MB onto zeolite

[AM] (mg L^{-1})	ΔH^o (kJ mol^{-1})	ΔS^o (J mol^{-1})	ΔG^o (kJ mol^{-1})			
			298.15 K	303.15 K	313.15 K	323.15 K
6.40	9.27	46.43	- 4.37	- 5.05	- 5.28	- 5.67
9.61	4.89	36.79	- 5.98	- 6.39	- 6.65	- 6.96
12.8	1.25	25.82	- 6.44	- 6.59	- 6.83	- 7.08
Average	5.14	36.35	- 5.61	- 6.01	- 6.26	- 6.57

Toxicity assessment

Toxicity evaluation results were summarized at Table 4. *V. fischeri* MB acute toxicity varied from 15.55 mg L^{-1} up to 18.64 mg L^{-1}, values that increased to 29.67 mg L^{-1} and 43.90 mg L^{-1} after zeolites adsorption, meaning a 2.35 times less toxic solution, after treatment.

The MB EC$_{50}$ (%, 48 h) values obtained for *D. similis* were 0.16 mg L^{-1} up to 0.43 mg L^{-1}. After zeolites adsorption treatment these values were 26.10 mg L^{-1} up to 47.80 mg L^{-1}. The efficacies for acute toxicity removal for bacteria and for Daphnis were on average 55.42 % and 99.18 %, respectively. Although *D. similis* response was very sensitive to methylene blue, after the zeolite adsorption the solution reduced substantially its harmful effects.

Results from solid waste classification tests showed that dye-saturated zeolite was considered neither corrosive nor reagent, according to ABNT norms. It was classified as non-inert waste, based on NBR 10004/2004 (Class II A, non-dangerous/non-inert) due to the presence of presence of heavy metals exceeding the maximum limit allowed [24].

Orbital Elec. J. Chem., Campo Grande, 2(3): 235-247, 2010

245

The residual fly ash fraction of zeolitic material contains an amount of readily leachable material deposited during cooling after combustion.

Table 4. Efficacy of zeolite adsorption for MB acute toxicity removal

EC_{50} Untreated (15 min, % v/v)	EC_{50} adsorved (15 min, % v/v)	TU Untreated	TU adsorved	Removal (%)
17.23 (*)	34.74	5.80	2.87	50.51
18.64 (*)	43.90	5.36	2.27	57.65
16.58 (*)	39.50	6.03	2.51	58.37
0.190 (**)	26.10	526	3.83	99.27
0.160(**)	47.80	625	2.09	99.66
0.430 (**)	31.47	233	3.17	98.63

(*) 15 min - *V. fischeri*; (**) 48h - *D.similis*

Conclusion

The present study showed that zeolite synthesized from fly ash can be used as an effective adsorbent for the removal of methylene blue dye from aqueous solution. It is observed from the experiments that about 80-94% removal is possible. The equilibrium data followed Temkin isotherm. The coal fly ash based adsorbent may be an alternative to more costly adsorbents for the treatment of aqueous waste containing methylene blue. Both lived-organisms evidenced that the proposed treatment resulted in a less toxic liquid residue. Yet, most importantly the results of this investigation demonstrated the great significance of toxicological assays associated with decolorization experiments.

Acknowledgements

References and Notes

[1]   Alcântara, M. R.; Daltin, D. *Quim Nova* **1996**, 19, 320.

[2]   Guaritini, C. C. I.; Zanoni, M. V. B. *Quim Nova* **2000**, 23, 71.

[3]   Zanoni, M. V.B.; Carneiro, P. A. *Ciência Hoje* **2001**, 29, 61.

[4]   Zollinger, H.; Colour Chemistry—Synthesis, Properties and Application of Organic Dyes and Pigment, New York: Willey-VCH, 2003.

[5]   Almeida, C.A.P.; Debacher, N. A.; Downsc, A. J.; Cotteta, L.; Mello, C. A. D. *J. Colloid Interface Sci.* **2009**, *332*, 46.

[6]   Gupta V. K.; Carrott, P. J. M.; Ribeiro-Carrot, M. M. L.; Suhas. *Crit. Rev. Environ. Sci. Technol.* **2009**, *39,* 783.

[7]   Bhatnagar, A.; Sillanpää, M. *Chem. Eng. J.* **2010**, *157*, 277.

[8]   Holler, H.; Wirsching, U. *Fortschr. Miner.* **1985**, *63*, 21.

[9]   Henmi, T. *Clay Sci*. **1987**, *6,* 277.

[10] Querol, X.; Alastuey, A.; Lopez-Soler, A.; Andres, J. M.; Juan, R.; Ferrer, P.; Ruiz,

C. R. *Environ. Sci.Technol*. **1997**, *31*, 2527.

[11] Shigemoto, N.; Hayashi, H.; Miyaura, K. *J. Mater. Sci.* **1993**, *28*, 4781.

[12] Querol, X.; Moreno, N.; Umaña, J. C.; Alastuey, A.; Hernández, E.; López-Soler A.; Plana, F. *Int. J. Coal Geol.* **2002,** *50,* 413.

[13] Rayalu, S. S.; Bansiwal, A. K.; Meshram, S. U.; Labhsetwar, N.; Devotta, S. *Catal. Sur. Asia* **2006**, *10*, 74.

[14] Fungaro, D. A.; Silva, M. G. *Quim. Nova* **2002,** *25,* 1081.

[15] Fungaro, D. A.; Flues, M. S-M; Celebroni, A. P. *Quim. Nova* **2004**, *27*, 582.

[16] Fungaro D. A.; Izidoro, J. C. *Quim. Nova* **2006,** *29,* 735.

[17] Fungaro, D. A.; Izidoro, J. C.; Almeida, R. S.; *Eclética Quim.* **2005**, *30*, 31.

[18] Fungaro, D. A.; Bruno, M., Grosche, L. C. *Desalin. Water Treat*. **2009**, *2*, 231.

[19] Ghosk, D.; Bhattacharyya, K. G. *Appl. Clay Sci.* **2002**, *20*, 295.

[20] Borrely, S. I.; Gonçalves, A .A.; Oikawa, H.; Duarte, C. L.; Rocha, F. R. *Radiat. Phys. Chem*. **2004**, *71*, 455.

[21] CETESB-COMPANHIA DE TECNOLOGIA DE SANEAMENTO AMBIENTAL. Relatório de qualidade das águas interiores do estado de São Paulo. Documento sem os anexos. São Paulo: CETESB, 2007. 521 p. Available from: http://www.cetesb.sp.gov.br/Agua/rios/publicacoes.asp. Acess March 2009.

[22] ABNT NBR 12713. Ecotoxicologia aquática - Toxicidade aguda - método de ensaio com *Daphnia spp* (*Cladocera, Crustacea*). São Paulo: ABNT, 2004. 21 p.

[23] ABNT NBR-15411-2. Ecotoxicologia aquática – Determinação do efeito inibitório de amostras de água sobre a emissão de luz de *Vibrio fischeri* (Ensaio de bactéria luminescente)*.* Parte 2 - Método utilizando bactérias desidratadas*,* 2006.

[24] NBR 10004 2004. Resíduos sólidos – Classificação. Rio de Janeiro.

[25] NBR 10005, 2004. Procedimento para obtenção de extrato lixiviado de resíduos sólidos. Rio de Janeiro.

[26] NBR 10006, 2004. Procedimento para obtenção de extrato solubilizado de resíduos sólidos. Riode Janeiro.

[27] ASTM standard specification for coal fly ash and raw or calcined natural pozzolan for use in concrete (C618-05). *Annual book of ASTM standards, concrete and aggregates*; American Society for Testing Materials: ASTM International, West Conshohocken, PA, 2005; Vol. 04.02

[28] Levandowski J.; Kalkreuth, W. *Int. J. Coal Geol.* **2009**, *77*, 269.

[29] White, S. C.; Case, E. D. *J. Mater. Sci.* **1990**, *25*, 5215.

[30] Covarrubias, C.; Garcia, R.; Arriagada, R.; Yanez, J.; Garland, M. T. *Microp. Mesop. Mat.* **2006**, *88*, 220.

[31] Varshney, K. G.; Khan, A. A.; Gupta, U.; Maheshwari, S. M. *Colloids Surf.* **1996**, *A133*, 19.

[32] Giles, C. H.; MacEwan, T. H.; Nakhwa, S. N.; Smith, D. *J. Chem. Soc. London* **1960,** 3973.

[33] Wang, S.; Li, H.; Xu, L. *J. Colloid Interface Sci*. **2006**, *295*, 71.

247

Orbital Elec. J. Chem., Campo Grande, 2(3): 235-247, 2010

Full Paper

Synthesis, antibacterial and antifungal activity of pyrazolyl-quinazolin-4(3*H*)-one derivatives

Navin B. Patel[a]*, Jaymin C. Patel[a], Sarvil D. Patel[a] and Gaman G. Barat[b]

[a]Department of Chemistry, Veer Narmad South Gujarat University, Surat 395007, Gujarat, India
[b]Department of Chemistry, Art's, Science and Commerce College, Pilvai (N.G.) 382850, Gujarat, India

ABSTRACT: *A series of pyrazolyl-quinazolin-4(3H)-ones* **6a-m** *have been synthesized from 2-[2-(phenylamino)phenyl]acetic acid by using efficient methods. An acid chloride of 2-[2-(phenylamino)phenyl]acetic acid on cyclization reaction with 5-iodo anthranilic acid yielded benzoxazinone* **2**, *which on condensation reaction with hydrazine hydrate afforded quinazolin-4(3H)-one* **3**. *Acetylation of compound* **3** *and then condensation with aromatic aldehydes led to the formation of chalcones* **5a-m** *which on subjected to reaction with phenyl hydrazine yielded the desired compounds* **6a-m**. *All the synthesized componds have been characterized by elemental analyses, IR and NMR spectra data. The title compounds have been screened against bacterial as well as fungal microorganisms. The potency of these compounds was calculated and compared with standard drugs i.e. Penicillin-G and Fluconazole. Some of the compounds showed very good antimicrobial activity.*

Keywords: *antimicrobial activity; chalcone; pyrazole; quinazolin-4(3H)-one*

Introduction

There are wide varieties of heterocycles which have been explored for developing biologically important molecules. Quinazolin-4(3*H*)-one have emerged as an important class of nitrogenated heterocycle that have attached synthetic interest because they possess pharmacological and therapeutic properties. Various quinazolin-4(3*H*)-one derivatives possess antibacterial, antifungal, analgesic, anti-inflammatory, anticonvulsant, anti HIV, antitubercular, anticancer, antiviral, CNS depressant, diuretic and hypolipidemic activities [1-9]. The large number of synthetic compounds with pyrazoline nucleus played a vital role in medicinal chemistry. These compounds are

---

* Corresponding author. E-mail: drnavin@satyam.net.in

known for their antibacterial, antifungal, antimycobacterial, analgesic, anti-inflammatory, anticancer, antiamoebic, molluscicidal, antinociceptive, antidepressant, anticonvulsant and antiviral activities [10-18]. Furthermore quinazolin-4(3*H*)-one incorporating pyrazoline nucleus possesses antitumor and antidiabetic activity [19]. Its halogenated derivatives showed potential antihyperlipidemic activity with no significant toxic side effects. There are broad spectrums of therapeutic properties of pyrazoline with quinazolin-4(3*H*)-one for the pharmacological activities.

In view of these important considerations, we report here synthesis of pyrazolyl-quinazolin-4(3*H*)-one, involves the base-catalyzed condensation of acetamido quinazolin-4(3*H*)-one with aromatic aldehydes to chalcones [18], which on subsequently undergoes cyclization reaction with phenyl hydrazine [17] led to the formation of the desired compounds. The title compounds were screened for their antibacterial and antifungal activities *in vitro*. The potency [20] of the respective compounds was calculated and compared with standard drugs.

Material and Methods

The Melting points were determined in open capillary tubes and are uncorrected. The IR spectra of the synthesized compounds were recorded on Perkin Elmer 1300 FTIR spectrometer using KBr pellets and frequencies are recorded in cm^{-1}. ^{1}H NMR and ^{13}C NMR spectra were recorded on Bruker Avance II 400 NMR spectrometer using CDCl$_3$ as a solvent. The chemical shifts are reported in (δ ppm) downfield from tetramethylsilane (TMS). Elemental analyses of newly synthesized compounds were carried out on Carlo Erba 1108 analyzer**.** The purities of all the compounds were checked by TLC on Merck silica gel 60 F254 using toluene: ethylacetate (8:2) as mobile phase and spots were visualized under UV radiation. 2-[2-(Phenylamino)phenyl]acetyl chloride **1** was synthesized by the literature procedure [21].

Synthesis of 6-iodo-2-[2-(phenylamino)benzyl]-4H-3,1-benzoxazin-4-one (2)

A mixture of 2-[2-(phenylamino)phenyl]acetyl chloride **1** (0.01 mol) and 5-iodo anthranilic acid (0.01 mol) in dry pyridine (20 mL) was stirred at 0-5 ºC for 1 h, further stirred for 1 h at room temperature. After completion of reaction, a pasty mass obtained, was washed thoroughly with sodium bicarbonate (5% w/v) to remove unreacted acid. A solid separated was filtered, dried and recrystallized from methanol. Yield: 65%, m.p. 287-290 °C; IR (KBr): 3441 (NH), 2926, 2854 (CH$_2$), 1745 (C=O), 1613 (C=N), 1145 (C-O), 617 (C-I) cm^{-1}; ^{1}H NMR (400 MHz, CDCl$_3$): δ 3.54 (s, 2H, CH$_2$), 6.37-8.18 (m, 12H, Ar-H), 9.15 (bs, 1H, NH); Anal. Calcd for C$_{21}$H$_{15}$IN$_2$O$_2$: C, 55.52; H, 3.33; N, 6.17. Found: C, 55.38; H, 3.26; N, 6.05%.

Synthesis of 3-Amino-6-iodo-2-[2-(phenylamino)benzyl]quinazolin-4(3H)-one

249

Orbital Elec. J. Chem., Campo Grande, 2(3): 248-262, 2010

(3)

A mixture of compound **2** (0.01 mol) and hydrazine hydrate (0.02 mol) in absolute ethanol (25 mL) was refluxed on water bath for 6-8 h. After completion of the reaction, it was slowly poured onto crushed ice cold water with continuous stirring. The solid thus obtained was filtered and washed several times with cold water. The crude product was dried and recrystallized from ethanol. Yield: 73%, m.p. 152-155 °C; IR (KBr): 3512-3394 (NH and NH_2), 2932, 2856 (CH_2), 1724 (C=O), 1610 (C=N), 612 (C-I) cm^{-1}; ^{1}H NMR (400 MHz, CDCl$_3$): δ 3.55 (s, 2H, CH_2), 5.74 (bs, 2H, NH_2), 6.38-8.18 (m, 12H, Ar-H), 9.16 (bs, 1H, NH); Anal. Calcd for $C_{21}H_{17}IN_4O$: C, 53.86; H, 3.66; N, 11.96. Found: C, 53.74; H, 3.57; N, 11.85%.

Synthesis of N-{6-iodo-4-oxo-2-[2-(phenylamino)benzyl]quinazolin-3(4H)-yl} acetamide (4)

To the solution of compound **3** (0.01 mol) in dry benzene (50 mL), acetyl chloride (0.01 mol) was added drop by drop at 0-5 °C over the period of 1 h with continuous shaking. After completion of the addition, the reaction mixture kept over night. The excess of solvent was distilled off under reduced pressure and then poured onto ice and shake well, the solid thus obtained was filtered and recrystallized from methanol. Yield: 70%, m.p. 185-188 °C; IR (KBr): 3452 (NH), 2929, 2851 (CH_2), 1727 (C=O), 1651 (C=O of amide), 1615 (C=N), 619 (C-I) cm^{-1}; ^{1}H NMR (400 MHz, CDCl$_3$): δ 2.24 (s, 3H, CH_3), 3.54 (s, 2H, CH_2), 6.37-8.18 (m, 12H, Ar-H), 9.15 (bs, 1H, NH), 10.35 (bs, 1H, NH); Anal. Calcd for $C_{23}H_{19}IN_4O_2$: C, 54.13; H, 3.75; N, 10.98. Found: C, 54.02; H, 3.68; N, 10.86 %.

General procedure for the synthesis of acrylamido-quinazolin-4(3H)-ones (5a-m)

To the solution of compound **4** (0.01 mol) in absolute ethanol (50 mL), substituted aromatic aldehydes (0.01 mol) in 2% NaOH was added and refluxed for 10-12 h. After completed the reaction, it was concentrated, cooled and poured onto ice. The solid thus obtained was filtered, washed with water and recrystallized from methanol.

6-Iodo-2-[2-(phenylamino)benzyl]-3-(phenylacrylamido)-quinazolin-4(3H)-one **(5a)**

Yield: 72%, m.p. 176-178 °C; IR (KBr): 3437 (NH), 2918, 2849 (CH_2), 1719 (C=O), 1664 (C=O), 1613 (C=N), 1576 (CH=CH), 623 (C-I) cm^{-1}; ^{1}H NMR (400 MHz, CDCl$_3$): δ 3.55 (s, 2H, CH_2), 6.37-8.18 (m, 17H, Ar-H), 6.77 (d, 1H, J = 16.6 Hz, =CHCO), 7.62 (d, 1H, J = 16.6 Hz, =CH-Ar), 8.85 (bs, 1H, CONH), 9.17 (bs, 1H, NH); ^{13}C NMR (100 MHz, CDCl$_3$): δ 30.57 (CH_2), 112.52-148.64 (26C, CH=CH and Ar-C), 162.14 (C=O), 168.11 (C=N), 173.24 (CONH); Anal. Calcd for $C_{30}H_{23}IN_4O_2$: C, 60.21; H, 3.87; N, 9.36. Found: C, 60.07; H, 3.78; N, 9.23%.

Orbital Elec. J. Chem., Campo Grande, 2(3): 248-262, 2010

250

6-Iodo-2-[2-(phenylamino)benzyl]-3-(2-hydroxyphenylacrylamido)-quinazolin-4(3H)-one (5b)

Yield: 66%, m.p. 164-167 °C; IR (KBr): 3546 (OH), 3442 (NH), 2924, 2850 (CH$_2$), 1722 (C=O), 1658 (C=O), 1615 (C=N), 1568 (CH=CH), 620 (C-I) cm^{-1}; ^{1}H NMR (400 MHz, CDCl$_3$): δ 3.54 (s, 2H, CH$_2$), 6.36-8.17 (m, 16H, Ar-H), 6.79 (d, 1H, *J* = 16.2 Hz, =CHCO), 7.57 (d, 1H, *J* = 16.2 Hz, =CH-Ar), 8.82 (bs, 1H, CONH), 9.16 (bs, 1H, NH), 10.36 (bs, 1H, OH); ^{13}C NMR (100 MHz, CDCl$_3$): δ 30.43 (CH$_2$), 112.17-155.69 (26C, CH=CH and Ar-C), 161.76 (C=O), 168.42 (C=N), 173.34 (CONH); Anal. Calcd for C$_{30}$H$_{23}$IN$_4$O$_3$: C, 58.64; H, 3.77; N, 9.12. Found: C, 58.55; H, 3.69; N, 9.18%.

6-Iodo-2-[2-(phenylamino)benzyl]-3-(3-hydroxyphenylacrylamido)-quinazolin-4(3H)-one (5c)

Yield: 71%, m.p. 178-181 °C; IR (KBr): 3539 (OH), 3454 (NH), 2932, 2856 (CH$_2$), 1725 (C=O), 1662 (C=O), 1616 (C=N), 1577 (CH=CH), 617 (C-I) cm^{-1}; ^{1}H NMR (400 MHz, CDCl$_3$): δ 3.56 (s, 2H, CH$_2$), 5.57 (bs, 1H, OH), 6.37-8.18 (m, 16H, Ar-H), 6.78 (d, 1H, *J* = 16.4 Hz, =CHCO), 7.60 (d, 1H, *J* = 16.4 Hz, =CH-Ar), 8.84 (bs, 1H, CONH), 9.17 (bs, 1H, NH); ^{13}C NMR (100 MHz, CDCl$_3$): δ 30.76 (CH$_2$), 112.08-159.27 (26C, CH=CH and Ar-C), 162.18 (C=O), 168.26 (C=N), 172.88 (CONH); Anal. Calcd for C$_{30}$H$_{23}$IN$_4$O$_3$: C, 58.64; H, 3.77; N, 9.12. Found: C, 58.77; H, 3.85; N, 9.05%.

6-Iodo-2-[2-(phenylamino)benzyl]-3-(4-hydroxyphenylacrylamido)-quinazolin-4(3H)-one (5d)

Yield: 78%, m.p. 193-196 °C; IR (KBr): 3552 (OH), 3445 (NH), 2934, 2853 (CH$_2$), 1720 (C=O), 1655 (C=O), 1609 (C=N), 1569 (CH=CH), 625 (C-I) cm^{-1}; ^{1}H NMR (400 MHz, CDCl$_3$): δ 3.58 (s, 2H, CH$_2$), 5.59 (bs, 1H, OH), 6.36-8.16 (m, 16H, Ar-H), 6.81 (d, 1H, *J* = 16.6 Hz, =CHCO), 7.62 (d, 1H, *J* = 16.6 Hz, =CH-Ar), 8.82 (bs, 1H, CONH), 9.16 (bs, 1H, NH); ^{13}C NMR (100 MHz, CDCl$_3$): δ 30.36 (CH$_2$), 112.31-157.29 (26C, CH=CH and Ar-C), 161.98 (C=O), 167.93 (C=N), 173.22 (CONH); Anal. Calcd for C$_{30}$H$_{23}$IN$_4$O$_3$: C, 58.64; H, 3.77; N, 9.12. Found: C, 58.56; H, 3.71; N, 9.23%.

6-Iodo-3-(2-chlorophenylacrylamido)-2-[2-(phenylamino)benzyl]quinazolin-4(3H)-one (5e)

Yield: 63%, m.p. 159-162 °C; IR (KBr): 3440 (NH), 2921, 2846 (CH$_2$), 1726 (C=O), 1653 (C=O), 1611 (C=N), 1581 (CH=CH), 742 (C-Cl), 618 (C-I) cm^{-1}; ^{1}H NMR (400 MHz, CDCl$_3$): δ 3.57 (s, 2H, CH$_2$), 6.37-8.17 (m, 16H, Ar-H), 6.78 (d, 1H, *J* = 16.4 Hz, =CHCO), 7.59 (d, 1H, *J* = 16.4 Hz, =CH-Ar), 8.79 (bs, 1H, CONH), 9.14 (bs, 1H, NH); ^{13}C NMR (100 MHz, CDCl$_3$): δ 30.18 (CH$_2$), 111.91-148.59 (26C, CH=CH and Ar-C), 162.06 (C=O), 168.35 (C=N), 173.42 (CONH); Anal. Calcd for C$_{30}$H$_{22}$ClIN$_4$O$_2$: C, 56.93; H, 3.50; N, 8.85. Found: C, 56.79; H, 3.62; N, 8.73%.

251

Orbital Elec. J. Chem.*, Campo Grande,* 2(3): 248-262, 2010

6-Iodo-3-(3-chlorophenylacrylamido)-2-[2-(phenylamino)benzyl]quinazolin-4(3H)-one (5f)

Yield: 61%, m.p. 171-174 °C; IR (KBr): 3454 (NH), 2928, 2853 (CH$_2$), 1718 (C=O), 1660 (C=O), 1607 (C=N), 1575 (CH=CH), 755 (C-Cl), 612 (C-I) cm^{-1}; ^{1}H NMR (400 MHz, CDCl$_3$): δ 3.54 (s, 2H, CH$_2$), 6.36-8.18 (m, 16H, Ar-H), 6.82 (d, 1H, *J* = 16.4 Hz, =CHCO), 7.62 (d, 1H, *J* = 16.4 Hz, =CH-Ar), 8.77 (bs, 1H, CONH), 9.15 (bs, 1H, NH); ^{13}C NMR (100 MHz, CDCl$_3$): δ 30.36 (CH$_2$), 112.24-148.25 (26C, CH=CH and Ar-C), 161.76 (C=O), 167.86 (C=N), 173.21 (CONH); Anal. Calcd for C$_{30}$H$_{22}$ClIN$_4$O$_2$: C, 56.93; H, 3.50; N, 8.85. Found: C, 56.81; H, 3.42; N, 8.97%.

6-Iodo-3-(4-chlorophenylacrylamido)-2-[2-(phenylamino)benzyl]quinazolin-4(3H)-one (5g)

Yield: 68%, m.p. 195-197 °C; IR (KBr): 3444 (NH), 2930, 2856 (CH$_2$), 1716 (C=O), 1663 (C=O), 1611 (C=N), 1573 (CH=CH), 738 (C-Cl), 622 (C-I) cm^{-1}; ^{1}H NMR (400 MHz, CDCl$_3$): δ 3.57 (s, 2H, CH$_2$), 6.37-8.18 (m, 16H, Ar-H), 6.85 (d, 1H, *J* = 16.2 Hz, =CHCO), 7.60 (d, 1H, *J* = 16.2 Hz, =CH-Ar), 8.81 (bs, 1H, CONH), 9.17 (bs, 1H, NH); ^{13}C NMR (100 MHz, CDCl$_3$): δ 30.54 (CH$_2$), 112.32-148.57 (26C, CH=CH and Ar-C), 162.16 (C=O), 167.89 (C=N), 173.33 (CONH); Anal. Calcd for C$_{30}$H$_{22}$ClIN$_4$O$_2$: C, 56.93; H, 3.50; N, 8.85. Found: C, 57.08; H, 3.38; N, 8.69%.

6-Iodo-2-[2-(phenylamino)benzyl]-3-(2-nitrophenylacrylamido)-quinazolin-4(3H)-one (5h)

Yield: 76%, m.p. 205-210 °C; IR (KBr): 3452 (NH), 2933, 2855 (CH$_2$), 1724 (C=O), 1659 (C=O), 1614 (C=N), 1580 (CH=CH), 1544, 1357 (NO$_2$), 619 (C-I) cm^{-1}; ^{1}H NMR (400 MHz, CDCl$_3$): δ 3.56 (s, 2H, CH$_2$), 6.38-8.19 (m, 16H, Ar-H), 6.83 (d, 1H, *J* = 16 Hz, =CHCO), 7.62 (d, 1H, *J* = 16 Hz, =CH-Ar), 8.84 (bs, 1H, CONH), 9.16 (bs, 1H, NH); ^{13}C NMR (100 MHz, CDCl$_3$): δ 30.32 (CH$_2$), 111.82-150.48 (26C, CH=CH and Ar-C), 162.29 (C=O), 168.06 (C=N), 172.94 (CONH); Anal. Calcd for C$_{30}$H$_{22}$IN$_5$O$_4$: C, 56.00; H, 3.45; N, 10.88. Found: C, 55.86; H, 3.56; N, 10.75%.

6-Iodo-2-[2-(phenylamino)benzyl]-3-(3-nitrophenylacrylamido)-quinazolin-4(3H)-one (5i)

Yield: 67%, m.p. 225-228 °C; IR (KBr): 3457 (NH), 2928, 2850 (CH$_2$), 1729 (C=O), 1654 (C=O), 1612 (C=N), 1578 (CH=CH), 1535, 1353 (NO$_2$), 611 (C-I) cm^{-1}; ^{1}H NMR (400 MHz, CDCl$_3$): δ 3.53 (s, 2H, CH$_2$), 6.37-8.40 (m, 16H, Ar-H), 6.82 (d, 1H, *J* = 16.2 Hz, =CHCO), 7.65 (d, 1H, *J* = 16.2 Hz, =CH-Ar), 8.86 (bs, 1H, CONH), 9.17 (bs, 1H, NH); ^{13}C NMR (100 MHz, CDCl$_3$): δ 30.24 (CH$_2$), 112.17-150.58 (26C, CH=CH and Ar-C), 161.87 (C=O), 168.15 (C=N), 173.06 (CONH); Anal. Calcd for C$_{30}$H$_{22}$IN$_5$O$_4$: C, 56.00; H, 3.45; N, 10.88. Found: C, 56.17; H, 3.52; N, 10.81%.

252

Orbital Elec. J. Chem., Campo Grande, 2(3): 248-262, 2010

6-Iodo-2-[2-(phenylamino)benzyl]-3-(4-nitrophenylacrylamido)-quinazolin-4(3H)-one **(5j)**

Yield: 65%, m.p. 243-245 °C; IR (KBr): 3443 (NH), 2927, 2852 (CH$_2$), 1722 (C=O), 1659 (C=O), 1608 (C=N), 1582 (CH=CH), 1540, 1361 (NO$_2$), 614 (C-I) cm^{-1}; ^{1}H NMR (400 MHz, CDCl$_3$): δ 3.55 (s, 2H, CH$_2$), 6.36-8.17 (m, 16H, Ar-H), 6.80 (d, 1H, *J* = 16.4 Hz, =CHCO), 7.61 (d, 1H, *J* = 16.4 Hz, =CH-Ar), 8.83 (bs, 1H, CONH), 9.18 (bs, 1H, NH); ^{13}C NMR (100 MHz, CDCl$_3$): δ 30.56 (CH$_2$), 112.27-148.32 (26C, CH=CH and Ar-C), 162.25 (C=O), 168.03 (C=N), 173.24 (CONH); Anal. Calcd for C$_{30}$H$_{22}$IN$_5$O$_4$: C, 56.00; H, 3.45; N, 10.88. Found: C, 55.89; H, 3.38; N, 10.96%.

6-Iodo-2-[2-(phenylamino)benzyl]-3-(2-methoxyphenylacrylamido)-quinazolin-4(3H)-one **(5k)**

Yield: 67%, m.p. 155-158 °C; IR (KBr): 3454 (NH), 2926, 2847 (CH$_2$), 1725 (C=O), 1661 (C=O), 1612 (C=N), 1584 (CH=CH), 1249, 1103 (C-O-C), 625 (C-I) cm^{-1}; ^{1}H NMR (400 MHz, CDCl$_3$): δ 3.54 (s, 2H, CH$_2$), 3.66 (s, 3H, OCH$_3$), 6.37-8.17 (m, 16H, Ar-H), 6.82 (d, 1H, *J* = 16 Hz, =CHCO), 7.64 (d, 1H, *J* = 16 Hz, =CH-Ar), 8.78 (bs, 1H, CONH), 9.14 (bs, 1H, NH); ^{13}C NMR (100 MHz, CDCl$_3$): δ 30.46 (CH$_2$), 61.23 (OCH$_3$), 112.12-156.44 (26C, CH=CH and Ar-C), 162.38 (C=O), 167.89 (C=N), 173.32 (CONH); Anal. Calcd for C$_{31}$H$_{25}$IN$_4$O$_3$: C, 59.25; H, 4.01; N, 8.91. Found: C, 59.17; H, 3.96; N, 8.83%.

6-Iodo-2-[2-(phenylamino)benzyl]-3-(4-methoxyphenylacrylamido)-quinazolin-4(3H)-one **(5l)**

Yield: 70%, m.p. 170-174°C; IR (KBr): 3443 (NH), 2924, 2853 (CH$_2$), 1715 (C=O), 1655 (C=O), 1614 (C=N), 1582 (CH=CH), 1241, 1105 (C-O-C), 617 (C-I) cm^{-1}; ^{1}H NMR (400 MHz, CDCl$_3$): δ 3.55 (s, 2H, CH$_2$), 3.64 (s, 3H, OCH$_3$), 6.37-8.18 (m, 16H, Ar-H), 6.79 (d, 1H, *J* = 16.4 Hz, =CHCO), 7.58 (d, 1H, *J* = 16.4 Hz, =CH-Ar), 8.76 (bs, 1H, CONH), 9.15 (bs, 1H, NH); ^{13}C NMR (100 MHz, CDCl$_3$): δ 30.62 (CH$_2$), 59.56 (OCH$_3$), 111.76-158.45 (26C, CH=CH and Ar-C), 161.82 (C=O), 167.88 (C=N), 173.19 (CONH); Anal. Calcd for C$_{31}$H$_{25}$IN$_4$O$_3$: C, 59.25; H, 4.01; N, 8.91. Found: C, 59.12; H, 4.11; N, 8.85%.

6-Iodo-2-[2-(phenylamino)benzyl]-3-(4-dimethylaminophenylacrylamido)-quinazolin-4(3H)-one **(5m)**

Yield: 72%, m.p. 144-148 °C; IR (KBr): 3448 (NH), 2935, 2860 (CH$_2$), 1717 (C=O), 1662 (C=O), 1618 (C=N), 1585 (CH=CH), 611 (C-I) cm^{-1}; ^{1}H NMR (400 MHz, CDCl$_3$): δ 2.86 (s, 6H, N(CH$_3$)$_2$), 3.56 (s, 2H, CH$_2$), 6.38-8.18 (m, 16H, Ar-H), 6.81 (d, 1H, *J* = 16.6 Hz, =CHCO), 7.62 (d, 1H, *J* = 16.6 Hz, =CH-Ar), 8.78 (bs, 1H, CONH), 9.16 (bs, 1H, NH); ^{13}C NMR (100 MHz, CDCl$_3$): δ 30.45 (CH$_2$), 46.72 (N-(CH$_3$)$_2$), 111.92-

253

Orbital Elec. J. Chem., Campo Grande, 2(3): 248-262, 2010

150.22 (26C, CH=CH and Ar-C), 162.17 (C=O), 168.27 (C=N), 172.86 (CONH); Anal. Calcd for $C_{32}H_{28}IN_5O_2$: C, 59.91; H, 4.40; N, 10.92. Found: C, 59.76; H, 4.28; N, 10.78%.

General procedure for the synthesis of pyrazolyl-quinazolin-4(3H)-ones (6a-m)

A mixture of compound **5a** (0.01 mol), phenyl hydrazine (0.01 mol) in absolute methanol (30 mL) was added few drops of glacial acetic acid and refluxed for 8-10 h. After completion of the reaction, excess of solvent was distilled off; the separated solid was filtered, washed with water and recrystallized from methanol. Similarly other pyrazol derivatives 6b-m were synthesized.

*6-Iodo-2-[2-(phenylamino)benzyl]-3-(1,5-diphenyl-4,5-dihydro-1H-pyrazol-3-yl-amino)quinazolin-4(3H)-one **(6a)***

Yield: 65%, m.p. 104-106 °C; IR (KBr): 3444 (NH), 2926, 2854 (CH$_2$), 1728 (C=O), 1613 (C=N), 615 (C-I) cm^{-1}; ^{1}H NMR (400 MHz, CDCl$_3$): δ 3.02 (dd, 1H, J_{ab} = 17.4 Hz, J_{ax} = 5.6 Hz, Ha), 3.46 (dd, 1H, J_{ba} = 17.4 Hz, J_{bx} = 12.2 Hz, Hb), 3.56 (s, 2H, CH$_2$), 5.47 (dd, 1H, J_{xb} = 12.2 Hz, J_{xa} = 5.6 Hz, Hx), 6.36-8.18 (m, 22H, Ar-H), 8.34 (bs, 1H, NH), 9.17 (bs, 1H, NH); ^{13}C NMR (100 MHz, CDCl$_3$): δ 30.48 (CH$_2$), 36.42 (CH$_2$ of pyrazole), 55.56 (CH of pyrazole), 112.45-148.67 (30C, Ar-C), 161.16 (C=N of pyrazole), 162.14 (C=O), 168.23 (C=N); Anal. Calcd for $C_{36}H_{29}IN_6O$: C, 62.80; H, 4.25; N, 12.21. Found: C, 62.63; H, 4.17; N, 12.09%.

*6-Iodo-2-[2-(phenylamino)benzyl]-3-[5-(2-hydroxyphenyl)-1-phenyl-4,5-dihydro-1H-pyrazol-3-yl-amino]quinazolin-4(3H)-one **(6b)***

Yield: 70%, m.p. 137-140 °C; IR (KBr): 3538 (OH), 3443 (NH), 2924, 2851 (CH$_2$), 1726 (C=O), 1608 (C=N), 619 (C-I) cm^{-1}; ^{1}H NMR (400 MHz, CDCl$_3$): δ 3.03 (dd, 1H, J_{ab} = 17.6 Hz, J_{ax} = 5.4 Hz, Ha), 3.46 (dd, 1H, J_{ba} = 17.6 Hz, J_{bx} = 11.8 Hz, Hb), 3.54 (s, 2H, CH$_2$), 5.51 (dd, 1H, J_{xb} = 11.8 Hz, J_{xa} = 5.4 Hz, Hx), 6.36-8.17 (m, 21H, Ar-H), 8.43 (bs, 1H, NH), 9.16 (bs, 1H, NH), 10.35 (bs, 1H, OH); ^{13}C NMR (100 MHz, CDCl$_3$): δ 30.56 (CH$_2$), 35.37 (CH$_2$ of pyrazole), 55.72 (CH of pyrazole), 112.15-155.82 (30C, Ar-C), 161.28 (C=N of pyrazole), 161.89 (C=O), 168.34 (C=N); Anal. Calcd for $C_{36}H_{29}IN_6O_2$: C, 61.37; H, 4.15; N, 11.93. Found: C, 61.26; H, 4.11; N, 11.85%.

*6-Iodo-2-[2-(phenylamino)benzyl]-3-[5-(3-hydroxyphenyl)-1-phenyl-4,5-dihydro-1H-pyrazol-3-yl-amino]quinazolin-4(3H)-one **(6c)***

Yield: 67%, m.p. 148-152 °C; IR (KBr): 3547 (OH), 3454 (NH), 2926, 2853 (CH$_2$), 1732 (C=O), 1614 (C=N), 621 (C-I) cm^{-1}; ^{1}H NMR (400 MHz, CDCl$_3$): δ 3.05 (dd, 1H, J_{ab} = 17.8 Hz, J_{ax} = 5.6 Hz, Ha), 3.48 (dd, 1H, J_{ba} = 17.8 Hz, J_{bx} = 12.4 Hz, Hb), 3.56 (s, 2H, CH$_2$), 5.52 (dd, 1H, J_{xb} = 12.4 Hz, J_{xa} = 5.6 Hz, Hx), 5.58 (bs, 1H, OH), 6.37-8.18 (m, 21H, Ar-H), 8.41 (bs, 1H, NH), 9.14 (bs, 1H, NH); ^{13}C NMR (100 MHz,

254

Orbital Elec. J. Chem., Campo Grande, 2(3): 248-262, 2010

CDCl$_3$): δ 30.32 (CH$_2$), 36.26 (CH$_2$ of pyrazole), 54.87 (CH of pyrazole), 112.46-159.58 (30C, Ar-C), 161.07 (C=N of pyrazole), 162.22 (C=O), 168.14 (C=N); Anal. Calcd for C$_{36}$H$_{29}$IN$_6$O$_2$: C, 61.37; H, 4.15; N, 11.93. Found: C, 61.28; H, 4.18; N, 11.98%.

6-Iodo-2-[2-(phenylamino)benzyl]-3-[5-(4-hydroxyphenyl)-1-phenyl-4,5-dihydro-1H-pyrazol-3-yl-amino]quinazolin-4(3H)-one (6d)

Yield: 68%, m.p. 161-164 °C; IR (KBr): 3555 (OH), 3446 (NH), 2930, 2849 (CH$_2$), 1723 (C=O), 1608 (C=N), 615 (C-I) cm^{-1}; ^{1}H NMR (400 MHz, CDCl$_3$): δ 3.07 (dd, 1H, J_{ab} = 17.6 Hz, J_{ax} = 5.4 Hz, Ha), 3.50 (dd, 1H, J_{ba} = 17.6 Hz, J_{bx} = 12 Hz, Hb), 3.57 (s, 2H, CH$_2$), 5.52 (dd, 1H, J_{xb} = 12 Hz, J_{xa} = 5.4 Hz, Hx), 5.59 (bs, 1H, OH), 6.36-8.18 (m, 21H, Ar-H), 8.39 (bs, 1H, NH), 9.16 (bs, 1H, NH); ^{13}C NMR (100 MHz, CDCl$_3$): δ 30.44 (CH$_2$), 36.51 (CH$_2$ of pyrazole), 55.35 (CH of pyrazole), 112.05-157.42 (30C, Ar-C), 161.24 (C=N of pyrazole), 162.13 (C=O), 168.02 (C=N); Anal. Calcd for C$_{36}$H$_{29}$IN$_6$O$_2$: C, 61.37; H, 4.15; N, 11.93. Found: C, 61.48; H, 4.23; N, 11.86%.

6-Iodo-3-[5-(2-chlorophenyl)-1-phenyl-4,5-dihydro-1H-pyrazol-3-yl-amino]-2-[2-(phenylamino)benzyl]quinazolin-4(3H)-one (6e)

Yield: 65%, m.p. 122-124 °C; IR (KBr): 3439 (NH), 2921, 2846 (CH$_2$), 1716 (C=O), 1613 (C=N), 742 (C-Cl), 624 (C-I) cm^{-1}; ^{1}H NMR (400 MHz, CDCl$_3$): δ 3.04 (dd, 1H, J_{ab} = 17.4 Hz, J_{ax} = 5.6 Hz, Ha), 3.49 (dd, 1H, J_{ba} = 17.4 Hz, J_{bx} = 12.2 Hz, Hb), 3.55 (s, 2H, CH$_2$), 5.47 (dd, 1H, J_{xb} = 12.2 Hz, J_{xa} = 5.6 Hz, Hx), 6.38-8.19 (m, 21H, Ar-H), 8.37 (bs, 1H, NH), 9.14 (bs, 1H, NH); ^{13}C NMR (100 MHz, CDCl$_3$): δ 30.16 (CH$_2$), 36.38 (CH$_2$ of pyrazole), 55.64 (CH of pyrazole), 112.23-148.79 (30C, Ar-C), 161.11 (C=N of pyrazole), 162.25 (C=O), 168.17 (C=N); Anal. Calcd for C$_{36}$H$_{28}$ClIN$_6$O: C, 59.80; H, 3.90; N, 11.62. Found: C, 59.69; H, 3.82; N, 11.54%.

6-Iodo-3-[5-(3-chlorophenyl)-1-phenyl-4,5-dihydro-1H-pyrazol-3-yl-amino]-2-[2-(phenylamino)benzyl]quinazolin-4(3H)-one (6f)

Yield: 71%, m.p. 119-123 °C; IR (KBr): 3447 (NH), 2924, 2850 (CH$_2$), 1719 (C=O), 1610 (C=N), 751 (C-Cl), 616 (C-I) cm^{-1}; ^{1}H NMR (400 MHz, CDCl$_3$): δ 3.02 (dd, 1H, J_{ab} = 17.6 Hz, J_{ax} = 5.6 Hz, Ha), 3.45 (dd, 1H, J_{ba} = 17.6 Hz, J_{bx} = 12 Hz, Hb), 3.53 (s, 2H, CH$_2$), 5.49 (dd, 1H, J_{xb} = 12 Hz, J_{xa} = 5.6 Hz, Hx), 6.37-8.18 (m, 21H, Ar-H), 8.41 (bs, 1H, NH), 9.17 (bs, 1H, NH); ^{13}C NMR (100 MHz, CDCl$_3$): δ 30.32 (CH$_2$), 36.55 (CH$_2$ of pyrazole), 55.74 (CH of pyrazole), 112.38-148.92 (30C, Ar-C), 161.29 (C=N of pyrazole), 162.41 (C=O), 167.84 (C=N); Anal. Calcd for C$_{36}$H$_{28}$ClIN$_6$O: C, 59.80; H, 3.90; N, 11.62. Found: C, 59.92; H, 3.96; N, 11.55%.

6-Iodo-3-[5-(4-chlorophenyl)-1-phenyl-4,5-dihydro-1H-pyrazol-3-yl-amino]-2-[2-(phenylamino)benzyl]quinazolin-4(3H)-one (6g)

Yield: 64%, m.p. 137-139 °C; IR (KBr): 3438 (NH), 2919, 2846 (CH$_2$), 1722

Orbital Elec. J. Chem*., Campo Grande,* 2(3): 248-262, 2010

255

(C=O), 1606 (C=N), 739 (C-Cl), 610 (C-I) cm^{-1}; ^{1}H NMR (400 MHz, CDCl$_3$): δ 3.05 (dd, 1H, J_{ab} = 17.8 Hz, J_{ax} = 5.4 Hz, Ha), 3.48 (dd, 1H, J_{ba} = 17.8 Hz, J_{bx} = 11.8 Hz, Hb), 3.56 (s, 2H, CH$_2$), 5.47 (dd, 1H, J_{xb} = 11.8 Hz, J_{xa} = 5.4 Hz, Hx), 6.38-8.17 (m, 21H, Ar-H), 8.38 (bs, 1H, NH), 9.16 (bs, 1H, NH); ^{13}C NMR (100 MHz, CDCl$_3$): δ 30.48 (CH$_2$), 36.33 (CH$_2$ of pyrazole), 55.52 (CH of pyrazole), 111.78-148.59 (30C, Ar-C), 161.44 (C=N of pyrazole), 162.57 (C=O), 168.16 (C=N); Anal. Calcd for C$_{36}$H$_{28}$ClIN$_6$O: C, 59.80; H, 3.90; N, 11.62. Found: C, 59.71; H, 3.87; N, 11.56%.

*6-Iodo-2-[2-(phenylamino)benzyl]-3-[5-(2-nitrophenyl)-1-phenyl-4,5-dihydro-1H-pyrazol-3-yl-amino]quinazolin-4(3H)-one **(6h)***

Yield: 70%, m.p. 143-146 °C; IR (KBr): 3455 (NH), 2930, 2854 (CH$_2$), 1728 (C=O), 1614 (C=N), 1552, 1365 (NO$_2$), 621 (C-I) cm^{-1}; ^{1}H NMR (400 MHz, CDCl$_3$): δ 3.01 (dd, 1H, J_{ab} = 17 Hz, J_{ax} = 5.2 Hz, Ha), 3.46 (dd, 1H, J_{ba} = 17 Hz, J_{bx} = 11.6 Hz, Hb), 3.54 (s, 2H, CH$_2$), 5.51 (dd, 1H, J_{xb} = 11.6 Hz, J_{xa} = 5.2 Hz, Hx), 6.37-8.17 (m, 21H, Ar-H), 8.42 (bs, 1H, NH), 9.14 (bs, 1H, NH); ^{13}C NMR (100 MHz, CDCl$_3$): δ 30.64 (CH$_2$), 36.57 (CH$_2$ of pyrazole), 55.82 (CH of pyrazole), 112.24-150.66 (30C, Ar-C), 161.28 (C=N of pyrazole), 162.23 (C=O), 168.36 (C=N); Anal. Calcd for C$_{36}$H$_{28}$IN$_7$O$_3$: C, 58.94; H, 3.85; N, 13.37. Found: C, 58.81; H, 3.76; N, 13.24%.

*6-Iodo-2-[2-(phenylamino)benzyl]-3-[5-(3-nitrophenyl)-1-phenyl-4,5-dihydro-1H-pyrazol-3-yl-amino]quinazolin-4(3H)-one **(6i)***

Yield: 73%, m.p. 156-160 °C; IR (KBr): 3460 (NH), 2934, 2852 (CH$_2$), 1733 (C=O), 1611 (C=N), 1541, 1358 (NO$_2$), 616 (C-I) cm^{-1}; ^{1}H NMR (400 MHz, CDCl$_3$): δ 3.03 (dd, 1H, J_{ab} = 17.4 Hz, J_{ax} = 5.6 Hz, Ha), 3.50 (dd, 1H, J_{ba} = 17.4 Hz, J_{bx} = 12.2 Hz, Hb), 3.55 (s, 2H, CH$_2$), 5.52 (dd, 1H, J_{xb} = 12.2 Hz, J_{xa} = 5.6 Hz, Hx), 6.36-8.39 (m, 21H, Ar-H), 8.45 (bs, 1H, NH), 9.18 (bs, 1H, NH); ^{13}C NMR (100 MHz, CDCl$_3$): δ 30.18 (CH$_2$), 36.42 (CH$_2$ of pyrazole), 55.58 (CH of pyrazole), 112.45-150.79 (30C, Ar-C), 161.09 (C=N of pyrazole), 162.12 (C=O), 168.23 (C=N); Anal. Calcd for C$_{36}$H$_{28}$IN$_7$O$_3$: C, 58.94; H, 3.85; N, 13.37. Found: C, 58.86; H, 3.78; N, 13.49%.

*6-Iodo-2-[2-(phenylamino)benzyl]-3-[5-(4-nitrophenyl)-1-phenyl-4,5-dihydro-1H-pyrazol-3-yl-amino]quinazolin-4(3H)-one **(6j)***

Yield: 69%, m.p. 173-176 °C; IR (KBr): 3439 (NH), 2924, 2852 (CH$_2$), 1727 (C=O), 1613 (C=N), 1550, 1367 (NO$_2$), 612 (C-I) cm^{-1}; ^{1}H NMR (400 MHz, CDCl$_3$): δ 3.02 (dd, 1H, J_{ab} = 17.2 Hz, J_{ax} = 5.2 Hz, Ha), 3.47 (dd, 1H, J_{ba} = 17.2 Hz, J_{bx} = 11.8 Hz, Hb), 3.57 (s, 2H, CH$_2$), 5.48 (dd, 1H, J_{xb} = 11.8 Hz, J_{xa} = 5.2 Hz, Hx), 6.37-8.17 (m, 21H, Ar-H), 8.42 (bs, 1H, NH), 9.16 (bs, 1H, NH); ^{13}C NMR (100 MHz, CDCl$_3$): δ 30.46 (CH$_2$), 36.57 (CH$_2$ of pyrazole), 55.72 (CH of pyrazole), 112.32-148.49 (30C, Ar-C), 161.17 (C=N of pyrazole), 162.36 (C=O), 168.34 (C=N); Anal. Calcd for C$_{36}$H$_{28}$IN$_7$O$_3$: C,

256

Orbital Elec. J. Chem., Campo Grande, 2(3): 248-262, 2010

58.94; H, 3.85; N, 13.37. Found: C, 59.02; H, 3.91; N, 13.52%.

*6-Iodo-2-[2-(phenylamino)benzyl]-3-[5-(2-methoxyphenyl)-1-phenyl-4,5-dihydro-1H-pyrazol-3-yl-amino]quinazolin-4(3H)-one **(6k)***

Yield: 70%, m.p. 122-124°C; IR (KBr): 3450 (NH), 2924, 2847 (CH$_2$), 1715 (C=O), 1609 (C=N), 1248, 1108 (C-O-C), 618 (C-I) cm^{-1}; ^{1}H NMR (400 MHz, CDCl$_3$): δ 3.05 (dd, 1H, J_{ab} = 17.8 Hz, J_{ax} = 5.6 Hz, Ha), 3.49 (dd, 1H, J_{ba} = 17.8 Hz, J_{bx} = 12.2 Hz, Hb), 3.54 (s, 2H, CH$_2$), 3.67 (s, 3H, OCH$_3$), 5.52 (dd, 1H, J_{xb} = 12.2 Hz, J_{xa} = 5.6 Hz, Hx), 6.38-8.19 (m, 21H, Ar-H), 8.44 (bs, 1H, NH), 9.14 (bs, 1H, NH); ^{13}C NMR (100 MHz, CDCl$_3$): δ 30.31 (CH$_2$), 36.42 (CH$_2$ of pyrazole), 55.53 (CH of pyrazole), 112.18-156.39 (30C, Ar-C), 161.03 (C=N of pyrazole), 162.21 (C=O), 167.83 (C=N); Anal. Calcd for C$_{37}$H$_{31}$IN$_6$O$_2$: C, 61.84; H, 4.35; N, 11.70. Found: C, 61.75; H, 4.31; N, 11.63%.

*6-Iodo-2-[2-(phenylamino)benzyl]-3-[5-(4-methoxyphenyl)-1-phenyl-4,5-dihydro-1H-pyrazol-3-yl-amino]quinazolin-4(3H)-one **(6l)***

Yield: 72%, m.p. 141-144 °C; IR (KBr): 3436 (NH), 2919, 2845 (CH$_2$), 1716 (C=O), 1610 (C=N), 1246, 1112 (C-O-C), 612 (C-I) cm^{-1}; ^{1}H NMR (400 MHz, CDCl$_3$): δ 3.01 (dd, 1H, J_{ab} = 17.6 Hz, J_{ax} = 5.4 Hz, Ha), 3.49 (dd, 1H, J_{ba} = 17.6 Hz, J_{bx} = 11.8 Hz, Hb), 3.55 (s, 2H, CH$_2$), 3.66 (s, 3H, OCH$_3$), 5.49 (dd, 1H, J_{xb} = 11.8 Hz, J_{xa} = 5.4 Hz, Hx), 6.37-8.18 (m, 21H, Ar-H), 8.40 (bs, 1H, NH), 9.16 (bs, 1H, NH); ^{13}C NMR (100 MHz, CDCl$_3$): δ 30.75 (CH$_2$), 36.61 (CH$_2$ of pyrazole), 55.34 (CH of pyrazole), 111.86-158.33 (30C, Ar-C), 160.79 (C=N of pyrazole), 162.11 (C=O), 168.24 (C=N); Anal. Calcd for C$_{37}$H$_{31}$IN$_6$O$_2$: C, 61.84; H, 4.35; N, 11.70. Found: C, 61.71; H, 4.28; N, 11.65%.

*6-Iodo-2-[2-(phenylamino)benzyl]-3-[5-(4-dimethylaminophenyl)-1-phenyl-4,5-dihydro-1H-pyrazol-3-yl-amino]quinazolin-4(3H)-one **(6m)***

Yield: 66%, m.p. 128-130 °C; IR (KBr): 3455 (NH), 2937, 2856 (CH$_2$), 1730 (C=O), 1614 (C=N), 615 (C-I) cm^{-1}; ^{1}H NMR (400 MHz, CDCl$_3$): δ 3.07 (dd, 1H, J_{ab} = 17.6 Hz, J_{ax} = 5.6 Hz, Ha), 3.51 (dd, 1H, J_{ba} = 17.6 Hz, J_{bx} = 12 Hz, Hb), 3.57 (s, 2H, CH$_2$), 5.52 (dd, 1H, J_{xb} = 12 Hz, J_{xa} = 5.6 Hz, Hx), 6.36-8.18 (m, 21H, Ar-H), 8.37 (bs, 1H, NH), 9.15 (bs, 1H, NH); ^{13}C NMR (100 MHz, CDCl$_3$): δ 30.29 (CH$_2$), 36.45 (CH$_2$ of pyrazole), 55.57 (CH of pyrazole), 111.75-150.38 (30C, Ar-C), 161.27 (C=N of pyrazole), 162.34 (C=O), 168.46 (C=N); Anal. Calcd for C$_{38}$H$_{34}$IN$_7$O: C, 62.38; H, 4.68; N, 13.40. Found: C, 62.25; H, 4.61; N, 13.29%.

Antimicrobial activity

The *in vitro* antimicrobial activity of compounds **6a-m** was carried out by cup-plate method [22]. Antibacterial activity was screened against two gram positive bacteria

Orbital Elec. J. Chem., Campo Grande, 2(3): 248-262, 2010

257

(*Staphylococcus aureus* ATCC 9144 and *Bacillus subtilis* ATCC 6633) and two gram negative bacteria (*Escherichia coli* ATCC 25922 and *Pseudomonas aeruginosa* ATCC 9027), by measuring the zone of inhibition on agar plates at two different concentrations 100 μg/mL and 50 μg/mL. While antifungal activity was tested by measuring the zone of inhibition on agar plates with two fungal species *Candida albicans* ATCC 10231 and *Aspergillus niger* ATCC 6275 at two different concentrations 20 μg/mL and 10 μg/mL. Penicillin-G was used as a standard antibacterial agent whereas fluconazole was used as a standard antifungal agent. The potency of the compounds was calculated by using the following formula [20]:
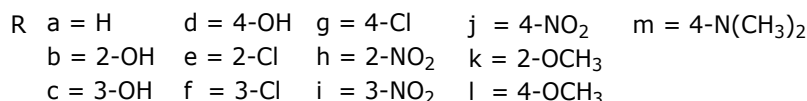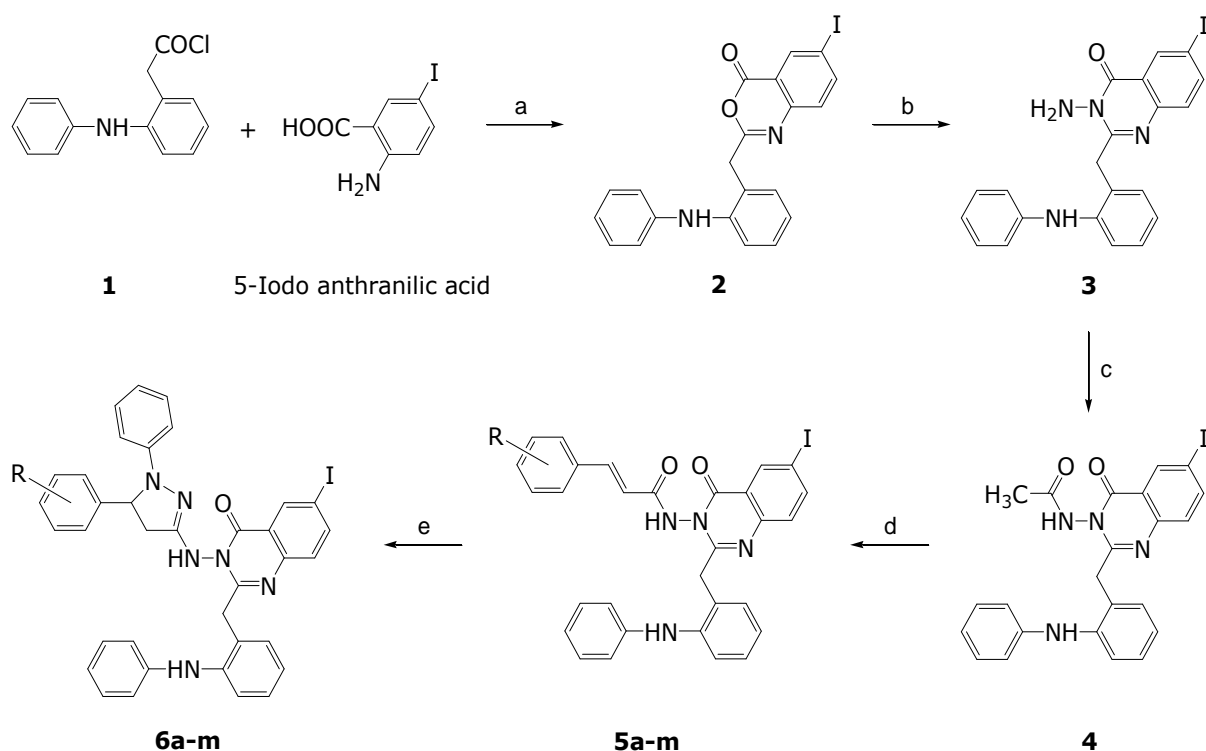
Potency = {antilog [(D/B)×I]}×M×F

Where F = dilution factor = 1 (same dilution used for standard and test); M = potency of standard compound = 100; I = $\log(C_H/C_L)$ of standard compound; D = (C_H+C_L) of test compound - (C_H+C_L) of standard compound; B = (C_H-C_L) of test compound + (C_H-C_L) of standard compound; C_H = Zone of inhibition at higher concentration; C_L = Zone of inhibition at lower concentration.

Results and Discussion

Chemistry

The title compounds pyrazolyl-quinazolin-4(3*H*)-ones **6a-m** were synthesized according to described process in Scheme 1. The structural elucidation of these compounds was carried out by elemental analyses as well as IR and NMR spectral data. IR spectra showed strong C=O and C=N stretching of quinazolinone at 1733-1715 cm^{-1} and 1618-1606 cm^{-1} respectively. The ^{1}H NMR spectra of compounds **6a-m** indicated that the -CH$_2$ protons of the pyrazoline ring resonated as a pair of doublet of doublets (Ha and Hb) due to geminal and vicinal coupling. The CH proton appeared as a doublet of doublet (Hx) due to vicinal coupling with the two magnetically nonequivalent protons of methylene group at position 4 of pyrazoline ring. The Ha proton which is *cis* to Hx resonates upfield in the range δ 3.01-3.08 as a doublet of doublet with coupling constant value *J* at around 17.5 Hz and 5.5 Hz while Hb, the other proton which is *trans* to Hx resonates downfield in the range δ 3.45-3.51 as a doublet of doublet with coupling constant value *J* at around 17.5 Hz and 12 Hz. The Hx proton which is vicinal to two methylene protons (Ha and Hb) resonates as a doublet of doublet in the range δ 5.45-5.52 with coupling constant value *J* at around 12 Hz and 5.5 Hz. In ^{13}C NMR spectra, signals at around δ 36, δ 55 and δ 161 confirms the presence of CH$_2$, CH and C=N of pyrazoline ring respectively, whereas C=O and C=N signals of quinazolinone ring are appear at around δ 162 and δ 168 respectively.

Scheme 1: Synthesis of pyrazolyl-quinazolin-4(3*H*)-ones **6a-m**

R a = H   d = 4-OH   g = 4-Cl   j = 4-NO₂   m = 4-N(CH₃)₂
   b = 2-OH   e = 2-Cl   h = 2-NO₂   k = 2-OCH₃
   c = 3-OH   f = 3-Cl   i = 3-NO₂   l = 4-OCH₃

Reagents and conditions: *(a) Pyridine, 0-5 °C; (b) Hydrazine hydrate, abs. ethanol, 6-8 h; (c) Acetyl chloride, benzene, 0-5 °C; (d) Aromatic aldehydes, abs. ethanol, 2 % NaOH, 10-12 h; (e) phenyl hydrazine, abs. methanol, glacial acetic acid, 8-10 h.*

The results of antibacterial activity are shown in Table 1. Compounds **6a** (R = H) and **6h** (R = 2-NO₂) showed good activity against gram positive bacteria *S. aureus* and *B. subtilis* while compound **6i** (R = 3-NO₂) possessed good activity against gram negative bacteria *E. coli* and *P. aeruginosa* as compared to standard drug penicillin-G. The remaining compounds exhibited moderate activities as compared to standard drugs. The results of antifungal activity are summarized in Table 2. The results shows that componds **6a** (R = H), **6e** (R = 2-Cl), **6g** (R = 4-Cl), **6h** (R = 2-NO₂) and **6m** (R = 4-N(CH₃)₂) showed good activity against *C. albicans* and moderate activity against *A. niger* except compound **6e** (R = 2-Cl) which displayed good activity against both fungi as compared to standard drug fluconazole. The remaining compounds possessed moderate activities against both fungi as compared to standard drug. Overall compound **6a** (R = H) showed very good activity against gram positive bacteria *B. subtilis* with potency of 63.61 % as compared to penicillin-G whereas compound **6e** (R = 2-Cl) exhibited very good activity with potency of 61.84 % against *C. albicans* as compared to fluconazole.

Table 1. Antibacterial activity of compounds **6a-m**

Compound	Zone of inhibition (mm)											
	S. aureus ATCC 9144			*B. subtilis* ATCC 6633			*E. coli* ATCC 25922			*P. aeruginosa* ATCC 9027		
	C_H	C_L	Pot %	C_H	C_L	Pot %	C_H	C_L	Pot %	C_H	C_L	Pot %
6a	16	12	57.87	17	13	63.61	6	0	40.81	7	0	48.61
6b	9	7	36.21	10	8	38.97	8	6	32.33	10	8	39.56
6c	11	9	40.19	12	10	44.19	8	6	32.33	10	8	39.56
6d	9	7	36.21	10	8	38.97	9	7	34.11	9	7	37.40
6e	7	0	48.23	7	0	45.27	6	0	40.81	7	0	48.61
6f	6	0	44.39	6	0	41.49	6	0	40.81	6	0	44.72
6g	6	0	44.39	7	0	45.27	7	0	44.45	7	0	48.61
6h	14	11	50.47	15	12	55.63	9	7	34.11	10	8	39.56
6i	11	9	40.19	12	10	44.19	16	12	54.75	15	12	55.43
6j	13	10	48.23	14	11	52.61	11	9	37.98	12	10	44.27
6k	10	8	38.15	11	9	41.49	11	8	41.30	12	10	44.27
6l	10	8	38.15	11	9	41.49	14	11	47.67	14	12	49.53
6m	8	6	34.37	9	7	36.59	6	0	40.81	7	0	48.61
Penicillin-G	30	25	100	27	21	100	31	25	100	28	23	100

C_H = Zone of inhibition at concentration 100 µg/mL, C_L = Zone of inhibition at concentration 50 µg/mL, Pot = Potency of compound (%) as compared to penicillin-G

Table 2. Antifungal activity of compounds **6a-m**

Compound	Zone of inhibition (mm)					
	C. albicans ATCC 10231			*A. niger* ATCC 6275		
	C_H	C_L	Pot %	C_H	C_L	Pot %
6a	14	11	55.58	13	10	48.51
6b	12	10	46.64	11	9	40.48
6c	9	7	38.84	8	6	33.78
6d	11	9	43.88	10	8	38.11
6e	16	13	61.84	15	12	53.99
6f	12	10	46.64	11	9	40.48
6g	14	12	52.69	13	11	45.67
6h	14	11	55.58	13	10	48.51
6i	11	9	43.88	10	8	38.11
6j	12	10	46.64	11	9	40.48
6k	9	7	38.84	8	6	33.78
6l	7	0	49.07	7	0	45.04
6m	14	11	55.58	13	10	48.51
Fluconazole	26	21	100	28	22	100

C_H = Zone of inhibition at concentration 20 µg/mL, C_L = Zone of inhibition at concentration 10 µg/mL, Pot = Potency of compound (%) as compared to fluconazole

Conclusion

The title compound was successfully synthesized using known methods. Phenyl substituted compound was found very active towards gram positive bacteria while 3-nitro phenyl substituted compound showed higher activity towards gram negative bacteria whereas 2-chloro phenyl substituted compound exhibited very good activity against fungi among the series. These findings give some idea about further research on this molecule with hope to get biologically active molecule.

Acknowledgements

References and Notes

[1]   Grover, G.; Kini, S. G. *Eur. J. Med. Chem.* **2006**, *41*, 256.

[2]   Alagarsamy, V.; Solomon, V. R.; Dhanabal, K. *Bioorg. Med. Chem*. **2007**, *15*, 235.

[3]   Laddha, S. S.; Bhatnagar, S. P. *Phosphorus, Sulfur, and Silicon* **2008**, *183*, 2262.

[4]   Alagarsamy, V.; Murugesan, S.; Dhanabal, K.; Murugan, M.; Clercq, E. I*ndian J. Pharm. Sci.* **2007**, *69*, 304.

[5]   Raghavendra, N. M.; Thampi, P.; Gurubasavarajaswamy, P. M.; Sriram, D. *Arch. Pharm.* **2007**, *340*, 635.

[6]   Agnihotri, A. K.; Shukla, S. K. *Arch. Pharm.* **1982**, *315*, 701.

[7]   Jatav, V.; Mishra, P.; Kashaw, S.; Stables, J. P. *Eur. J. Med. Chem.* **2008**, *43*, 135.

[8]   Maarouf, A. R.; El-Bendary, E. R.; Goda, F. E. *Arch. Pharm.* **2004**, *337*, 527.

[9]   Kurogi, Y.; Inoue, Y.; Tsutsumi, K.; Nakamura, S.; Nagao, K.; Yoshitsugu, H.; Tsuda, Y. *J. Med. Chem*. **1996**, *39*, 1433.

[10] Berghot, M. A.; Moawad, E. B. *Eur. J. Pharm. Sci*. **2003**, *20*, 173.

[11] Zampieri, D.; Mamolo, M. G.; Laurini, E.; Scialino, G.; Banfi, E.; Vio, L. *Bioorg. Med. Chem*. **2008**, *16*, 4516.

[12] Khode, S.; Maddi, V.; Aragade, P.; Palkar, M.; Ronad, P. K.; Mamledesai, S.; Thippeswamy, A. H. M.; Satyanarayana, D. *Eur. J. Med. Chem*. **2009**, *44*, 1682.

[13] Havrylyuk, D.; Zimenkovsky, B.; Vasylenko, O.; Zaprutko, L.; Gzella, A.; Lesyk, R. *Eur. J. Med. Chem*. **2009**, *44*, 1396.

[14] Budakoti, A.; Bhat, A. R.; Azam, A. *Eur. J. Med. Chem.* **2009**, *44*, 1317.

[15] Barsoum, F. F.; Hosni, H. M.; Girgis, A. S. *Bioorg. Med. Chem*. **2006**, *14*, 3929.

[16] Kaplancikli, Z. A.; Turan-Zitouni, G.; Ozdemir, A.; Can, O. D.; Chevallet, P. *Eur. J. Med. Chem.* **2009**, *44*, 2606.

[17] Ozdemir, Z.; Kandilci, H. B.; Gumusel, B.; Calis, U.; Bilgin, A. A. *Eur. J. Med. Chem.* **2007**, *42*, 373.

[18] El-Sabbagh, O. I.; Baraka, M. M.; Ibrahim, S. M.; Pannecouque, C.; Andrei, G.;

Snoeck, R.; Balzarini, J.; Rashad, A. A. *Eur. J. Med. Chem*. **2009**, *44*, 3746.

[19] Panda, J.; Srinivas, S. V.; Rao, M. E.; Panda, C. S. *J. Indian Chem. Soc.* **2002**, *79*, 770.

[20] Microbial assay of antibiotic. Eur. Pharmacopeia 2004, 4, 160.

[21] Furniss, B. S.; Hannaford, A. J.; Smith, P. W. G.; Tatchell, A. R. Vogel's Textbook of Practical Organic Chemistry, 5th Ed., New York: John Wiley and Sons, 1989.

[22] Barry, A. L. The Antimicrobial Susceptibility Test, Principles and Practices, Philadelphia, PA, USA:^Illus lea and febiger, 976.

262

Orbital Elec. J. Chem*., Campo Grande,* 2(3): 248-262, 2010

Full Paper

A facile microwave assisted one-pot synthesis of novel 1-methylhexahydroquinazolin-5(6H)-ones and bis-1-methylhexahydroquinazolin-5(6H)-ones

Madhusudhan Saha[a], Enamul Karim[a], Philippe Helissey[b], Jai N. Vishwakarma[a]*, Rishanlang Nongkhlaw[c]

(This paper is dedicated to Rev. Fr. Dr. Stephen Mavely on his 60th Birth Anniversary)

[a]Organic Research Lab., Department of Chemistry, St. Anthony's College, Shillong-793 001, India
[b]Laboratoire de Chimie Thérapeutique, UMR CNRS N°8638, Université Paris Descartes, Faculté des Sciences Pharmaceutiques et Biologiques, 4-Avenue de L'Observatoire, 75270 Paris Cedex 06 (France)
[c]Department of Chemistry, North-Eastern Hill University, Shillong-793 022, India

ABSTRACT: *Novel hexahydroquinazolin-5(6H)-ones **3a-j** have been synthesized in good yields by the reaction of enaminones **2a-b** with primary amines and formaldehyde under the influence microwaves. Enaminones **2a-b** have also been reacted with diamines and formaldehyde under similar conditions resulting in hitherto unreported bis-hexahydroquinazolin-5(6H)-ones **4a-d** and **5a-d**. The structures of the molecules have been established with the help of spectral and analytical data.*

***Keywords**: hexahydroquinazolin-5(6H)-ones; bis-hexahydroquinazolin-5(6H)-ones; dimedone; enaminone; 1,3-cyclohexanedione*

Introduction

Keeping in view the biological properties of octahydroquinazolines [1-3], we have recently reported [4, 5] the synthesis of hexahydroquinazolin-5(6H)-ones bearing phenyl and benzyl groups in position 1 of the ring and bis-hexahydroquinazolin-5(6H)-ones bearing phenyl group in position 1 of the ring. The biological properties of these molecules are under investigation. We now wish to report herein a short MW assisted

---

* Corresponding author. E-mail: jnvishwakarma@rediffmail.com

synthesis of hexahydroquinazolin-5(6H)-ones and bis-hexahydroquinazolin-5(6H)-ones bearing methyl group in position 1 of quinazoline ring.

Material and Methods

Melting points were recorded by open capillary method and are uncorrected. The IR spectra were recorded on a Perkin-Elmer 983 spectrometer. ^{1}H NMR (300 MHz) spectra were recorded on Bruker ACF-300 spectrometer. The chemical shifts (δ ppm) and the coupling constants (Hz) are reported in the standard pattern with reference to TMS as internal reference. FAB-mass spectra (MS) were measured on JEOL 3SX 102/DA-6000 Mass spectrometer using Argon as the FAB gas and *m*-nitrobenzylalcohol as the matrix. Elemental analyses were performed on a Vario-EL III instrument. Microwave irradiation was carried out in a domestic MW oven (Samsung CE2733G) operating at 2450 MHz. Enaminones **2a** and **2b** were synthesized by our reported procedure [6].

Synthesis of 1,3-substituted-1,2,3,4,7,8-hexahydroquinazolines (3a-e) and 1,3-substituted-7,7-dimethyl-1,2,3,4,7,8-hexahydroquinazolines (3f-j)

General procedure: A mixture of primary amine (1 mmol) and formaldehyde (2 mmol, 40% aqueous solution) in 1 mL of methanol was stirred for 5 minutes and to this was added a solution of enaminone **2** (1 mmol) in 4 mL methanol in one portion. The resulting reaction mixture was irradiated in a domestic microwave oven for 2-4 minutes at 180 watt. At the end of the reaction (tlc), methanol was distilled off under reduced pressure to give a gum which was purified by using chromatographic column (silica gel, EtOAc) to isolate **3a-j** in 57-89 % yields.

1-Methyl-3-phenyl-1,2,3,4,7,8-hexahydroquinazolin-5(6H)-one (3a). Dark brown gum; yield 61%; IR (KBr): 1542 (νC=C), 1605 (νC=O) cm^{-1}; ^{1}H NMR (CDCl$_3$): δ 1.95-2.00 (m, 2H, C$_7$-H), 2.33 (t, 2H, J=6.3 Hz, C$_8$-H), 2.45 (t, 2H, J=6.3 Hz, C$_6$-H), 2.96 (s, 3H, N-CH$_3$), 4.18 (s, 2H, C$_4$-H), 4.57 (s, 2H, C$_2$-H), 6.87-6.98 (m, 3H, aromatic), 7.17-7.28 (m, 2H, aromatic); MS: m/z 243.2 (MH$^+$). Anal. Calcd for C$_{15}$H$_{18}$N$_2$O (242.32): C, 75.52; H, 8.20; N, 10.36. Found: C, 75.39; H, 8.16; N, 10.41%.

1-Methyl-3-benzyl-1,2,3,4,7,8-hexahydroquinazolin-5(6H)-one (3b). Dark brown gum; yield 84%; IR (KBr): 1559 (νC=C), 1636 (νC=O) cm^{-1}; ^{1}H NMR (CDCl$_3$): δ 1.90-2.01 (m, 2H, C$_7$-H), 2.31 (t, 2H, J=6.0 Hz, C$_8$-H), 2.45 (t, 2H, J=6.3 Hz, C$_6$-H), 2.89 (s, 3H, N-CH$_3$), 3.58 (s, 2H, N$_3$-CH$_2$), 3.66 (s, 2H, C$_4$-H), 3.85 (s, 2H, C$_2$-H), 7.26-7.39 (m, 5H, aromatic); MS: m/z 257.2 (MH$^+$). Anal. Calcd for C$_{16}$H$_{20}$N$_2$O (256.34): C, 74.97; H, 7.86; N, 10.93. Found: C, 74.91; H, 7.80; N, 10.99%.

1-Methyl-3-tolyl-1,2,3,4,7,8-hexahydroquinazolin-5(6H)-one (3c). Dark brown gum; yield 63%; IR (KBr): 1548 (νC=C), 1611 (νC=O) cm^{-1}; ^{1}H NMR (CDCl$_3$): δ 1.87-2.00 (m, 2H, C$_7$-H), 2.28 (s, 3H, Ar-CH$_3$), 2.33 (m, 2H, C$_8$-H), 2.43 (m, 2H, C$_6$-H), 2.94 (s, 3H, N-

CH$_3$), 4.15 (s, 2H, C$_4$-H), 4.55 (s, 2H, C$_2$-H), 6.87-6.91 (m, 4H, aromatic); MS: m/z 257.2 (MH$^+$). Anal. Calcd for C$_{16}$H$_{20}$N$_2$O (256.34): C, 74.97; H, 7.86; N, 10.93. Found: C, 74.89; H, 7.82; N, 10.88%.

1-Methyl-3-(4-chlorophenyl)-1,2,3,4,7,8-hexahydroquinazolin-5(6H)-one *(3d)*. Pale yellow solid; yield 57%; mp 132^{0}C; IR (KBr): 1542 (νC=C), 1611 (νC=O) cm^{-1}; ^{1}H NMR (CDCl$_3$): δ 1.96 (m, 2H, C$_7$-H), 2.40 (t, 2H, J=6.0 Hz, C$_8$-H), 2.43 (t, 2H, J=6.6 Hz, C$_6$-H), 2.99 (s, 3H, N-CH$_3$), 4.14 (s, 2H, C$_4$-H), 4.54 (s, 2H, C$_2$-H), 6.89 (d, 2H, J=8.8 Hz, aromatic), 7.19 (d, 2H, J=8.8 Hz, aromatic); MS: m/z 277.2 (MH$^+$). Anal. Calcd for C$_{15}$H$_{17}$ClN$_2$O (276.76): C, 65.10; H, 6.19; N, 10.12. Found: C, 65.25; H, 6.14; N, 10.06%.

1,3-Dimethyl-1,2,3,4,7,8-hexahydroquinazolin-5(6H)-one (3e). Dark brown gum; yield 70%; IR (KBr): 1636 (νC=O) cm^{-1}; ^{1}H NMR (CDCl$_3$): δ 1.90-2.02 (m, 2H, C$_7$-H), 2.32 (t, 2H, J=6.0 Hz, C$_8$-H), 2.44 (t, 2H, J=6.6 Hz, C$_6$-H), 2.90 (s, 3H, N$_3$-CH$_3$), 2.97 (s, 3H, N$_1$-CH$_3$), 3.42 (s, 2H, C$_4$-H), 3.82 (s, 2H, C$_2$-H); MS: m/z 181.1 (MH$^+$). Anal. Calcd for C$_{10}$H$_{16}$N$_2$O (180.25): C, 66.63; H, 8.95; N, 15.54. Found: C, 66.81; H, 8.89; N, 15.61%.

1,7,7-Trimethyl-3-phenyl-1,2,3,4,7,8-hexahydroquinazolin-5(6H)-one *(3f).* Pale yellow solid; yield 80%; mp 140^{0}C; IR (KBr): 1540 (νC=C), 1599 (νC=O) cm^{-1}; ^{1}H NMR (CDCl$_3$): δ 1.01 (s, 6H, C$_7$-CH$_3$), 2.22 (s, 2H, C$_8$-H), 2.25 (s, 2H, C$_6$-H), 2.99 (s, 3H, N$_1$-CH$_3$), 4.18 (s, 2H, C$_4$-H), 4.62 (s, 2H, C$_2$-H), 6.90-6.97 (m, 3H, aromatic), 7.22-7.25 (m, 2H, aromatic) ; MS: m/z 271.2 (MH$^+$). Anal. Calcd for C$_{17}$H$_{22}$N$_2$O (270.37): C, 75.52; H, 8.20; N, 10.36. Found: C, 75.70; H, 8.15; N, 10.32%.

1,7,7-Trimethyl-3-benzyl-1,2,3,4,7,8-hexahydroquinazolin-5(6H)-one *(3g).* Pale yellow solid; yield 85%; mp 142^{0}C; IR (KBr): 1566 (νC=C), 1609 (νC=O) cm^{-1}; ^{1}H NMR (CDCl$_3$): δ 1.10 (s, 6H, C$_7$-CH$_3$), 2.19 (s, 2H, C$_8$-H), 2.32 (s, 2H, C$_6$-H), 2.93 (s, 3H, N$_1$-CH$_3$), 3.67 (s, 2H, C$_4$-H), 3.77 (s, 2H, N$_3$-CH$_2$), 3.99 (s, 2H, C$_2$-H), 7.28-7.37 (m, 5H, aromatic); MS: m/z 284.8 (MH$^+$). Anal. Calcd for C$_{18}$H$_{24}$N$_2$O (284.40): C, 76.02; H, 8.51; N, 9.85. Found: C, 76.16; H, 8.47; N, 9.90%.

1,7,7-Trimethyl-3-tolyl-1,2,3,4,7,8-hexahydroquinazolin-5(6H)-one *(3h).* Pale yellow solid; yield 89%; mp 132^{0}C; IR (KBr): 1540 (νC=C), 1594 (νC=O) cm^{-1}; ^{1}H NMR (CDCl$_3$): δ 1.02 (s, 6H, C$_7$-CH$_3$), 2.22-2.39 (m, 7H, C$_8$-H + C$_6$-H + Ar-CH$_3$), 2.97 (s, 3H, N$_1$-CH$_3$), 4.16 (s, 2H, C$_4$-H), 4.59 (s, 2H, C$_2$-H), 6.87 (d, 2H, J=8.1Hz, aromatic), 7.05 (d, 2H, J=8.1Hz, aromatic); MS: m/z 284.8 (MH$^+$) Anal. Calcd for C$_{18}$H$_{24}$N$_2$O (284.40): C, 76.02; H, 8.51; N, 9.85. Found: C, 75.92; H, 8.59; N, 9.80%.

1,7,7-Trimethyl-3-(4-chlorophenyl)-1,2,3,4,7,8-hexahydroquinazolin-5(6H)-one *(3i).* Pale yellow solid; yield 75%; mp 174^{0}C; IR (KBr): 1540 (νC=C), 1600 (νC=O) cm^{-1}; ^{1}H NMR (CDCl$_3$): δ 1.01 (s, 6H, C$_7$-CH$_3$), 2.12-2.24 (m, 4H, C$_8$-H + C$_6$-H), 2.99 (s, 3H, N$_1$-

265

Orbital Elec. J. Chem., Campo Grande, 2(3): 263-270, 2010

CH$_3$), 4.15 (s, 2H, C$_4$-H), 4.60 (s, 2H, C$_2$-H), 6.87 (d, 2H, J= 8.1Hz, aromatic), 7.19 (d, 2H, J= 8.1Hz, aromatic); MS: m/z 305.1 (MH$^+$) Anal. Calcd for C$_{17}$H$_{21}$N$_2$OCl (304.81): C, 66.99; H, 6.94 N, 9.19. Found: C, 66.80; H, 6.99; N, 9.23%.

1,3,7,7-Tetramethyl-1,2,3,4,7,8-hexahydroquinazolin-5(6H)-one (3j). Dark brown gum; yield 78%; IR (KBr): 1560 (νC=C), 1595 (νC=O) cm^{-1}; ^{1}H NMR (CDCl$_3$): δ 1.08 (s, 6H, C$_7$-CH$_3$), 2.18 (s, 2H, C$_8$-H), 2.28 (s, 2H, C$_6$-H), 2.41 (s, 3H, N$_3$-CH$_3$), 2.95 (s, 3H, N$_1$-CH$_3$), 3.45 (s, 2H, C$_4$-H), 3.86 (s, 2H, C$_2$-H); MS: m/z 209.2 (MH$^+$). Anal. Calcd for C$_{12}$H$_{20}$N$_2$O (208.30): C, 69.19; H, 9.68; N, 13.45. Found: C, 69.05; H, 9.65; N, 13.53%.

Synthesis of bis-Quinazolines 4a-d and 5a-d.

General Procedure: A mixture of diamine (0.5 mmol) and formaldehyde (2 mmol, 40% aqueous solution) in 1.5 mL methanol was shaken at room temperature for 5 minutes. To this mixture, a solution of enaminone **2** (1 mmol) in 5 mL methanol was added in one lot and the resulting mixture was irradiated in a domestic microwave oven for 2-4 minutes at 180 watt. At the end of the reaction (monitored by tlc), methanol was distilled off under reduced pressure to give a gum which was purified by using chromatographic column (silica gel, EtOAc) yielding **4** and **5** in 55-60% yields.

3,3′-(Ethane-1,2-diyl)bis(1-methyl-1,2,3,4,7,8-hexahydroquinazoline-5(6H)-one) **(4a)**. Dark brown gum; yield 55%; IR (KBr): 1543(νC=C), 1668 (νC=O) cm^{-1}; ^{1}H NMR (CDCl$_3$): δ 1.90-1.92 (m, 4H, C$_7$-H + C$_{7'}$-H), 2.27 (t, 4H, J=6.3 Hz, C$_8$-H + C$_{8'}$-H), 2.42 (t, 4H, J=6.0 Hz, C$_6$-H + C$_{6'}$-H), 2.68 (s, 4H, -CH$_2$-CH$_2$-), 2.93 (s, 6H, N$_1$-CH$_3$ + N$_{1'}$-CH$_3$), 3.47 (s, 4H, C$_4$-H + C$_{4'}$-H), 3.98 (s, 4H, C$_2$-H + C$_{2'}$-H), MS: m/z 359.2 (MH$^+$). Anal. Calcd for C$_{20}$H$_{30}$N$_4$O$_2$ (358.48): C, 67.01; H, 8.44; N, 15.63. Found: C, 67.21; H, 8.40; N, 15.69%.

3,3′-(Butane-1,4-diyl)bis(1-methyl-1,2,3,4,7,8-hexahydroquinazoline-5(6H)-one) **(4b)**. Dark brown gum; yield 56%; IR (KBr): 1538 (νC=C), 1653 (νC=O) cm^{-1}; ^{1}H NMR (CDCl$_3$): δ 1.52-1.58 (m, 4H, C$_7$-H + C$_{7'}$-H), 1.95 (t, 4H, J=6.0 Hz, C$_8$-H + C$_{8'}$-H), 2.22-2.27 (m, 4H, -CH$_2$CH$_2$CH$_2$CH$_2$-), 2.45 (t, 4H, J=6.0 Hz, C$_6$-H + C$_{6'}$-H), 2.95 (s, 6H, N$_1$-CH$_3$ + N$_{1'}$-CH$_3$), 3.43 (s, 4H, -CH$_2$CH$_2$CH$_2$CH$_2$-), 3.88 (s, 4H, C$_4$-H + C$_{4'}$-H), 4.98 (s, 4H, C$_2$-H + C$_{2'}$-H); MS: m/z 387.1 (MH$^+$). Anal. Calcd for C$_{22}$H$_{34}$N$_4$O$_2$ (386.53): C, 68.36; H, 8.87; N, 14.49. Found: C, 68.21; H, 8.22; N, 14.60%.

3,3′-(Ethane-1,2-diyl)bis(1,7,7-trimethyl-1,2,3,4,7,8-hexahydroquinazoline-5(6H)-one) **(4c)**. Dark brown gum; yield 60%; IR (KBr): 1557 (νC=C), 1669 (νC=O) cm^{-1}; ^{1}H NMR (CDCl$_3$): δ 1.06 (s, 12H, C$_7$-CH$_3$ + C$_{7'}$- CH$_3$), 2.17 (s, 4H, C$_8$-H + C$_{8'}$-H), 2.27 (s, 4H, C$_6$-H + C$_{6'}$-H), 2.68 (s, 4H, -CH$_2$-CH$_2$-), 2.99 (s, 6H, N$_1$-CH$_3$ + N$_{1'}$-CH$_3$), 3.55 (s, 4H, C$_4$-H + C$_{4'}$-H), 4.03 (s, 4H, C$_2$-H + C$_{2'}$-H); MS: m/z 415.3 (MH$^+$). Anal. Calcd for C$_{24}$H$_{38}$N$_4$O$_2$ (414.58): C, 69.53; H, 9.24; N, 13.51. Found: C, 69.35; H, 9.28; N, 13.59%.

3,3′-(Butane-1,4-diyl)bis(1,7,7-trimethyl-1,2,3,4,7,8-hexahydroquinazoline-5(6H)-one)

266

Orbital Elec. J. Chem., Campo Grande, 2(3): 263-270, 2010

(4d). Dark brown gum; yield 58%; IR (KBr): 1557 (νC=C), 1650 (νC=O) cm^{-1}; ^{1}H NMR (CDCl$_3$): δ 1.06 (s, 12H, C$_7$-CH$_3$ + C$_{7'}$-CH$_3$), 1.55 (s, 4H, -CH$_2$C*H$_2$*C*H$_2$*CH$_2$-), 2.16 (s, 4H, C$_8$-H + C$_{8'}$-H), 2.26 (s, 4H, C$_6$-H + C$_{6'}$-H), 2.40 (s, 4H, -C*H$_2$*CH$_2$CH$_2$C*H$_2$*-), 2.89 (s, 6H, N$_1$-CH$_3$ + N$_{1'}$-CH$_3$), 3.47 (s, 4H, C$_4$-H + C$_{4'}$-H), 3.91 (s, 4H, C$_2$-H + C$_{2'}$-H); MS: m/z 443.3 (MH$^+$). Anal. Calcd for C$_{26}$H$_{42}$N$_4$O$_2$ (442.64): C, 70.35; H, 9.56; N, 12.66. Found: C, 70.21; H, 9.51; N, 12.61%.

3,3′-(1,4-phenylene)bis(1-methyl-1,2,3,4,7,8-hexahydroquinazoline-5(6H)-one) **(5a).** Dark brown gum; yield 60%; IR (KBr): 1516 (νC=C), 1541 (νC=O) cm^{-1}; ^{1}H NMR (CDCl$_3$): δ 1.84-1.94 (m, 4H, C$_7$-H + C$_{7'}$-H), 2.38 (t, 4H, J=6.0 Hz, C$_8$-H + C$_{8'}$-H), 2.52 (t, 4H, J=1.8 Hz, C$_6$-H + C$_{6'}$-H), 2.97 (s, 6H, N$_1$-CH$_3$ + N$_{1'}$-CH$_3$), 4.14 (s, 4H, C$_4$-H + C$_{4'}$-H), 4.54 (s, 4H, C$_2$-H + C$_{2'}$-H), 6.90-6.96 (m, 4H, aromatic); MS: m/z 407.1 (MH$^+$). Anal. Calcd for C$_{24}$H$_{30}$N$_4$O$_2$ (406.52): C, 70.91; H, 7.44; N, 13.78. Found: C, 70.75; H, 7.50; N, 13.69%.

3,3′-(biphenyl-4,4′-diyl)bis(1-methyl-1,2,3,4,7,8-hexahydroquinazoline-5(6H)-one) **(5b).** Dark brown gum; yield 55%; IR (KBr): 1533 (νC=C), 1609 (νC=O) cm^{-1}; ^{1}H NMR (CDCl$_3$): δ 1.86-1.90 (m, 4H, C$_7$-H + C$_{7'}$-H), 2.21 (t, 4H, J=6.3 Hz, C$_8$-H + C$_{8'}$-H), 2.51 (t, 4H, J=1.8 Hz, C$_6$-H + C$_{6'}$-H), 2.94 (s, 6H, N$_1$-CH$_3$ + N$_{1'}$-CH$_3$), 4.05 (s, 4H, C$_4$-H + C$_{4'}$-H), 4.47 (s, 4H, C$_2$-H + C$_{2'}$-H), 6.68-6.88 (m, 8H, aromatic); MS: m/z 483.7 (MH$^+$). Anal. Calcd for C$_{30}$H$_{34}$N$_4$O$_2$ (482.62): C, 74.66; H, 7.10; N, 11.61. Found: C, 74.47; H, 7.15; N, 11.66%.

3,3′-(1,4-phenylene)bis(1,7,7-trimethyl-1,2,3,4,7,8-hexahydroquinazoline-5(6H)-one) **(5c).** Dark brown gum in 56% yield; IR (KBr) 1548 (νC=C), 1647 (νC=O) cm^{-1}; ^{1}H NMR (CDCl$_3$): δ 1.01 (s, 12H, C$_7$-CH$_3$ + C$_{7'}$-CH$_3$), 2.17 (s, 4H, C$_8$-H + C$_{8'}$-H), 2.25 (s, 4H, C$_6$-H + C$_{6'}$-H), 2.95 (s, 6H, N$_1$-CH$_3$ + N$_{1'}$-CH$_3$), 4.10 (s, 4H, C$_4$-H + C$_{4'}$-H), 4.53 (s, 4H, C$_2$-H + C$_{2'}$-H), 6.87-6.91 (m, 4H, aromatic), MS: m/z 463.4 (MH$^+$) Anal. Calc. for C$_{28}$H$_{38}$N$_4$O$_2$ (462.63): C, 72.69; H, 8.28; N, 12.11. Found: C, 72.51; H, 8.24; N, 12.17%

3,3′-(biphenyl-4,4′-diyl)bis(1,7,7-trimethyl-1,2,3,4,7,8-hexahydroquinazoline-5(6H)-one) **(5d).** Dark brown gum; 57% yield; IR (KBr): 1533 (νC=C), 1609 (νC=O) cm^{-1}; ^{1}H NMR (CDCl$_3$): δ 1.02 (s, 12H, C$_7$-CH$_3$ + C$_{7'}$-CH$_3$), 2.20 (s, 4H, C$_8$-H + C$_{8'}$-H), 2.25 (s, 4H, C$_6$-H + C$_{6'}$-H), 3.00 (s, 6H, N$_1$-CH$_3$ + N$_{1'}$-CH$_3$), 4.21 (s, 4H, C$_4$-H + C$_{4'}$-H), 4.63 (s, 4H, C$_2$-H + C$_{2'}$-H), 6.95-7.05 (m, 4H, aromatic), 7.43-7.48 (m, 4H, aromatic); MS: m/z 539.3 (MH$^+$). Anal. Calcd for C$_{34}$H$_{42}$N$_4$O$_2$ (538.72): C, 75.80; H, 7.86; N, 10.40. Found: C, 75.64; H, 7.81; N, 10.47%.

Results and Discussion

Thus, when 3-methylaminocyclohexenone (**2a**) was treated with aniline and formaldehyde under the influence of microwaves, a product was obtained in 61% yields

267

Orbital Elec. J. Chem., Campo Grande, 2(3): 263-270, 2010

which was characterized as 1-methyl-3-phenyl-1,2,3,4,7,8-hexahydroquinazolin-5(6H)-one (**3a**) on the basis of analytical and spectral data. The reaction of **2a** with other primary amines and formaldehyde behaved in a similar manner and octahydroquinazolines **3b-e** were isolated in 57-84% yields (scheme 1).

Scheme 1

	R	n
4a	H	0
4b	H	2
4c	Me	0
4d	Me	2

	R	
2a	H	
2b	Me	

	R	n
5a	H	1
5b	H	2
5c	Me	1
5d	Me	2

	R	R_1
3a	H	Ph
3b	H	PhCH$_2$
3c	H	4-MePh
3d	H	4-ClPh
3e	H	Me
3f	Me	Ph
3g	Me	PhCH$_2$
3h	Me	4-MePh
3i	Me	4-ClPh
3j	Me	Me
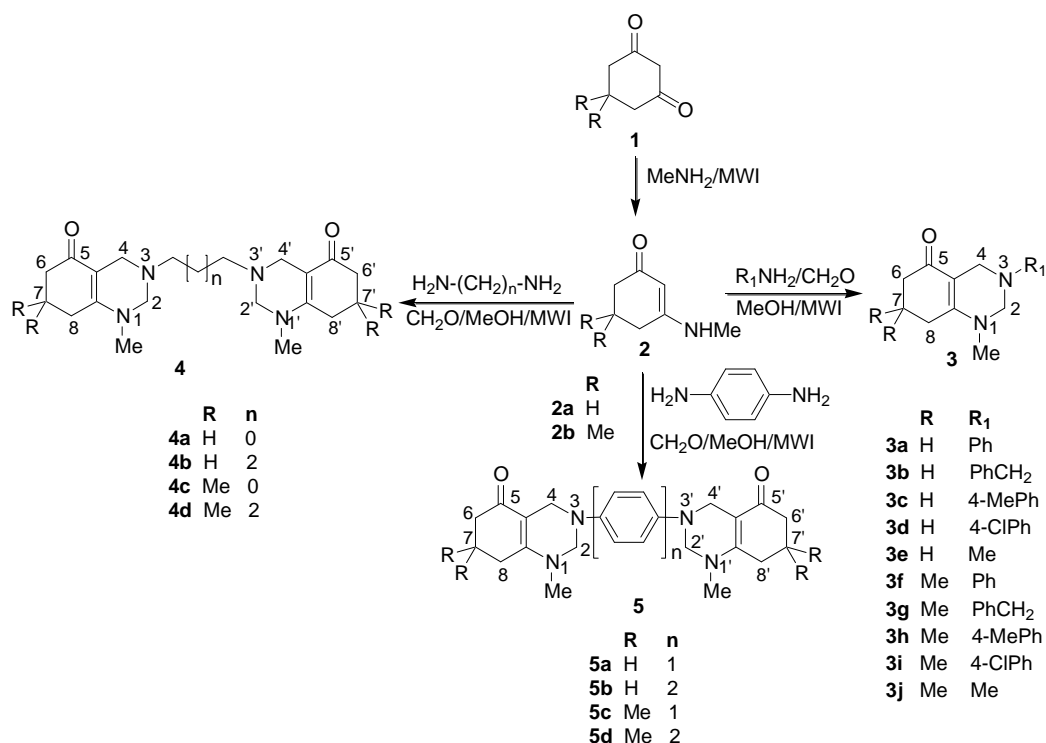
The infrared spectra of **3a-e** showed strong peaks in the region of 1540 to 1636 cm^{-1} due to extensively delocalized double bonds and carbonyl groups [6]. In the ^{1}H NMR spectra of **3a-e**, the methylene protons at C-2 resonated near 4.50 ppm except in **3b** and **3e** where they appeared in the vicinity of 3.80 ppm. This lowering in chemical shift could be attributed to the absence of delocalization of N-3 lone pair of electrons. Probably a similar explanation could be extended for the appearance of CH$_2$ protons at C-4 close to 4.15 ppm except in **3b** and **3e** where they were found to resonate near 3.50 ppm. While CH$_2$ protons at C-7 appeared as multiplets in the range of 1.90-2.00 ppm, those at C-6 and C-8 resonated close to 2.40 and 2.30 ppm, respectively. The methyl protons at N-1 gave singlets close to 2.90 ppm.

The Reactions of **2b** with formaldehyde and primary amines were subsequently examined under similar conditions and the expected 1-methyl-3-alkyl/aralkyl/aryl-7,7-dimethyl-5-oxo-1,2,3,4,5,6,7,8-octahydroquinazolines **3f-j** were isolated in 75-89% yields, whose structures could be established with the help of analytical and spectral data. The infrared spectra of **3f-j** showed strong peaks in the region of 1540 to 1609 cm^{-1}. The ^{1}H NMR spectra of tetrahydropyrimidine rings of **3f-j** were found to have a similar

268

Orbital Elec. J. Chem., Campo Grande, 2(3): 263-270, 2010

pattern as those of **3a-e.** However, the six methyl protons at C-7 appeared as sharp singlets around 1.00 ppm and the CH_2 protons at C-6 and C-8 resonated in ranges of 2.25-2.99 and 2.18-2.24 ppm, respectively.

Encouraged by the successful synthesis of octahydroquinazolines **3a-j**, we then turned our attention to the synthesis of bis-octahydroquinazolines. Thus, when enaminone **2a** was reacted with 1,2-diaminoethane and formaldehyde under the influence of microwaves in methanol, a product **4a** was isolated in 55% yield, the structure of which was established to be 3,3'-(ethane-1,2-diyl)bis(1-methyl-1,2,3,4,7,8-hexahydroquinazolin-5(6H)-one based on analytical and spectral data. The compound **2a** gave the corresponding product **4b** under identical conditions on reaction with 1,4-diaminobutane and formaldehyde. We were thus able to connect two octahydroquinazoline rings through flexible aliphatic chains. Subsequently, with the intention to connect the two octahydroquinazoline rings through aromatic linkers, enaminones **2** were reacted with aromatic diamines and formaldehyde to give **5** in 55-60% yields (scheme 1), the structures of which could be established with the help of spectral and analytical data.

The infrared spectra of **4a-d** and **5a-d** showed strong peaks in the range of 1516-1669 cm^{-1} due to extensive delocalization of the enaminone moiety. The ^{1}H NMR spectra of these dimers were found to have the same pattern as in the monomeric octahydroquinazolines except that the signals due to CH_2 protons of ethylene linkers appeared at 2.68 ppm while those in butylene appeared in the ranges of 2.45-2.46 and 1.55-2.17ppm. The dimeric structures of **4a-d** and **5a-d** were further supported by their mass spectra.

Conclusion

The present paper describes an efficient, clean, simple, fast and environment friendly strategy for the synthesis of hitherto unknown octahydroquinazolines and bis-octahydroquinazolines from easily accessible starting materials in good yields with promising biological properties. The methodology reported herein is an example of multi-component reactions (MCRs).

Acknowledgements

269

Orbital Elec. J. Chem., Campo Grande, 2(3): 263-270, 2010

spectra.

References and Notes

[1] Sarac, S.; Yarim, M.; Ertan, M.; Kilic, F. S.; Erol, K. *Arzneim-Forsc Drug Res.* **2002**, *52*, 27.

[2] Yarim, M.; Sarac, S.; Kilic, F. S.; Erol, K. *Farmaco* **2003**, *58*, 17.

[3] Hamama, W.S.; Hammouda, M.; Afsahi, E. M. *Z. Naturforsch* **1988**, *43B*, 483.

[4] Chanda, K.; Dutta, M. C.; Vishwakarma, J. N. *Indian J. Chem.* **2006**, *45B*, 1076.

[5] Chanda, K.; Dutta, M. C.; Nongkhlaw, R. L.; Vishwakarma, J. N. *E-J. Chem.* **2009**, *7*, 281.

[6] Chanda, K.; Dutta, M. C.; Vishwakarma, J. N. *Indian J. Chem.* **2004**, *43B*, 2475.

270

Orbital Elec. J. Chem., Campo Grande, 2(3): 263-270, 2010

Full Paper

Synthesis, characterization and study of antibacterial activity of some novel tetrazole derivatives

Subramaniyan Arulmurugan [a], Helen P. Kavitha*[a], Bathey R. Venkatraman[b]

[a]Research Department of Chemistry, SRM University, Ramapuram Campus, Chennnai-89, Tamilnadu, India
[b]PG & Research Dept. of Chemistry, Periyar EVR College, Tiruchirapalli-23, Tamil Nadu, India

ABSTRACT: *This work aims at synthesizing novel tetrazole derivatives from phenothiazine. Phenothiazine is first converted into corresponding nitrile by reacting it with aldehyde, sodium metabisulphite and sodium cyanide. The nitrile on treatment with NaN3/DMF yielded the tetrazole derivative. In this work two tetrazole derivatives, viz., Dimethyl-{4-[phenothiazin-10-yl-(1H-tetrazol-5-yl)methyl]-phenyl}-amine and 10-[(4-Methoxy-phenyl)-(1H-tetrazole-5-yl)-methyl-10H-phenothiazine were prepared. The compounds were synthesized in good yields and their structures were confirmed by IR, ^{1}H-NMR, mass and elemental analysis. The tetrazole compounds were screened for antimicrobial activity against bacteria and fungi. The results of the study show that the compounds present good antimicrobial activity.*

Keywords: *phenothiazine; nitrile; tetrazole; antibacterial activity*

Introduction

The chemistry of nitrogen-sulfur heteroatom containing aromatic compounds is becoming more popular as an area of research. Phenothiazine derivatives have shown diverse biological activities including tranquilizers [1], anti-inflammatory [2], antimalarial [3], antipsychotropic [4], antimicrobial [5], antitubercular [6-7], antitumour [8-10] and stimulation of the penetration of anticancer agents *via* the blood-brain barior. They bind to physical targets or receptors, producing many possible mechanisms of actions [11]. Phenothiazines are inexpensive and widely available. A slight variation in the substitution pattern on the phenothiazine nucleus often causes a marked difference in substitution

---

* Corresponding author. E-mail: helenkavithap@yahoo.co.in

pattern on the phenothiazine nucleus often causes a marked difference in activities. It has been reported [12] that some phenothiazine inhibit intracellular replication of viruses including human immunodeficiency viruses (HIV). Some of the derivatives of phenothiazine have also been reported to exhibit significant anticancer activities [13-14].

Tetrazoles are medicinally important heterocycles incorporated in a large number of drugs [15-16]. They are reported to possess anti-inflammatory [17-18], analgesic [19], ulcer therapeutic and coccidiostatic properties [20]. The tetrazole function is metabolically more stable than the acid function. A close similarity between the acidic character of the tetrazole group and carboxylic acid group have inspired medicinal chemists to synthesize substituted tetrazoles as potential medicinal agents. Attracted by the biological importance of phenothiazine and tetrazole moieties and continuing our work to synthesize some tetrazole derivatives starting from phenothiazine [21], we have synthesized two tetrazoles from phenothiazine with a view to screen the compounds for antimicrobial activity.

Material and Methods

All the melting points are uncorrected. Infrared spectra were recorded on Bruker IFS 66V FTIR spectrometer and Perkin Elmer Nr. PE 257 Infrared spectrometer using potassium bromide discs. NMR spectra were recorded on EM-390 NMR spectrometer and EM-390 Varian 90 MHz spectrometer. Mass spectra were recorded on FINNEGAN MAT 8230 spectrometer.

Synthesis

Preparation of (Substituted-phenyl)-phenothiazin-10-yl-acetonitrile (2a, b)

Aldehyde (0.05 mol) was added to a stirred solution of sodium metabisulphite (0.05 mol) in 20 mL of water. After fifteen minutes, phenothiazine (0.05 mol) was added. The reaction mixture was stirred for thirty minutes and then it was cooled in an ice-bath. A solution of sodium cyanide (0.05 mol) in 20 mL of water was added drop wise and the stirring was continued for six hours. The reaction flask was kept aside overnight. The product obtained was filtered off and washed with excess of water. The dried sample was recrystallized from aqueous ethanol.

Preparation of Dimethyl-{4-[phenothiazin-10-yl-(1H-tetrazol-5-yl)-methyl]-phenyl}-amine. (3)a

To a mixture of nitrile **2** (0.01 mol), sodium azide (0.01 mol) and ammonium chloride (0.1 mol), 10 mL of dimethylformamide was added. The content of the flask was heated in oil bath for seven hours, maintaining the temperature at 125 °C. The solvent was removed under reduced pressure. Distilled water (100 mL) was added to the flask

Orbital Elec. J. Chem., Campo Grande, 2(3): 271-276, 2010

272

and the solution was acidified with concentrated hydrochloric acid to pH 2. The solution was cooled to 5 °C in an ice bath. The product was removed by filtration, washed repeatedly with water and dried. The crude tetrazole was recrystallized from aqueous methanol.

(4-Dimethylamino-phenyl)-phenothiazin-10-yl-acetonitrile (2a)

Yield 62%. Melting Point: 80-82 °C. IR (KBr pellet, cm^{-1}): 2220 (Nitrile), ^{1}H NMR (90 MHz, CDCl$_3$): 7.3 (s, 8H, ArH), 6.8 (d, 2H, o-protons), 6.8 (d, 2H, m-protons), 3.1 (s, 6H, dimethyl protons), 4.3 (s, 1H, CH proton). MS (m/z): 358 [M+1]+ (20%), 50 (100%). Elemental Analysis: Calculated: C, 73.92; H, 5.36; N, 11.75. Found: C, 73.89; H, 5.42; N, 11.79.

(4-Methoxy-phenyl)-phenothiazin-10-yl-acetonitrile(2b)

Yield 65%. Melting Point: 162-164 °C, IR (KBr pellet, cm-1): 2220 (Nitrile), ^{1}H NMR (90 MHz, CDCl$_3$): 7.2-7.4 (s, 8H, ArH), 7.9 (d, 2H m-protons), 7.0 (d, 2H, o-protons), 3.9 (s, 3H, methoxy protons), 4.5 (s, 1H, CH proton). MS (m/z): 344 [M+1]+ (20%), 198 (100%). Elemental Analysis: Calculated: C, 73.23; H, 4.68; N, 8.13; Found: C, 73.29; H, 4.72; N, 8.21.

Dimethyl-{4-[phenothiazin-10-yl-(1H-tetrazol-5-yl)-methyl]-phenyl}-amine. (3a)

Yield 70%. Melting Point: 160-163 °C. IR (KBr pellet, cm^{-1}): 3341(s), 3184(w) 3053(w), 2918(w), 1597(s) 1572(m) 1263(w), 1244(w), 1063(m), 1035(w), 750(s), 738(s), 717(m). ^{1}H NMR (90 MHz, CDCl$_3$): 6.9-7.3 (m, 8H, ArH), 7.8 (d, 2H, m-protons), 6.6 (d, 2H, o-protons), 3.1 (s, 6H, (CH$_3$)$_2$-N- protons), 4.7 (s,1H, CH proton). MS (m/z): 400 [M+1]+ (20%), 334 (100%). Elemental Analysis: Calculated: C, 65.98; H, 5.03; N, 20.98. Found: C, 65.94; H, 5.08; N, 20.95.

10-[(4-Methoxy-phenyl)-(1H-tetrazole-5-yl)-methyl]-10H-phenothiazine(3b)

Yield 45%. Melting Point: 140-142 °C. IR (KBr pellet, cm^{-1}): 3341(s), 3184(w) 3099(w), 3054(w), 1598(s) 1572(w) 1248(w), 1079(s), 1035(s), 751(s), 737(m), 717(m). ^{1}H NMR (90 MHz, CDCl$_3$): 7.3 (m, 8H, ArH), 7.45 (d, 2H, o-protons), 7.0 (d, 2H, o-protons), 3.9 (s, 3H, (CH$_3$- protons), 4.6(s,1H, CH proton). MS (m/z): 387 (100%). Elemental Analysis: Calculated: C, 65.10; H, 4.42; N, 18.08. Found: C, 65.21; H, 4.38; N, 18.13.

Antimicrobial Assay

The antimicrobial activity for the given samples was carried out by Disc Diffusion Technique (Indian Pharmacopoeia 1996, Vol II, A-105). The test microorganisms of Gram positive *Staphylococcus aureus* and Gram negative *Escherichia coli* and fungus *Candida*

273

Orbital Elec. J. Chem*., Campo Grande*, 2(3): 271-276, 2010

albicans, Aspergillus niger were obtained from National Chemical Laboratory (NCL), India, and maintained by periodical sub culturing on Nutrient agar and Sabourad dextrose medium both bacteria and fungus respectively. The effect produced by the sample was compared with the effect produced by the positive control (Reference standard Ciprofloxazin 5 μg/disc for bacteria and Fluconazole 10 μg/disc for fungal). The result indicated that compounds were active against all the four organisms with reference to standard. The results are shown in the Table 1.

Table 1 – Antimicrobial screening results of the compounds

S. No.	Microorganism	Weight of the compound per disc, μg	Diameter zone of inhibition in mm		
			3a	3b	Std
1	Staphylococcus aureus (NCIM 2079)	50	14	11	41
2	Escherichia coli (NCIM 2065)	50	12	16	41
3	Candida albicans (NICM 3102)	50	13	15	22
4	Aspergillus Niger (NICM 105)	50	12	14	22

Results and Discussion

Scheme 1
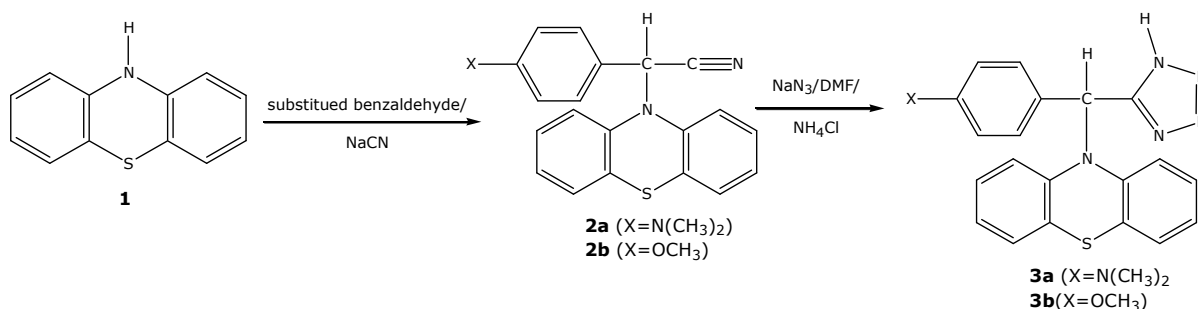
The two new tetrazole derivatives synthesized in this work were characterized by IR, ^{1}H NMR, mass and elemental analysis. In the FTIR spectra, the presence of absorption bands at 1063 and 1035 cm^{-1} (**3a**) and 1079 and 1035 cm^{-1} (**3b**)confirm the presence of tetrazole ring in the synthesized compounds. Similarly, the presence of N-N=N is evidenced by the absorption bands at 1263 and 1248 cm^{-1} for the compounds **3a** and **3b**, respectively. ^{1}H NMR spectra also show convincing evidence regarding the structure of the compound. A singlet observed at δ 3.9, a doublet observed at δ 7.0 and δ 7.45 and a multiplet centered at δ 7.3 confirms the structure of **3b**. Similar observations were found for the compound **3a**. In the mass spectra, the appearance of molecular ion peaks at m/z 400 and m/z 387 confirm the compounds **3a** and **3b**, respectively.

274

Orbital Elec. J. Chem., Campo Grande, 2(3): 271-276, 2010

From the analysis of the data in the antimicrobial assay, it is observed that the two tetrazole compounds synthesized in this study show fairly good antibacterial and antifungal activity against the test organisms, but the activity is less than the standard drugs. The efficiency of the compound **3a** is found to be more when compared with **3b** in activity against staphylococcus, where as the compound **3b** is more active than **3a** against *Escherichia coli*. But the activity **3a** and **3b** are comparable against the fungi.

Conclusion

In conclusion, we have synthesized two new tetrazole compounds following a simple and efficient method. The compounds were isolated in good yield. The synthesized compounds showed fairly good activity against the test microorganisms.

Acknowledgements

References and Notes

[1]   Ei-Said, M. K. *Pharmazie* **1981**, *36*, 86-89.

[2]   Tilak, S. R. et al. *Indian drugs*.**1998**, *35*, 221.

[3]   Dominguez, J. N.; López, S.; Charris, J.; Iarruso, L.; Lobo, G.; Semenov, A.; Olson, J. E.; Rosenthal, P. J. *J. Med. Chem.* **1997**, *40, 2726*.

[4]   Lin, G.; Midha, K. K.; Hawes, E. M. *J. Heterocycl. Chem.* **1991**, *28*, 215.

[5]   Raval, J.; Desai, K. K. *ARKIVOC*, **2005**, *(xiii)*, 21.

[6]   Viveros, M.; Amaral, L. *Int. J. Antimicrob. Ag.* **2001**, *17*, 225.

[7]   Amaral, L.; Kristiansen, J. E. *Int. J. Antimicrob. Ag*. **2000**, *14*, 173.

[8]   Motohashi, N. Kurihara, T.; Satoh, K.; Sakagami, H.; Mucsi, I.; Pusztai, R.; Szabó, M.; Molnár, J. *Anticancer Res.* **1999,** *19*, 1837.

[9]   Motohashi, N.; Kawase, M.; Saito, S.; Sakagami, H. *Curr. Drug Targets* **2000**, *1*, 237.

[10] Kurihara, T.; Motohasho, N.; Pang, G. L.; Higano, M.; Kiguchi, K.; Molnar, J. *Anticancer Res.* **1996***, 16*, 2757.

[11] Ghosh, N.; Chattopadhyay, U. *In Vivo* **1993**, *7*. 435.

[12] Floyd, R. A.; Scheider, J. E.; Zhu, Y. Q.; North, T. W.; Schinazi, F. *Proc. Am. Assoc. Cancer. Res.* **1993**, *34*, 359.

[13] Kurihara, T.; Motohashi, N.; Sakagami, H. H.; Molnar, J. *Anticancer Res*. **1999**, *19*, 4081.

[14] Kurihara, T.; Nojima, K.; Sakagami, H.; Motohashi, N.; Molnar, J. *Anticancer Research.* **1999**, *19*, 3895.

[15] Katritzky, A. R.; Jain, R.; Petrukhin, R.; Denisenko, S.; Schelenz, T. *SAR QSAR Environ. Res.* **2001**, *12*, 259-266.

[16] Hiriyanna, S. G; Basavaiah, K.; Dhayanithi, V.; Bindu, A.; Sudhaker, P.; Pati, H. N.

275

Orbital Elec. J. Chem., Campo Grande, 2(3): 271-276, 2010

Anal. Chem. Indian J. **2008**, *7*, 568-572.

[17] Aliasaghar, H.; Khalili, D.; De Clercq, E.; Salmi, C.; Brunel, J. M. *Molecules* **2007**, *12*, 1720.

[18] Mohite, P. B.; Pandhare, R. B.; Khanage, S. G.; Bhaskar, V. H. *Journal of Pharmacy Research*, **2010**, *3, 43.*

[19] Bachar, S. C.; Lahiri, S. C. *Pharmazie* **2004**, *59*, 435.

[20] Hallinan, E. A.; Tsymbalov, S.; Dorn, C. R.; Pitzele, B. S.; Hansen, D. W. Jr. *J. Med. Chem*. **2002**, *45*, 1686.

[21] Venkatraman, B. R.; Kavitha, H. P. *Molbank* **2009**, M621.

276

Orbital Elec. J. Chem*., Campo Grande*, 2(3): 271-276, 2010

Full Paper

Synthesis, physicochemical and antimicrobial studies of first row transition metal complexes with quinoline derivatives nitroquinolino[3,2-*b*][1,5]benzodiazepine and nitroquinolino[3,2-*b*][1,5]benzoxazepine

Neeraj Sharma*, Neelam Sharma

Department of Biotechnology, GLA Group of Institution, Mathura (UP), India

ABSTRACT: *Metal complexes of Mn (II), Cu (II), Ni (II) and Co (II) with quinoline derivatives have been synthesized and characterized by elemental analysis, molar conductance, magnetic movement, electronic spectra, thermal analysis and IR spectral data. The molecular formula of complexes corresponds to $[ML(NO_3)_2]$ where M = Mn, Cu, Ni, Co, Zn, Fe, or Cr. The physicochemical and IR spectral data shows that the ligand coordinates to the metal ion in bidentate fashion (through the C=N and N-H groups). The antimicrobial studies of ligand and its metal, metal complexes have been screened for selected bacteria (E. Coli, S. typhi, B. subtilis and S. aureus) and fungi (A. flavous, A. niger, P. triticena and F. species). Antimicrobial studies shows that the Mn (II) complexes are more toxic than other metal complexes. Magnetic susceptibility measurements reveal octahedral geometry around the metal ion. The complexes were found to be non electrolyte in nature on the basis of low value of molar conductance.*

Keywords: antimicrobial activity; quinoline derivatives; metal complexes; spectral study

Introduction

Quinoline, 1-azenaphthalene, is an aromatic nitrogen compound and characterized by a double ring structure contains benzene fused to pyridine at two adjacent carbon atoms. Quinoline family compounds are widely used as a parent compound to make drugs (especially antimalarial medicine), fungicides, biocides, alkaloids, dyes, rubber chemical and flavoring reagents. They have antiseptic, antipyretic and antiperiodic properties [1]. They are also used as catalyst, corrosion inhibitor, and preservative and

---

* Corresponding author. E-mail: dr_neerajsharmaagra@yahoo.com

as solvent forresin and terpenes. They are used in transition metal complex catalyst chemistry for uniform polymerization and luminescence chemistry [2]. The 8-(diethylaminohexyl amino)-6-methoxy-4-methyl quinoline is highly effective against the protozoan parasite *Trypanosoma cruzi* which is the agent of Chagas disease [3] and the 2-(2-methylquinolin-4-ylamino)-N-phenylacetamide is more active than the standard antileishmanial drug sodium antimony gluconate [4]. Dynemicin A and streptonigrin are naturally occurring members of the class of antitumors, antibiotics whose synthesis are based on the utilization of performed quinoline derivatives [5]. Cryptolepine (5-methyl-5H-indolol[3,2-b]quinoline) major cryptolepis sanguinolenta alkaloid displays a plenty of pharmacological effects, such as antimuscarinic, noradrenergic receptor antagonistic, vasodilative, antithrombotic, antiplasmodial and first of all cytotoxic activities [6-8]. Quinoline containing drugs, particularly 4-aminoquinolines, have a long and successful history as antimalarials [1, 9]. Transition metal complexes of quinoline derivatives have also been reported [10, 11].

Material and Methods

All the chemicals used were of AR grade and purified by standard methods. Melting points were determined in open capillaries and are uncorrected. The 1:1 stoichiometric ratio was confirmed by Fengers mass estimation method [12]. The complexes were purified by recrystallization and TLC. The IR spectra in a KBr matrix were recorded on Perkin Elmer 842-spectrophotometer at CDRI, LUCKNOW and elemental analysis of C, H, N, were carried out at NCl pure. The Thermo gravimetric analysis of metal complex was carried out at a constant heating rate 10 ^{o}C/min up to temperature 1000 ^{o}C on a TGA instrument model Perkins Elmer (Pyris Diamond) UV-visible spectra were measured on a SHIMADZU double beam spectrophotometer using N,N'-dimethylformamide   as a solvent at 10^{-3} M concentration.

Chemistry

Synthesis of Nitroquinolino [3,2-b] [1,5] benzodiazepine (Scheme 1)

The mixture of 2-chloro-6-nitroquinoline-3-carbaldehyde dissolved in small amount of acetic acid and *o*-phenylenediammine was taken in a 100 mL borosil beaker and a pinch of potassium iodide was then added. The whole mixture was made into slurry and was irradiated by placing the beaker in a microwave oven for about 30 minutes. The product obtained was poured into ice-cold water; the solid separated was filtered, dried and recrystallized.

Synthesis of Nitroquinolino [3,2-b] [1,5] benzoxazepine (Scheme 1)

The mixture of 2-aminophenol, KOH and DMSO were taken in a 100 mL borosil beaker and in another beaker were taken 2-chloro-6-nitroquinoline-3-carbaldehyde and

278

Orbital Elec. J. Chem. | Vol 2 || No. 3 || 277-287 2010 |

small amount of KI. The mixture was irradiated for about five minute in a microwave oven. The product was then hydrolysed by pouring into ice-cold water. The final product separated as a solid on acidification with dilute HCl was then filtered, dried and purified.

Synthesis of Metal Complexes (Scheme 1)

Metal complexes were prepared by the mixing of equimolar solutions of ligands nitroquinolino[3,2-b][1,5]benzodiazepine, nitroquinolino[3,2-b][1,5]benzoxazepine and metal nitrate solutions. The stoichiometry of the complexes of the ligands **A** and **B** (0.025 M) with Mn (II), Cu (II), Ni (II) and Co (II) (0.025 M) metal ions was found by carrying out potentiometric titration against standard (0.1 M) NaOH solution in ethanol – water mixture. The pH of the reaction mixture was adjusted between 7.5 to 8.5. The coloured precipitates were filtered washed several times with hot water followed by ethanol to free it form the soluble impurities. The resulting coloured solids were dried in an oven at 100 ^{o}C and stored in desiccators over anhydrous $CaCl_2$. The complexes were purified by recrystallization and TLC in silica Gel – G.

Scheme 1

X = NH, Nitroquinolino[3,2-b][1,5]benzodiazepine (**A**)
X = O, Nitroquinolino[3,2-b][1,5]benzoxazepine (**B**)

$M(NO_3)_2$ aq.

[ML(NO$_3$)$_2$]
M= Co (II), Ni (II), Mn (II), Cu (II)
L= Nitroquinolino[3,2-b][1,5]benzodiazepine (**A**) or
nitroquinolino[3,2-b][1,5] benzoxazepine (**B**)
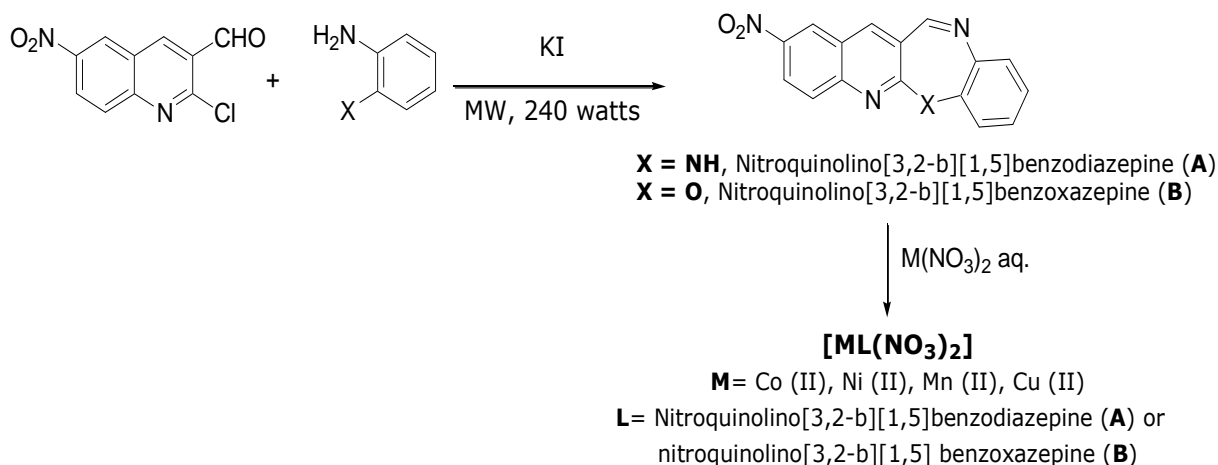
Antimicrobial Activity

The biological experiments for determining antimicrobial activity of ligands and their metal complexes have been done by serial dilution method [13]. In this technique the solutions of different concentrations (viz. 250 ppm, 500 ppm, 750 ppm and 1000 ppm) were prepared in dimethylformamide. The graded dilution of the test compounds in a suitable nutrient (agar) and PDA medium were inoculated with the organisms under examination using aseptic techniques in an incubator at 37 ºC . The antibacterial and antifungal activity of ligands and their metal complexes have been screened in vitro, against bacteria (*Bacillus subtilis, Staphylococcus aureus, Escherichia coli and Salmonella typhi*) and fungi (*Aspergillus flavous, Aspergillus niger, Penicillium triticena and Fusarium species).*

279

Orbital Elec. J. Chem. | Vol 2 || No. 3 || 277-287 2010 |

The percentage of growth inhibition was calculated by measuring the diameter of the microbial colony in the control and test plates by the following expression:

$$\% \text{ inhibition} = \frac{C - T}{C} \times 100$$

Where:

C = diameter of microbial colony in millimeter in control plate.

T =   diameter of microbial colony in treated (test) plate.

Results and Discussion

The complexes are microcrystalline colored powder, stable at room temperature, and are soluble in DMF and DMSO. The elemental analyses were satisfactory, show that the complexes have a ligand to metal ratio of 1:1, and have the general formula $[ML(NO_3)_2]$, where M = Co (II), Ni (II), Mn (II), Cu (II) and L = Nitroquinolino[3,2-b] [1,5]benzodiazepine and nitroquinolino[3,2-b][1,5]benzoxazepine. The molar conductance value (11.30–21.6 mhos cm^2 mol^{-1}) indicates the nonelectrolytic nature of the complexes. The data are presented in Table 1.

Table 1. Analytical and physical data of ligands and their metal complexes

Compound	Yield %	Mol. Wt..	M. C.[a] mhos cm^2 mol$^-$	Magnetic moment μeff BM	$\lambda_{max.}$	Elemental analysis[b] %			
						C	H	N	Metal
$C_{16}H_{10}N_4O_2$	82	314	11.3	-		61.14	3.18	17.83	-
$C_{16}H_9N_3O_3$	84	315	11.9	-		60.95	2.85	13.33	-
MnA(NO$_3$)$_2$	81	492.9	12.7	1.87	10000 17600 22400	38.95	2.03	11.36	11.14
MnB(NO$_3$)$_2$	80	493.9	12.3	1.96	10200 17800 22200	38.87	1.82	8.50	11.12
CuA(NO$_3$)$_2$	76	501.5	17.62	1.91	13100 17300	38.29	1.99	11.17	12.66
CuB(NO$_3$)$_2$	89	502.5	17.7	1.94	13600 17500	38.20	1.79	8.36	12.64
CoA(NO$_3$)$_2$	82	496.9	20.3	4.87	10100 17300 22300	38.64	2.01	11.27	11.85
CoB(NO$_3$)$_2$	82	497.9	20.7	4.96	10200 17200 22400	38.56	1.81	8.43	11.82
NiA(NO$_3$)$_2$	78	496.7	21.4	3.03	11600 17900 12640	38.65	2.01	11.27	11.81
NiB(NO$_3$)$_3$	79	497.7	21.6	3.06	12300 18400 25300	38.58	1.81	8.44	11.79

[a] Molar conductivity, [b] Found

280

Orbital Elec. J. Chem. | Vol 2 || No. 3 || 277-287 2010 |

IR Spectral analyses

The IR spectra of complexes are compared with that of free ligands to determine the changes that might have taken place during complexation. The important bands and assignments of ligands and their complexes are summarized in Table 2. The band at 1658 cm^{-1} and 1651 cm^{-1} in the free ligands   NitroQBD(A) and NitroQBO(B), respectively attributed to υ (C =N) [14, 15] undergoes the shifting to lower region in all the complexes, indicating the participation of azomethine nitrogen in complexation. In all the complexes the band assigned to v(N-H) in ligand NitroQBD (A) (3330 cm^{-1}) shows lowering compared to the ligand indicating the involvement of N-H group in coordination. In all the complexes the band assigned to v(C-O-C) in ligand NitroQBO(B) (1022 cm^{-1}) shows lowering compared to the ligand indicating the involvement of C-O-C group in coordination. The presence of new bands in the region 428 cm^{-1} - 500 cm^{-1} in all the complexes is attributed to v(M-N) and v(M-O) linkage [16-18]. Other strong bands around 1360 cm^{-1} and 860 cm^{-1} in all complexes, suggest monodentate coordination of –NO$_2$ group in the complexes [19]. The results indicate that the ligands are bidentate in nature [20-23].

Table 2. IR spectral data of ligands and its metal complexes

Compounds	v(C=N)	v(N-H)	v(C-O-C)	v(M-N)	v(M-O)	v(M-NO$_3$)
C$_{16}$H$_{10}$N$_4$O$_2$ (A)	1658	3330		-	-	-
C$_{16}$H$_9$N$_3$O$_3$ (B)	1651		1022	-	-	-
[MnA(NO$_3$)$_2$]	1645	3318		440		1350, 865
[MnB(NO$_3$)$_2$]	1630		998	458	530	1345, 843
[CuA(NO$_3$)$_2$]	1648	3320		467		1320, 865
[CuB(NO$_3$)$_2$]	1631		990	449	542	1332, 840
[CoA(NO$_3$)$_2$]	1638	3315		428		1342, 855
[CoB(NO$_3$)$_2$]	1625		1012	432	525	1355, 864
[NiA(NO$_3$)$_2$]	1635	3312		432		1343, 820
CuB(NO$_3$)$_2$]	1630		1005	428	545	1365, 865

Thermo Gravimetric Analysis

The results of thermo gravimetric analysis of metal complexes were recorded in below. The results of thermo gravimetric analysis of metal complexes showed that the final residue was the metal carbide as well as well as metal oxide and weight of residue was in good agreement with the theoretically calculated weight of metal carbide as well as metal oxide. The residue left have higher weight [24] then metal oxide, probably part shows the presence of metal carbide formed simultaneously on heating the complexes at about 1000 ^{0}C. The thermal decomposition of metal complexes can be expressed as presented in the tables 3-10:

281

Orbital Elec. J. Chem. | Vol 2 || No. 3 || 277-287 2010 |

Table 3. Decomposition scheme of Mn (II) complex with ligand **A**

Decomposition scheme	Temp. rang (^{o}C)	Weight loss % Found (calc.)
$Mn(C_{16}H_{10}N_4O_2)(NO_3)_2$		
↓	206-324	13.89 (14.40)
$Mn(C_9H_5NO)(NO_3)_2$		
↓	510-660	26.29 (26.74)
$MnO + Mn_3C$ + other volatile oxides of C, H, N		
↓	1003	53.42 (52.98)
$MnO + Mn_3C$		

Table 4. Decomposition scheme of Mn (II) complex with ligand **B**

Decomposition scheme	Temp. rang (^{o}C)	Weight loss % Found (calc.)
$Mn(C_{16}H_9N_3O_3)(NO_3)_2$		
↓	206-324	13.89 (14.40)
$Mn(C_9H_5NO)(NO_3)_2$		
↓	510-660	26.29 (26.74)
$MnO + Mn_3C$ + other volatile oxides of C, H, N		
↓	1003	53.42 (52.98)
$MnO + Mn_3C$		

Table 5. Decomposition scheme of Cu (II) complex with ligand **A**

Decomposition scheme	Temp. rang (^{o}C)	Weight loss % Found (calc.)
$Cu(C_{16}H_9N_3O_3)(NO_3)_2$		
↓	194-393	13.02 (13.28)
$Cu(C_{14}H_{10}NO)(NO_3)_2$		
↓	488-586	32.18 (32.47)
$CuO + Cu_2C_2$ + other volatile oxides of C, H, N		
↓	1004	48.31(49.03)
$CuO + Cu_2C_2$		

Table 6. Decomposition scheme of Cu (II) complex with ligand **B**

Decomposition scheme	Temp. rang (^{o}C)	Weight loss % Found (calc.)
$Cu(C_{16}H_9N_3O_3)(NO_3)_2$		
↓	194-393	13.02 (13.28)
$Cu(C_{14}H_{10}NO)(NO_3)_2$		
↓	488-586	32.18 (32.47)
$CuO + Cu_2C_2$ + other volatile oxides of C, H, N		
↓	1004	48.31(49.03)
$CuO + Cu_2C_2$		

Table 7. Decomposition scheme of Co (II) complex with ligand **A**

Decomposition scheme	Temp. rang (^{o}C)	Weight loss % Found (calc.)
$Co(C_{16}H_{10}N_4O_2)(NO_3)_2$		
↓	106-286	13.78(13.23)
$Co(C_9H_5NO)(NO_3)_2$		
↓	397-586	26.51 (26.01)
$CoO + Co_3C$ + other volatile oxides of C, H, N		
↓	908	55.17 (56.37)
$CoO + Co_3C$		

Orbital Elec. J. Chem. | Vol 2 | | No. 3 | | 277-287 2010 |

282

Table 8. Decomposition scheme of Co (II) complex with ligand **B**

Decomposition scheme	Temp. rang (^{o}C)	Weight loss % Found (calc.)
$Co(C_{16}H_9N_3O_3)(NO_3)_2$ $\downarrow$ $Co(C_9H_5NO)(NO_3)_2$	106-286	13.78(13.23)
$\downarrow$	397-586	26.51 (26.01)
$CoO + Co_3C +$ other *volatile oxides of C, H, N* $\downarrow$ $CoO + Co_3C$	908	55.17 (56.37)

Table 9. Decomposition scheme of Ni (II) complex with ligand **A**

Decomposition scheme	Temp. rang (^{o}C)	Weight loss % Found (calc.)
$Ni(C_{16}H_{10}N_4O_2)(NO_3)_2$ $\downarrow$ $Ni(C_9H_5NO)(NO_3)_2$	195-439	29.64 (30.65)
$\downarrow$	516-662	26.15(25.81)
$NiO + Ni_3C +$ other *volatile oxides of C, H, N* $\downarrow$ $NiO + Ni_3C$	1005	38.55 (39.89)

Table 10. Decomposition scheme of Ni (II) complex with ligand **B**

Decomposition scheme	Temp. rang (^{o}C)	Weight loss % Found (calc.)
$Ni(C_{16}H_9N_3O_3)(NO_3)_2$ $\downarrow$ $Ni(C_9H_5NO)(NO_3)_2$	195-439	29.64 (30.65)
$\downarrow$	516-662	26.15(25.81)
$NiO + Ni_3C +$ other *volatile oxides of C, H, N* $\downarrow$ $NiO + Ni_3C$	1005	38.55 (39.89)

Electronic spectra and magnetic moment of complexes

Electronic spectra of Co (II) complexes shows three bands in the region 10100-9800, 17700 – 17100 cm^{-1} and 22300-21700 cm^{-1} which may be assigned to $^4T_{1g}(F) \rightarrow$ $^4T_{2g}(F)$, $^4A_{2g}(F)$ and $^4T_{1g}(P)$ transitions, respectively, which indicate octahedral geometry of both the Co (II) complexes which is further supported by high μ_{eff} value in the range 4.85-4.96 B.M. for both the Co (II) complexes [25, 26]. The Ni (II) complexes shows three bands in the regions 12600-11500 cm^{-1}, 18800- 7800 $cm^{-1}$and 26300-25200 cm^{-1} which may be assigned to$^3A_{2g}(F) \rightarrow$ $^3T_{2g}(F)$, $^3T_{1g}(F)$ and $^3T_{1g}(P)$ transitions respectively, which indicate octahedral geometry of all the Ni (II) complexes which is further supported by the μ_{eff} value in the range 3.03-3.06 B.M. for all the Ni (II) complexes [27].The electronic spectra of both the Cu (II) complexes shows two bands in the region 13800-13-200 cm^{-1} and 18000-17200 cm^{-1} which may be assigned to the transition $^2Eg \rightarrow$ $^2T_{2g}$ and charge transfer band respectively [28]. The electronic spectra of Cu (II) complexes suggesting an octahedral geometry around central metal ion which

283

Orbital Elec. J. Chem. | Vol 2 || No. 3 || 277-287 2010 |

is further supported by μ_{eff} value in the range 1.91-1.94 B.M. Electronic spectra of Mn (II) complexes under study show two bands in the range 14100–14700 cm^{-1} and 20480–21550 cm^{-1} corresponding to the spin allow transition $^4A_{2g} \rightarrow {}^4T_{2g}$ (V$_1$) & $^4A_{2g} \rightarrow {}^4T_{2g}$ (F) (V$_2$). The transition $^4A_{2g} \rightarrow {}^4T_{1g}$ (P) (V$_3$) is usually not observed in UV region due to charge transfer bond. The above transition suggests the octahedral geometry for the complex [29]. The electronic spectra of the Mn (II) complexes suggesting an octahedral geometry around central metal ion which is further supported by the μ_{eff} value in t range 1.87–1.96 B.M.

Antimicrobial Studies

The antibacterial and antifungal activity of ligands **A** and **B** and its metal complexes were screening *in vitro*, against bacteria (*Bacillus subtilis, Staphylococcus aureus, Escherichia coli and Salmonella typhi*) and fungi (*Aspergillus flavous, Aspergillus niger, Penicillium triticena and Fusarium species*).   The results are recorded in tables 11 and 12.

The results of biocidal activities show that the percentage of zone of inhibition of 500 ppm concentration is the best. The percentage of growth inhibition capacities of metal complexes follows the following order against different bacteria and fungi:

Bactericidal activities of metal

E. coli: Cu (II) > Mn (II) > Co (II) > Ni (II)

S. typhi: Cu (II) ≈ Mn(II) > Co (II) > Ni (II)

S. aureus: Cu (II) > Mn (II) > Co (II) > Ni (II)

B. subtilis: Mn (II) ≈ Cu (II) > Co (II) ≈ Ni (II)

Fungicidal activities of metal complexes

A. flavous: Cu (II) > Mn (II)   > CO (II) > Ni (II)

A. niger: Cu (II) > Mn (II) > Co (II) > Ni (II)

P. triticena: Cu (II) > Mn (II)   > Co (II) ≈ Ni (II)

F. species: Cu (II) > Mn (II) > Co (II) > Ni (II)

The results indicate that the Cu (II) complex is more toxic compared to other complexes, as well as Cu (II) complex is more effective towards bacteria *E. coli* compared to other microbes. The overall results obtained from the above studies confirm that with increase in the concentration of the complexes the activity almost remains unchanged or is slightly increase.

Orbital Elec. J. Chem. | Vol 2 || No. 3 || 277-287 2010 |

284

Table 11. Percentage of zone of inhibition of ligands and their metal complexes against fungi

Compounds	A. flavous				A. niger				P. triticena				F. species			
	% Conc. In ppm				% Conc. In ppm				% Conc. In ppm				% Conc. In ppm			
	250	500	750	1000	250	500	750	1000	250	500	750	1000	250	500	750	1000
$C_{16}H_{10}N_4O_2$ (A)	39.50	54.00	62.66	64.00	39.50	54.00	62.66	64.00	39.50	54.00	62.66	64.00	39.50	54.00	62.66	64.00
$C_{16}H_9N_3O_3$ (B)	39.50	54.00	62.66	64.00	39.50	54.00	62.66	64.00	39.50	54.00	62.66	64.00	39.50	54.00	62.66	64.00
$[MnA(NO_3)_2]$	39.50	62.66	69.13	71.55	39.50	62.66	69.13	71.55	39.50	62.66	64.00	69.13	39.50	62.66	64.00	69.13
$[MnB(NO_3)_2]$	39.50	62.66	64.00	69.13	39.50	62.66	69.13	71.55	39.50	62.66	69.13	71.55	39.50	64.00	69.13	71.55
$[CoA(NO_3)_2]$	39.50	69.13	71.55	75.00	39.50	69.13	71.55	75.00	39.50	69.13	71.55	75.00	39.50	69.13	71.55	75.00
$[CoB(NO_3)_2]$	39.50	69.13	71.55	75.00	39.50	69.13	71.55	75	39.50	69.13	71.55	75.00	39.50	69.13	71.55	75.00
$[CuA(NO_3)_2]$	47.84	71.55	71.55	47.84	39.50	62.66	69.13	71.55	39.50	62.66	69.13	71.55	39.50	62.66	69.13	71.55
$[CuB(NO_3)_2]$	47.84	71.55	71.55	75.00	47.84	71.55	71.55	75.00	47.84	71.55	71.55	75.00	47.84	71.55	71.55	75.00
$[NiA(NO_3)_2]$	39.50	62.66	69.13	71.55	39.50	62.66	69.13	71.55	39.50	62.66	69.13	71.55	39.50	62.66	69.13	71.55
$[NiB(NO_3)_2]$	39.50	62.66	69.13	71.55	39.50	62.66	69.13	71.55	39.50	62.66	69.13	71.55	39.50	62.66	69.13	71.55

Table 12. Percentage of zone of inhibition of ligands and their metal complexes against bacteria

Compounds	E. coli				S. typhi				S. aureus				B. subtilis			
	% Conc. In ppm				% Conc. In ppm				% Conc. In ppm				% Conc. In ppm			
	250	500	750	1000	250	500	750	1000	250	500	750	1000	250	500	750	1000
$C_{16}H_{10}N_4O_2$ (A)	39.50	54.00	62.66	64.00	39.50	54.00	62.66	64.00	39.50	54.00	62.66	64.00	39.50	54.00	62.66	64.00
$C_{16}H_9N_3O_3$ (B)	39.50	54.00	62.66	64.00	39.50	54.00	62.66	64.00	39.50	54.00	62.66	64.00	39.50	54.00	62.66	64.00
$[MnA(NO_3)_2]$	39.50	62.66	69.13	71.55	39.50	62.66	69.13	71.55	39.50	62.66	64.00	69.13	39.50	62.66	64.00	69.13
$[MnB(NO_3)_2]$	39.50	62.66	64.00	69.13	39.50	62.66	69.13	71.55	39.50	62.66	69.13	71.55	39.50	64.00	69.13	71.55
$[CoA(NO_3)_2]$	39.50	69.13	71.55	75.00	39.50	69.13	71.55	75.00	39.50	69.13	71.55	75.00	39.50	69.13	71.55	75.00
$[CoB(NO_3)_2]$	39.50	69.13	71.55	75.00	39.50	69.13	71.55	75	39.50	69.13	71.55	75.00	39.50	69.13	71.55	75.00
$[CuA(NO_3)_2]$	47.84	75.00	75.00	75.00	39.50	62.66	69.13	71.55	39.50	62.66	69.13	71.55	39.50	62.66	69.13	71.55
$[CuB(NO_3)_2]$	47.84	71.55	71.55	75.00	47.84	71.55	71.55	75.00	47.84	71.55	71.55	75.00	47.84	71.55	71.55	75.00
$[NiA(NO_3)_2]$	39.50	62.66	69.13	71.55	39.50	62.66	69.13	71.55	39.50	62.66	69.13	71.55	39.50	62.66	69.13	71.55
$[NiB(NO_3)_2]$	39.50	62.66	69.13	71.55	39.50	62.66	69.13		39.50	62.66	69.13	71.55	39.50	62.66	69.13	71.55

Acknowledgements

References and Notes

[1] O'Neill, P. M.; Bray, P. G.; Hawley, S. R.; Ward, S. A.; Park, B. K. *Pharmacology & Therapeutics* **1998**, *77*, 29.

[2] Gupta, A.; Sirohi, R.; Kishore, D. *J. Indian Chem. Soc*. **2004**, *81*, 163.

[3] Chiari, E.; Oliveira, A. B.; Prado, M. A.; Alves, R. J.; Galvão, L. M.; Araujo, F. G. *Antimicrob. Agents Chemother. **1996**,* 40, 613.

[4] Sahu, N. S. ; Pal, C. ; Mandal, N. B. *Bioorg. Med.Chem.* **2002***, 10*, 1687.

[5] Bringmann, G.; Reichert, Y.; Kane, V. *Tetrahedron* **2004***,* 60, 3539.

[6] Jonckers, T. H. M.; van Miert, S.; Cimanga, K. *J. Med. Chem.* **2002***, 45*, 3497.

[7] Dassonneville, L.; Lansiaux, A.; Wattelet, A. *Eu. J. Pharmacol.* **2002***, 409*, 9.

[8] Godlewska, J.; Badowska-Roslonek, K.; Ramza, J.; Kaczmarek, L.; Peczynska-Czoch, W.; Opolski, A. *Radiology and Oncology* **2004***, 38*, 137.

[9] Foley, M.; Tilley, L. *Pharmacology & Therapeutics* **1998***, 79*, 55.

[10] Rivera, D. G.; Peseke, K.; Jomarrón, I.; Montero, A.; Molina, R.; Coll, F. *Molecules* **2003***, 8*, 444.

[11] Black, S. I.; Young, G. B. *Polyhedron* **1998***, 8*, 585.

[12] Job, P.   *Ann. Chim*. **1928**, *9*, 113.

[13] Quasted, J. H. *J. Gen. Microbial* **1996**, *45*, 14.

[14] Colthup, N. B.; Daly, L. H.; Wiberley, S. E. Introduction to IR and Raman spectroscopy.   New York: Academic press, 1964.

[15] Bellamy, L. J. The IR spectra of complex molecules. New York: Wiley, 1966.

[16] Black, S. I.; Young, G. B. *Polyhedron* **1989***,* 8, 585.

[17] Addison, C. C.; Logan, N. Advances in Inorganic Chemistry and Radiochemistry. New York, NY, USA: Academic Press, 1964.

[18] Bhojya Naik, H. S.; Chetana, P. R.; Revanasiddappa, H. D. *J. Indian Chem. Soc.* **2002***, 79*, 955.

[19] Nakamoto, K.; Morimoto, Y.; Martell, A. E. *J. Phys. Chem.* **1962**, *66*, 46.

[20] Gao, W. T.; Zheng, Z. *Molecules* **2002***, 7*, 511.

[21] Grevea, S.; Vill, V.; Friedrichsena, W. *Z. Naturforsch., B: J. Chem. Sci.* **2002***, 57B*, 677.

[22] Plourde, G. L. ; Fisher, B. B. *Molecules* **2002***, 7*, 315.

[23] Black, S. I.; Young, G. B. *Polyhedron* **1989***, 8*, 585.

[24] Narula, A. K. *J. Indian Chem. Soc.* **1991**, *68*, 313.

[25] Lever, A. B. P. *Inorganic Electron Spectroscopy.* Amsterdam, The Netherlands: Elsevier,   1968.

[26] Huheey, J. E. Inorganic Chemistry: Principles of Structure and Reactivity. New York, NY, USA: Harper and Row, 1980.

286

Orbital Elec. J. Chem. | Vol 2 | | No. 3 | | 277-287 2010 |

[27] Drago, R. S. Physical Methods in Inorganic Chemistry*.* New York, NY, USA: Rein Hold, 1965.

[28] Sastri, C. V.; Eswaramoorthy, D.; Giribabu, L.; Maiya, B. G. *J. Inorg. Biochem.* **2003***, 94*, 138.

[29] Prasad, R. N.; Mathur, M. *J. Serb. Chem. Soc.* **2002***, 67*, 825.

287

Orbital Elec. J. Chem. |Vol 2||No. 3||277-287 2010|

Full Paper

Eletrodos monocristalinos de platina para eletrocatálise de oxidação de metano

Mayara Munaretto, Douglas Henrique Fockink, Valderi Pacheco Santos*

Universidade Estadual do Oeste do Paraná - UNIOESTE, Colegiado de Química, Centro de Engenharias e Ciências Exatas, Campus de Toledo, Rua da Faculdade, 645, Jardim Santa Maria, Cep 85.903-000, Toledo, Paraná, Brasil

Platinum single crystal electrodes for the electrocatalysis of methane oxidation

ABSTRACT: *The main objective of this paper is to characterize the voltammetric profiles of platinum single crystals of low Miller indexes Pt(100) and Pt(110) and study their catalytic activities on the oxidation of methane. In this way, it was developed a metallic surface modified by presence of other metal oxide, which presents catalytic activity for this reaction. It is well known that the electrooxidation of methane (CH_4) leads mainly to the formation of CO_2 and H_2O, however, the oxidation can also lead to the formation of CO, a reaction intermediate that has strong interaction with metal surfaces, such as platinum. This molecule tends to accumulate on the platinum surface and to passive it, due to the self-poisoning, decreasing its catalytic activity. Therefore, the main aim of this work was the development of a platinum electrode modified by deposition of titanium oxide, which presented electrocatalytic properties for the oxidation of methane.*

Keywords: Platinum single crystal electrodes; electrooxidation of methane; titanium deposition; electrocatalysis.

Introdução

Platina em processos eletródicos

A platina, por ser um metal nobre e apresentar estabilidade em diversos meios eletrolíticos, é muito utilizada como eletrodo em processos eletrocatalíticos. A sua principal vantagem em relação a outros metais nobres, é que ela possui alta capacidade de adsorção de espécies orgânicas e inorgânicas [1].

---

* Corresponding author. E-mail: vpacheco@unioeste.br

O estudo da platina em processos eletródicos tem o objetivo de aplicá-la como ânodo em sistemas denominados células a combustível. Estes dispositivos convertem energia química em energia elétrica a partir de um processo de combustão fria. No ânodo, o hidrogênio flui para o catalisador onde é dissociado em prótons e elétrons e no cátodo as moléculas de oxigênio reagem com os elétrons para formar água. Já em células específicas com oxidação direta de pequenas moléculas orgânicas (DOFC) a energia elétrica é gerada a partir da oxidação destas moléculas no ânodo, formando CO_2, enquanto o oxigênio é reduzido formando água no cátodo [2].

Eletrooxidação de metano

A eletrooxidação de metano sobre platina ocorre em soluções aquosas de ácido fosfórico, sulfúrico ou perclórico. O potencial de oxidação da molécula orgânica em solução ácida é determinado pela reação de eletrooxidação do hidrogênio adsorvido. Tem-se isso como evidência da reação de desidrogenação do metano na superfície da platina durante o processo de oxidação [3].

O estudo da adsorção de metano por diferentes técnicas eletroquímicas indica que o eletrodo contém uma camada adicional das espécies de carbono, que são consideradas como espécies parcialmente oxigenadas. Na polarização anódica do eletrodo a reação de eletrooxidação de metano ocorre em potenciais que precedem a evolução de oxigênio produzindo CO_2 e íons H^+ com praticamente 100% de eficiência [3].

A adsorção de metano nos eletrodos de platina é estudada de duas maneiras. Uma mantendo-se o tempo de adsorção constante e variando-se o potencial de adsorção e outra mantendo-se o potencial constante enquanto se varia o tempo de deposição [3]. No presente trabalho, manteve-se o potencial constante, na faixa de adsorção de hidrogênio (50 mV) antes de fazer os voltamogramas, com o objetivo de forçar a adsorção de metano no eletrodo, tendo-se em vista que a adsorção desta molécula de forma espontânea (em potencial de circuito aberto) não ocorre de forma significativa sobre platina. O tempo de adsorção foi definido no sentido de se obter um recobrimento limite de metano na superfície.

Eletrodos Modificados

Os eletrodos de platina têm se mostrado pouco eficientes quando empregados isoladamente, já que potenciais excessivamente altos são necessários para obter densidades de corrente satisfatórias. Neste sentido, tem-se buscado adicionar outros metais à platina, os quais modificam as propriedades superficiais do eletrodo e favorecem a oxidação de moléculas orgânicas em potenciais mais baixos [4-6]. Os principais metais utilizados juntamente com a platina na confecção de superfícies eletrocatalíticas são: Ru, Os, Rh, Sn, Ti, entre outros. Estes metais apresentam uma

289

Orbital Elec. J. Chem., Campo Grande, 2(3): 288-302, 2010

importante característica em comum, a capacidade de formação de espécies oxigenadas em sua superfície em potenciais mais baixos que aquele observado sobre a platina [7].

É bem conhecido na literatura que o aumento da atividade catalítica de um eletrodo de platina em reações de oxidação de pequenas moléculas orgânicas, após adição de outros metais, dê-se por meio de um mecanismo bifuncional, segundo o qual, estes metais atuam como sítios ativos que promovem a transferência de espécies oxigenadas para a molécula orgânica adsorvida em suas vizinhanças [7, 8]. Entretanto, estudos recentes têm mostrado também que alguns metais, quando combinados com a platina, melhoram a atividade catalítica do eletrodo por meio de um efeito eletrônico de redução da energia de adsorção da molécula de CO, a partir da interação entre os orbitais 4d e 5d destes metais [9, 10].

A modificação de um eletrodo de platina pura pode ser feita por meio da eletrodeposição de uma película de outro material metálico, de um óxido do mesmo ou de outro metal ou ainda de um polímero eletroquimicamente ativo. Quando se trata da deposição de um filme metálico, a reação deixa de ocorrer sobre o metal de base do eletrodo e passa a ocorrer somente sobre o novo metal [11], observando-se propriedades eletrocatalíticas totalmente diferentes.

Deste modo, tem-se dado grande atenção ao estudo em nível fundamental de superfícies eletrocatalíticas lisas, tais como depósitos metálicos superficiais [12, 13] ou mesmo ligas metálicas reais [14-17], embora o estudo com estas últimas seja mais difícil, uma vez que na superfície destas ligas pode ocorrer segregação, perdendo-se o controle das quantidades de cada metal na superfície, ainda que, no seio da liga metálica a composição não varie. Além disso, os altos potenciais usados para limpeza do eletrodo podem provocar a perda dos metais menos nobres, alterando-se também a composição superficial. Já com depósitos metálicos superficiais, a superfície do eletrodo é renovada ao final de cada ensaio, favorecendo a correlação entre a atividade catalítica da superfície e sua composição.

Tanto em estudos envolvendo eletrodepósitos como em estudos com ligas reais, o sistema Pt-Ru tem apresentado maior atividade catalítica para a oxidação de metanol [18-20], em comparação com outros eletrodos binários compostos por platina e um segundo metal [7], inclusive o ósmio [21]. Porém, estudos recentes demonstraram que eletrodos ternários do tipo Pt-Ru-Os apresentam melhor atividade catalítica para esta reação, quando comparados ao eletrodo Pt-Ru [15, 16, 21]. Estas informações confirmam uma nova tendência: a utilização de um método combinatório para o desenvolvimento de eletrodos ternários e quaternários compostos por diferentes proporções de Pt, Ru, Os, Ir e/ou Rh, os quais podem apresentar propriedades eletrocatalíticas promissoras para aplicações em células a combustível com oxidação

Orbital Elec. J. Chem., Campo Grande, 2(3): 288-302, 2010

290

direta de pequenas moléculas orgânicas [22].

O principal desafio no desenvolvimento de superfícies eletrocatalíticas para a oxidação de pequenas moléculas orgânicas reside ainda no tempo de vida útil do eletrodo, devido ao processo de envenenamento superficial provocado pela forte adsorção das espécies intermediárias formadas nestas reações. Outro problema é o alto custo dos metais envolvidos na preparação destes catalisadores. Por estes motivos, os eletrocatalisadores de aplicação tecnológica apresentam apenas uma pequena quantidade destes metais dispersos como nanopartículas em um substrato de carbono [23, 24].

O titânio é um metal muito passivo, ou seja, não é facilmente oxidado por agentes oxidantes médios. O seu potencial padrão é de 1,63 V e esse elevado valor positivo indica que o titânio metálico não pode ser depositado a partir de soluções aquosas mediante redução catódica.

Os estados de oxidação mais comuns para o titânio são, +4, +3 e +2. O mais estável e mais importante estado de oxidação é +4, pois na natureza o titânio é encontrado principalmente na forma de rutilo (TiO_2) [25].

Esse metal tem a propriedade de absorver hidrogênio. Além disso, pode adsorver oxigênio em quantidades consideráveis, formando soluções sólidas [25]. A fácil adsorção de oxigênio neste metal torna-o interessante para a aplicação em estudos de eletrocatálise de processos oxidativos.

A interação entre platina e titânio, a qual tem se mostrado eletrocataliticamente eficaz, incentivou a investigação do comportamento eletroquímico de depósitos de platina/titânio a partir de vários métodos. Sabe-se que o TiO_2 é um material semicondutor, o qual tem sido amplamente aplicado em células solares fotoeletroquímicas, na degradação fotoeletrocatalítica de contaminantes orgânicos e em dispositivos eletrocrômicos. As propriedades eletroquímicas dos eletrodos modificados com TiO_2 em diferentes eletrólitos têm sido amplamente estudadas por técnicas de voltametria, cronoamperometria e impedância e espectroeletroquímica [26].

Geralmente, estes eletrodos são obtidos por quatro métodos, como por exemplo, processo de eletrodeposição, pirólise térmica de metais, processo sol-gel e revestimento comercial de TiO_2. No entanto, os dois primeiros métodos só podem ser preparados usando-se um substrato de titânio, enquanto os dois últimos métodos exigem temperatura elevada para reforçar a estabilidade do filme de óxido sobre o substrato [26].

De acordo com Mentus [27], um método eficaz de se produzir camadas de Pt/TiO_2 é a partir da eletrodeposição ou mesmo deposição espontânea de platina sobre um

Orbital Elec. J. Chem., Campo Grande, 2(3): 288-302, 2010

291

eletrodo de titânio, a partir de uma solução de ácido hexacloroplatínico (H_2PtCl_6). Segundo o autor, as superfícies produzidas a partir desse método mostraram-se altamente reprodutíveis em termos de composição e estrutura, além de apresentarem alta atividade catalítica e resposta eletroquímica bem definida.

No presente trabalho, optou-se pela modificação superficial de eletrodos monocristalinos de platina pela deposição eletroquímica de titânio a partir de uma solução de Ti^{3+}.

Material e Métodos

Obtenção dos voltamogramas de platina antes e após borbulhamento de gás metano

Os eletrodos Pt(100) e Pt(110), previamente tratados termicamente em chama de hidrogênio por tempos em torno de 30 minutos e resfriados em atmosfera inerte, foram caracterizados por voltametria cíclica em solução eletrolítica de H_2SO_4 (*Vetec a 95-99%*) 0,1 mol L^{-1} saturada com nitrogênio (*Linde a 99,999%*), com velocidade de varredura de 100 mV s^{-1} e em configuração de menisco, dentro de uma célula eletroquímica de duplo compartimento confeccionada em vidro, cujo modelo é demonstrado na Figura 1, entre os potenciais de 0,05 e 1,6 V tendo como eletrodo de referência um Eletrodo Reversível de Hidrogênio. Todos os procedimentos envolvidos neste trabalho foram realizados em temperatura ambiente (~25ºC).
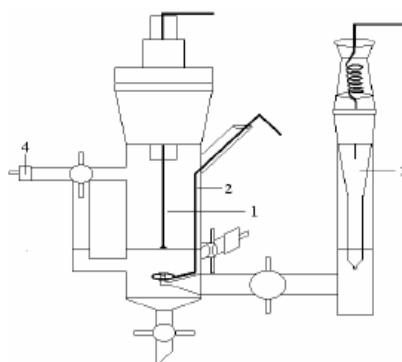
Figura 1. Modelo de célula eletroquímica de vidro utilizada. **1.** Eletrodo de trabalho; **2.** Contra-eletrodo; **3.** Eletrodo de referência (ERH); **4.** Borbulhador de nitrogênio.

Em seguida, estudou-se eletroquimicamente a atividade catalítica dos eletrodos Pt(100) e Pt(110) na oxidação do metano, devido às duas superfícies apresentarem propriedades totalmente diferentes: enquanto a primeira consiste de uma superfície idealmente lisa, a segunda apresenta defeitos regulares em forma de degraus, tornando interessante a comparação.

292

Orbital Elec. J. Chem., Campo Grande, 2(3): 288-302, 2010

Realizou-se o procedimento da mesma forma que o anterior, porém borbulhando-se na solução excesso de gás metano (*Aga a 99,995%*). Neste sentido, saturou-se previamente a solução eletrolítica com gás metano durante cerca de 5 minutos e provocou-se a adsorção do gás sobre a superfície em condições de potencial controlado (50 mV) durante 10 minutos, registrando-se em seguida os primeiros ciclos voltamétricos de oxidação de metano entre 0,05 e 1,5 V vs. ERH, com velocidade de varredura de 100 mV s^{-1}.

Deposição de titânio sobre os eletrodos de platina

As deposições de titânio sobre os eletrodos monocristalinos de platina foram realizadas partindo-se de uma solução de tricloreto de titânio (*Vetec a 15%*) diluída em ácido sulfúrico 0,1 mol L^{-1} obtendo-se uma concentração de 10% de titânio. Os depósitos foram obtidos por deposição espontânea (em potencial de circuito aberto) durante diferentes tempos que variaram entre 5 e 720 segundos.

Após cada deposição, registrou-se os primeiros ciclos voltamétricos dos eletrodos entre 0,05 e 1,0 V vs. ERH com velocidade de varredura de 100 mV s^{-1}, para caracterização eletroquímica de titânio. Evitaram-se potenciais maiores que 1,0 V, a fim de que não ocorresse a dessorção dos depósitos de titânio.

Obtenção dos voltamogramas dos eletrodos de platina modificados após borbulhamento de gás metano

Após a caracterização voltamétrica da superfície, iniciou-se o estudo da atividade catalítica do eletrodo Pt-Ti na eletrooxidação de metano. Para isto, optou-se por analisar as superfícies com o maior grau de recobrimento possível de titânio obtido por deposição espontânea, cerca de 27% para Pt(110) e 36% para Pt(100). Nesta etapa, assim como na seção 2.2, saturou-se previamente a solução eletrolítica com gás metano durante cerca de 5 minutos e provocou-se a adsorção do gás sobre a superfície em condições de potencial controlado (50 mV) durante 10 minutos, registrando-se em seguida os primeiros ciclos voltamétricos de oxidação de metano entre 0,05 e 1,5 V vs. ERH, com velocidade de varredura de 100 mV s^{-1}.

Resultados e Discussão

Identidade voltamétrica dos eletrodos monocristalinos de platina

Os voltamogramas cíclicos da Pt(100) e Pt(110) em solução de H_2SO_4 0,1 mol L^{-1} estão representados nas Figuras 2 e 3, respectivamente. Uma característica comum aos voltamogramas dos dois eletrodos é a presença de picos bastante agudos, característicos de cada face. Estes picos ocorrem como conseqüência da alta organização superficial dos eletrodos, isenta de defeitos, devido ao processo de tratamento térmico realizado

Orbital Elec. J. Chem., Campo Grande, 2(3): 288-302, 2010

293

previamente.
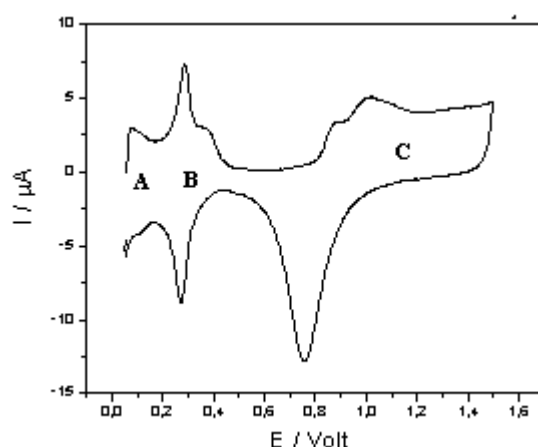
Figura 2. Voltamograma cíclico da Pt(100) em H_2SO_4 0,1mol L^{-1}, a 100 mV s^{-1}.

O voltamograma da Pt(100) apresenta picos característicos nas regiões A e B, que são bem diferentes daqueles existentes no voltamograma do eletrodo de platina policristalina. A Pt(100) possui máximos nesses potenciais e segundo Clavilier et al. [1, 28-30] o pico intenso em torno de 0,3 V é atribuído ao processo de dessorção de hidrogênio fortemente adsorvido sobre as plataformas formadas pelo plano atômico (100), nas quais o hidrogênio interage com 4 átomos de platina.

A diminuição drástica do pico em 0,3 V e o aumento do pico em torno de 0,2 V, bem como o alargamento de um pico entre 0,05 e 0,2 V, são indícios de que o eletrodo sofreu reestruturação superficial. Estas características devem-se à dessorção de hidrogênio fracamente adsorvido sobre os degraus existentes entre as ilhas formadas no eletrodo após a reconstrução superficial, quando aplicados potenciais maiores que 0,8 V (região C) [31, 32]. A partir deste potencial ocorre a formação de óxidos superficiais sobre a Pt(100). Segundo Conway et al. [33], as espécies oxigenadas responsáveis pela reconstrução superficial do eletrodo são Pt(OH)$_{ads}$ e PtO(H$_2$O)$_{ads}$.
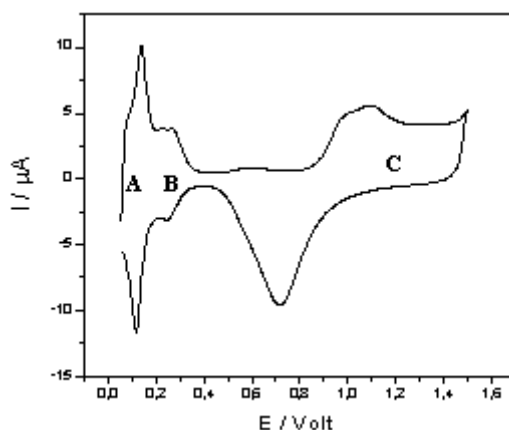
Figura 3. Voltamograma cíclico da Pt(110) em H_2SO_4 0,1mol L^{-1}, a 100 mV s^{-1}.

294

Orbital Elec. J. Chem*., Campo Grande,* 2(3): 288-302, 2010

No voltamograma cíclico da Pt(110), observa-se um pico intenso em 0,125 V (região A) correspondente ao hidrogênio fracamente adsorvido sobre os sítios em forma de degraus, comuns a esta face [34, 35, 36] (vide Figura 4), nos quais o hidrogênio se coordena com um ou dois átomos de platina.

Nas condições de potencial em que a adsorção de espécies oxigenadas é favorecida (região C, entre 0,8 e 1,45 V), a Pt(110) sofre reestruturação superficial por causa da perda de fileiras intercaladas de átomos na direção (110) [34, 36, 37]. Esta transição de estrutura forma microfacetas com orientação (111) sobre o eletrodo, conforme mostra a Figura 4. Isto provoca um alargamento do pico característico da Pt(110) (região A), diminuindo sua intensidade em relação a região B.
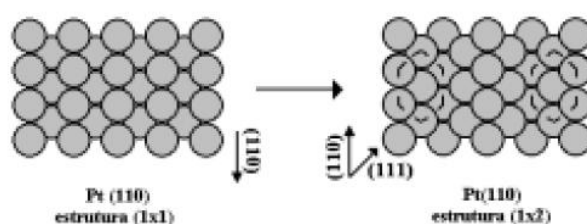
Figura 4. Reconstrução superficial típica, sofrida pela face (110) após um primeiro ciclo voltamétrico do eletrodo até potenciais em que a adsorção de oxigênio é favorecida.

Perfis voltamétricos de oxidação de metano sobre os eletrodos de platina

Os voltamogramas cíclicos dos eletrodos monocristalinos de platina, após o borbulhamento de gás metano, são mostrados nas Figuras 5 e 6.
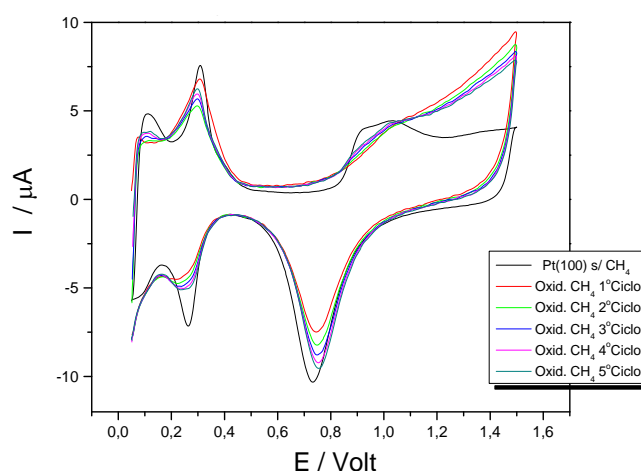
Figura 5. Voltamogramas de oxidação de metano sobre Pt(100), a 100 mV s^{-1}.

A partir dos baixos valores de corrente anódica acima daqueles atribuídos à oxidação da platina (figuras 5 e 6), é possível observar a pequena quantidade de metano adsorvido sobre os eletrodos de platina, o qual é totalmente oxidado e dessorvido do eletrodo em poucos ciclos voltamétricos. Isto é um forte indício de que o metano tem

Orbital Elec. J. Chem., Campo Grande, 2(3): 288-302, 2010

295

fraca interação com a superfície de platina, mesmo em 50 mV. Outro aspecto é que a quantidade de metano na dupla camada elétrica do eletrodo é muito pequena, pelo fato de o metano ser pouco solúvel no eletrólito ($\sim$ 1,5 10^{-3} mol L^{-1} ou 24 ppm [38]).
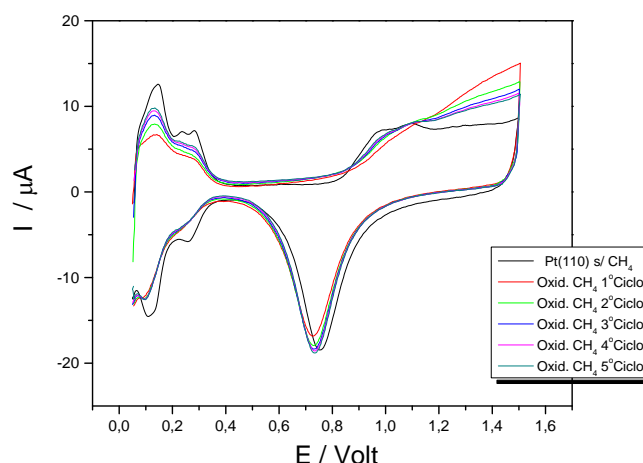

Figura 6. Voltamogramas de oxidação de metano sobre Pt(110), a 100 mV s^{-1}.

Ainda que as correntes observadas no eletrodo (100) sejam menores que aquelas no eletrodo (110), isto é apenas um efeito de área ativa, visto que o último eletrodo apresenta maior superfície. Entretanto, observa-se que as correntes atribuídas à oxidação de metano são proporcionalmente maiores no eletrodo (100), o que sugere que a interação da molécula orgânica é mais favorecida sobre as plataformas (100) que sobre os degraus (110).

Perfis voltamétricos dos eletrodos modificados

Nas Figuras 7 e 8, encontram-se respectivamente os voltamogramas da Pt(100) e Pt(110) modificadas com depósito espontâneo de titânio, a partir de soluções de cloreto de titânio III a 10%.
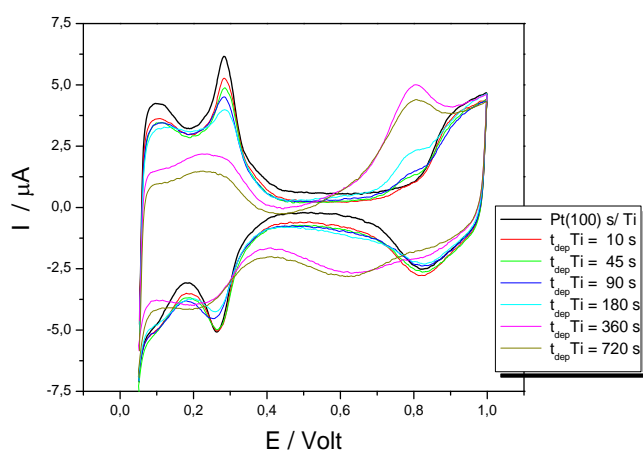
Figura 7. Voltamogramas da Pt(100) após diferentes tempos de deposição de titânio entre 10 e 720 s , com velocidade de varredura de 100 mV s^{-1}.

296

Orbital Elec. J. Chem*., Campo Grande, 2(3): 288-302, 2010*

Na Figura 7 surge uma onda anódica em potenciais ligeiramente menores que os observados na platina pura (entre 0,6 e 0,9 V), atribuída à oxidação dos depósitos de titânio [26]. A deposição de titânio sobre Pt(100) é efetiva, mas os graus de recobrimento de titânio estimados a partir da supressão dos picos de dessorção de hidrogênio não superam 36% de uma monocamada.
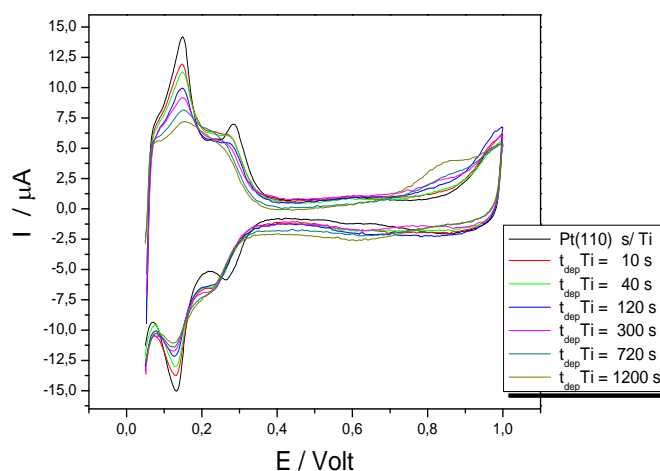
Figura 8. Voltamogramas da Pt(110) após diferentes tempos de deposição de titânio entre 10 e 1200 s , com velocidade de varredura de 100 mV s^{-1}.

A partir dos voltamogramas da Figura 8, é possível observar que o grau de recobrimento dos depósitos sobre Pt(110) é menor que sobre Pt(100). Isto pode ser devido à forte presença de degraus na face (110), o que torna a interação do depósito mais fraca, uma vez que esta interação ocorre nos topos dos degraus. Dessa forma, obteve-se um valor de recobrimento não maior que 27% mesmo após tempos mais longos de deposição.

O método de estimativa de grau de recobrimento dos depósitos baseou-se no fato de que os voltamogramas indicam que a adsorção de hidrogênio não ocorre sobre os depósitos, cuja composição é preferencialmente óxido de titânio [26]. Desta forma, pode-se determinar o grau de recobrimento de hidrogênio sobre cada eletrodo modificado e a partir da comparação desses valores com aquele obtido sobre platina pura é possível estimar o recobrimento dos depósitos nos eletrodos [39], utilizando-se as equações 1 e 2:

$$\theta_H = \frac{Q^H_{Pt-Ti}}{Q^H_{Pt}} \quad (1) \qquad \theta_{Ti} = 1 - \theta_H \quad (2)$$

onde, θ_H é o grau de recobrimento de hidrogênio, θ_{Ti} é o grau de recobrimento dos depósitos de titânio, Q^H_{Pt-Ti} é a carga de hidrogênio na superfície de platina modificada

297

Orbital Elec. J. Chem., Campo Grande, 2(3): 288-302, 2010

com depósito de titânio e $Q^H{}_{Pt}$ é a carga de hidrogênio na superfície de platina pura.

As cargas de oxidação de hidrogênio e os respectivos graus de recobrimento dos depósitos de titânio são apresentados nas tabelas 1 e 2, respectivamente.

Tabela 1. Valores das cargas de oxidação de hidrogênio e dos respectivos graus de recobrimento dos depósitos de titânio sobre Pt(100), v = 100 mV s^{-1}

$t_{deposição}$ Ti (s)	Q^H (I.t)	θ_{Ti}
0	1,01 10^{-6} / v	0
10	9,94 10^{-7} / v	0,02
45	9,22 10^{-7} / v	0,09
90	9,04 10^{-7} / v	0,11
180	8,38 10^{-7} / v	0,17
360	7,17 10^{-7} / v	0,29
720	6,48 10^{-7} / v	0,36

Tabela 2. Valores das cargas de oxidação de hidrogênio e dos respectivos graus de recobrimento dos depósitos de titânio sobre Pt(110) , v = 100 mV s^{-1}

| $t_{deposição}$ Ti (s)	Q^H (I.t)	θ_{Ti}
0	1,91 10^{-6} / v	0
10	1,75 10^{-6} / v	0,08
40	1,70 10^{-6} / v	0,11
120	1,55 10^{-6} / v	0,19
300	1,45 10^{-6} / v	0,24
720	1,40 10^{-6} / v	0,27
1200	1,40 10^{-6} / v	0,27

Apesar de os valores de θ_{Ti} sobre Pt(100) parecerem não ter atingido um valor máximo após 720 s de deposição, quando estimados a partir da supressão dos picos de hidrogênio, a onda anódica correspondente à oxidação dos depósitos de titânio não apresenta nenhum acréscimo efetivo após os tempos de deposição de 360 e 720 s, dando um forte indício de que o grau de recobrimento não vai além dos 36% de uma monocamada.

Os baixos graus de recobrimento desses depósitos sobre ambos os eletrodos de platina estão de acordo com a formação preferencial de óxido de titânio sobre a superfície, uma vez que estes não têm a mesma capacidade de interação química com a platina que teria o titânio metálico, além da repulsão lateral entre os átomos de oxigênio, o que limita significativamente os valores dos graus de recobrimento. A formação preferencial de TiO$_2$ a partir da deposição espontânea de titânio está de acordo com a literatura, que demonstra que a formação de titânio metálico é dificultada mesmo em condições de eletrodeposição catódica [25].

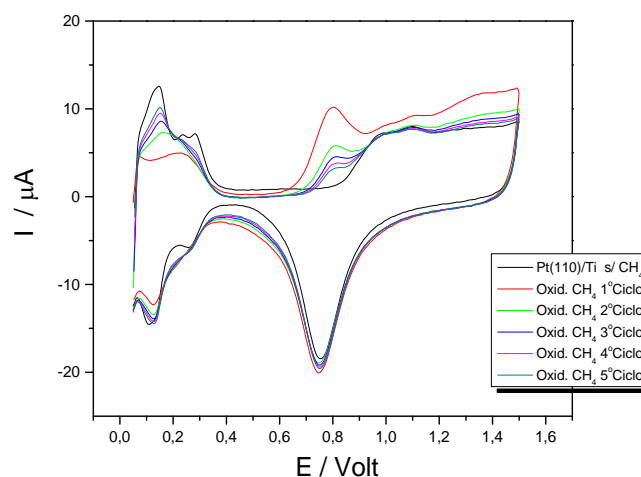### *Perfis voltamétricos de oxidação de metano sobre os eletrodos modificados*

Os perfis voltamétricos de oxidação de metano sobre os eletrodos de platina com depósitos de titânio são bem diferentes daqueles observados nos eletrodos de platina

Orbital Elec. J. Chem., Campo Grande, 2(3): 288-302, 2010

298

sem depósitos. Para Pt(100) com depósitos de titânio (Figura 9) pode-se observar o surgimento de uma onda anódica entre 0,5 e 0,9 V, atribuída ao processo de oxidação da molécula orgânica [40].
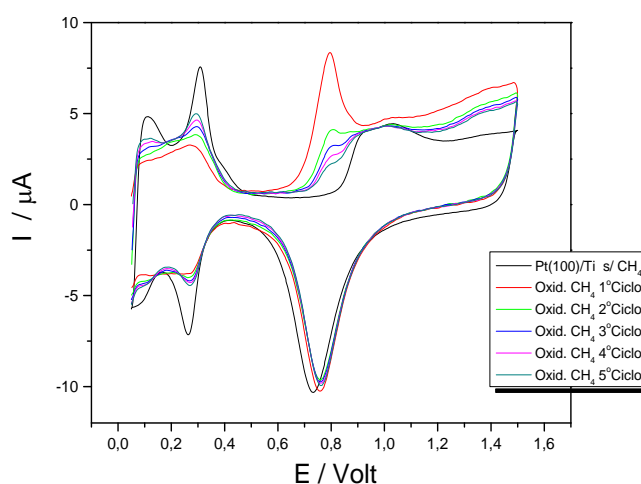
Figura 9. Voltamogramas de oxidação de metano sobre Pt(100)/Ti, a 100 mV s^{-1}.

No voltamograma para Pt(110) (Figura 10), também é possível observar o surgimento da onda anódica entre 0,5 e 0,9 V. Entretanto, esta onda é bem menos intensa que a observada sobre o eletrodo de Pt(100) modificado.

Figura 10. Voltamogramas de oxidação de metano sobre Pt(110)/Ti, a 100 mV s^{-1}.

O processo de oxidação de metano sobre os eletrodos modificados, ocorre em potenciais bem menores que aqueles observados para platina pura, dando um forte indício da influência dos depósitos de titânio no aumento na atividade catalítica do eletrodo sobre a reação.

Um aspecto que deve ser considerado em ambos os voltamogramas (Figuras 9 e 10) é que a presença do metano adsorvido e oxidado no 1º ciclo fornece uma espécie de blindagem ao depósito de titânio, evitando que este seja dessorvido no 1º ciclo. Assim, a

299

Orbital Elec. J. Chem*., Campo Grande,* 2(3): 288-302, 2010

onda anódica que ocorre entre 0,6 e 0,9 V do 2º ciclo em diante pode estar associada somente à oxidação progressiva dos depósitos de titânio até a dessorção total e recuperação do perfil voltamétrico da platina após alguns ciclos.

Conclusão

A deposição de titânio no eletrodo de platina foi obtida com êxito, uma vez que houve o aparecimento de uma onda anódica em potenciais menores do que aqueles observados na platina pura. No entanto, os valores de grau de recobrimento foram considerados baixos, pois na Pt(100) não ultrapassou 36% e na Pt(110) não ultrapassou 27% de uma monocamada. Esta última foi menor devido a sua superfície em forma de degraus, o que torna a interação entre platina e titânio mais fraca.

O metano mostrou-se uma molécula orgânica de difícil adsorção sobre os eletrodos de platina, já que os valores de corrente anódica foram baixos, ficando apenas um pouco acima daqueles atribuídos à oxidação da platina. Isto se deve à pequena quantidade de metano na solução devido à sua baixa solubilidade em água.

Já a oxidação da molécula orgânica nos eletrodos modificados pela deposição de titânio mostrou-se mais eficiente do que sobre a platina pura, uma vez que as correntes de oxidação foram ligeiramente maiores e o processo ocorreu em potenciais bem menores do que aqueles observados nos eletrodos de platina não modificados.

Agradecimentos

Referências e Notas

[1]   Feliu, J. M.; Rodes, A.; Orts, J. M.; Clavilier, J. *Pol. J. Chem*. **1994**, *68*, 1575.

[2]   Vielstich, W. Fuel Cells: Modern processes for the electrochemical production of energy. New York: Wiley, 1970.

[3]   Sustersic, M. G.; Córdova, R.; Triaca, W. E.; Arvia, A. J. *J. Electrochemical* **1980**, *127*, 1242.

[4]   Souza, J. P. I.; Rabelo, F. J. B.; Moraes, I. R.; Nart, F. C. *J. Electroanal. Chem*. **1997**, *420*, 17.

[5]   Pacheco Santos, V.; Tremiliosi-Filho, G. *J. Electroanal. Chem*. *2003*, *554-555*, 395.

[6]   Souza, J. P. I.; Queiroz, S. L.; Bergamaski, K.; Gonzalez, E. R.; Nart, F. C. J*. Phys. Chem.* **2002**, *106*, 9825.

[7]   Janssen, M. M. P.; Moolhuysen, J. *Electrochim. Acta* **1976**, *21*, 869.

[8]   Gasteiger, H. A.; Markovic, N.; Ross, P. N.; Cairns, E. J. *J. Phys. Chem.* **1993**, *97*, 12020.

Orbital Elec. J. Chem*., Campo Grande*, 2(3): 288-302, 2010

300

[9] Christoffersen, E.; Liu, P.; Ruban, A.; Skriver, H. L.; Norskov, J. K. *J. Catal*. **2001**, *199*, 123.

[10] Babu, P. K.; Kim, H. S.; Oldfield, E.; Wieckowski, A. *J. Phys. Chem*. **2003**, *107*, 7595.

[11] Ticianelli, E. A.; Gonzalez, E. R.; Eletroquímica: Princípios e Aplicações; 2ª Ed., São Paulo: Editora da Universidade de São Paulo, 2005.

[12] Schmidt, V. M.; Ianniello, R.; Pastor, E.; González, S. *J. Phys. Chem*. **1996**, *100*, 17901.

[13] Ianniello, R.; Schmidt, V. M.; Rodríguez, J. L.; Pastor, E. *J. Electroanal. Chem*. **1999**, *471*, 167.

[14] Liu, R.; Iddir, H.; Fan, Q.; Hou, G.; Bo, A.; Ley, K. L.; Smotkin, E. S.; Sung, Y. E.; Kim, H.; Thomas, S.; Wieckowski, A. *J.Phys. Chem*. 2000, **104**, 3518.

[15] Ley, K. L.; Liu, R.; Pu, C.; Fan, Q.; Leyarovska, N.; Segre, C.; Smotkin, E. S. *J. Electr. Soc*. **1997**, *144*, 1543.

[16] Gurau, B.; Viswanathan, R.; Liu, R.; Lafrenz, T. J.; Ley, K. L.; Smotkin, E. S.; Reddington, E.; Sapienza, A.; Chan, B. C.; Mallouk, T. E.; Sarangapani, S. *J. Phys. Chem.* **1998**, *102*, 9997.

[17] Kokoh, K. B.; Hahn, F.; Belgsir, E. M.; Lamy, C.; Andrade, A. R.; Olivi, P.; Motheo, A. J.; Tremiliosi-Filho, G. *Electrochim. Acta* **2004**, *49*, 2077.

[18] Tremiliosi-Filho, G.; Kim, H.; Chrzanowski, W.; Wieckowski, A.; Grzybowska, B.; Kulesza, P. *J. Electroanal. Chem*. **1999**, *467*, 143.

[19] Chrzanowski, W.; Kim, H.; Tremiliosi-Filho, G.; Wieckowski, A.; Grzybowska, B.; Kulesza, P. *J. New Mat. Electrochem. Syst*. **1998**, *1*, 31.

[20] Frelink, T.; Visscher, W.; Van Veen, J. A. R. *Surf. Sci*. *1995*, *335*, 353.

[21] Crown, A.; Kim, H.; Lu, G. Q.; Moraes, I. R. de; Rice, C.; Wieckowski, A. *J. New Mat. Electrochem. Syst*. *2000*, *3*, 275.

[22] Reddington, E.; Sapienza, A.; Gurau, B.; Viswanathan, R.; Sarangapani, S.; Smotkin, E. S.; Mallouk, T. E. *Science* **1998**, *280*, 1735.

[23] Radmilovic, V.; Gasteiger, H. A.; Ross, Jr. P. N. *J. Catal*. **1995**, *154*, 98.

[24] Delime, F.; Léger, J. -M.; Lamy, C. *J. Appl. Electrochem*. **1998**, *28*, 27.

[25] Ohlweiler, O. A.; Química Inorgânica. São Paulo: Edgard Blücher, 1971-1972, v. 2.

[26] Zhanga, J.; Yanga, C.; Changb, G.; Zhua, H.; Oyamab, M. *Mater. Chem. Phys*. **2004**, **88**, 398.

[27] Mentus, S. V. *Electrochim. Acta* **2005**, **50**, 3609.

[28] Clavilier, J.; Armand, D. *J. Electroanal. Chem*. **1986**, *199*, 187.

[29] Clavilier, J.; Armand, D.; Sun, S. G.; Petit, M. *J. Electroanal. Chem*. **1986**, *205*, 267.

[30] Rodes, A.; Clavilier, J. *J. Electroanal. Chem*. **1992**, *338*, 317.

[31] Furuya, N.; Shibata, M. J*. Electroanal. Chem*. **1999**, *467*, 85.

[32] Kolb, D. M. *Electrochim. Acta* **2000**, *45*, 2387.

[33] Angerstein-Kozlowska, H.; Conway, B. E.; Sharp, W. B. A. *Electroanal. Chem. Interf. Electrochem*. **1973**, *43*, 9.

[34] Kibler, L. A.; Cuesta, A.; Kleinert, M.; Kolb, D. M. J*. Electroanal. Chem*. **2000**, *484*,

301

Orbital Elec. J. Chem*., Campo Grande*, 2(3): 288-302, 2010

73.

[35] Gómez, R.; Clavilier, J. *J. Electroanal. Chem*. **1993**, *354*, 189.

[36] Markovic, N. M.; Grgur, B. N.; Lucas, C. A.; Ross, P. N. *Surf. Sci*. **1997**, *384*, 805.

[37] Speller, S.; Kuntze, J.; Rauch, T.; Bömermann, J.; Huck, M.; Aschoff, M.; Heiland, W. *Surf. Sci*. **1996**, *366*, 251.

[38] Disponível em: http://www.gamagases.com.br/propriedades_metano.htm. Acesso em outubro de 2009.

[39] Pacheco Santos, V.; Del Colle, V.; Bezerra, R. M.; Tremiliosi-Filho, G. *Electrochim. Acta* **2004**, *49*, 1221.

[40] Hamelin, A. Modern Aspects of Electrochemistry. New York: Plenum Press, 1985, v.16.

302

Orbital Elec. J. Chem*., Campo Grande,* 2(3): 288-302, 2010

Full Paper

Synthesis, characterization and antibacterial activity of new salicylhydrazide containing azopyrazoles

Bhupendra P. Patel*, Hasmukh S. Patel, Purvesh J. Shah

Department of Chemistry, Sardar Patel University, Vallabh Vidyanagar- 388120, India

ABSTRACT: *Various ethyl-2-substituted phenyl hydrazono-3-oxobutyrate (2a-h) condensation with 2-hydroxy benzoic acid hydrazide (3) to afford 1-(2-hydroxybenzoyl)-3-methyl-4-(2- substituted phenyl hydrazono)-1H-pyrazol-5(4H)-one (4a-h). The structures of all these compounds (4a-h) were recognized on basis of analytical and spectral data. The newly synthesized compounds were evaluated for their antimicrobial activity against various bacteria and fungi.*

Keywords: *pyrazoline-5-one; salicylhydrazide; antimicrobial activity; spectral studies*

Introduction

The arylazopyrazoles are generally prepared by combination of aryl-azo-ethyl actoacetate derivatives and hydrazine derivatives [1-6]. Hydrazide and their heterocyclised products display diverse biological activities including antibacterial, antifungicidal, analgesic, anti-inflammatory properties [7-21].These heterocyclic systems find wide use in medicine, agriculture and industry. One of the hydrazides, 2-hydroxy benzoic acid hydrazide (i.e. salicylhydrazide) and their condensed products play a vital role in medicinal chemistry [22-24]. Hence, it was thought of interest to merge both of arylazopyrazole and salicylhydrazide moieties which may enhance the drug activity of compounds to some extent, or they might possess some of the above mentioned biological activities. From this point of view, the objective of the present work is to prepare new derivatives of salicylhydrazide containing arylazopyrazole moiety. Hence the present communication comprises the synthesis of 1-(2-hydroxybenzoyl)-3-methyl-4-(2-substituted phenyl hydrazono)-1H-pyrazol-5(4H)-one (4a-h).

---

* Corresponding author. E-mail: drbppatel1948@yahoo.com

Material and Methods

Materials

All chemicals used were of laboratory grade. Salicylhydrazide were prepared by reported method [25].

Measurement

Melting points were determined in open capillary tubes and were uncorrected. The IR spectra were recorded in KBr pellets on a Nicolet 400D spectrometer and ^{1}H NMR and ^{13}C NMR spectra were recorded in DMSO with TMS as internal standard on a Bruker spectrometer at 400 MHz and 100 MHz, respectively. LC-MS of all novel samples taken on LC-MSD-Trap-SL_01046 instrument. Purity of compound was checked by TLC on silica gel plates and the spots were visualized by UV lamp.

Chemistry

Synthesis of ethyl-2-substituted phenyl hydrazono-3-oxobutyrate (2a-h)

Substituted aniline (**1a-h**) (0.01mole) was dissolved in a mixture of HCl (8 mL) and water (6 mL) and cooled to 0 °C in ice bath. To it a cold aqueous solution of sodium nitrate (0.03 mole) was added. The diazonium salt solution was filtered into a cooled solution of ethyl acetoacetate (0.01 mole) and sodium acetate (0.12 mole) in ethanol (50 mL). The resulting solid was washed with water and recrystallized from EtOH/MeOH. The yields, melting points and other characterization data of these compounds are given in Table 1.

Synthesis of 1-(2-hydroxybenzoyl)-3-methyl-4-(2-substituted phenyl hydrazono)-1H-pyrazol-5(4H)-one (4a-h)

To ethyl-2-substituted phenyl hydrazono-3-oxobutyrate (**2a-h**) (0.002 mole) dissolved in glacial acetic acid (20 mL), a solution of 2-hydroxy benzoic acid hydrazide (**3**) (0.002 mole) in 25 mL of glacial acetic acid was added and the mixture was refluxed 10-12 hrs. It was then cooled and allowed to stand overnight. The resulting solid was filtered off dried and crystallized from methanol. The yields, melting points and other characterization data of these compounds are given in Table 2.

Biological Screening

Antibacterial activities

Antibacterial activities of all the compounds were studied against gram-positive bacteria (*Bacillus subtilis and Staphylococcus aureus*) and gram-negative Bacteria (*E. coli, Salmonella typhi and Klebsiella promioe*) at a concentration of 50 µg/mL by agar cup plate method [26]. Methanol system was used as control in this method. Under similar

Orbital Elec. J. Chem*., Campo Grande,* 2(3): 303-310, 2010

304

conditions, using tetracycline as a standard for comparison, we carried out a control experiment. The area of inhibition of measured in millimeters Table 3.

Antifungal activity

The fungicidal activity of all the compounds (**4a-h**) was studied at 1000 ppm concentration in vitro plant pathogenic organisms listed in Table 4. The antifungal activities of all the samples were measured on each of these plant pathogenic strains on potato dextrose agar (PDA) medium. Such a PDA medium contained potato 200 gms, dextrose 20 gms, agar 20 gms and water 1 liter five days old cultures were employed. The compounds to be tested were suspended (1000 ppm) in a PDA medium and autoclaved at 120 °C for 15 min. at 15 atm pressure. These medium were poured into sterile Petri plate and the organisms were inoculated after cooling the Petri plate. The percentage inhabitation for fungi was calculated after 5 days using the formula given below.

Percentage of inhibition = 100(X-Y)/X
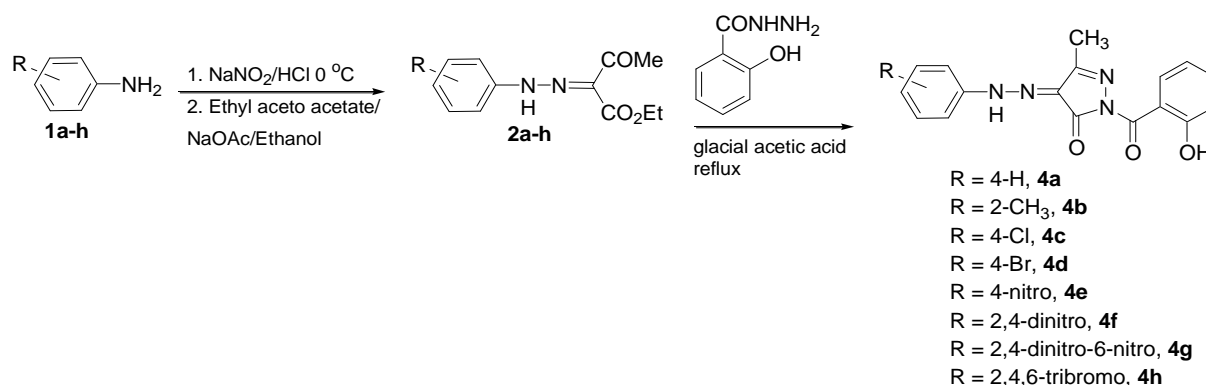
Where, X: Area of colony in control plate

Y: Area of colony in test plate

The fungicidal activity all compounds (**4a-h**) are shown in Table 4.

Results and Discussion

Our synthetic approach is shown in scheme 1.

Scheme 1

R = 4-H, **4a**
R = 2-CH$_3$, **4b**
R = 4-Cl, **4c**
R = 4-Br, **4d**
R = 4-nitro, **4e**
R = 2,4-dinitro, **4f**
R = 2,4-dinitro-6-nitro, **4g**
R = 2,4,6-tribromo, **4h**

It was observed that ethyl-2-substituted phenyl hydrazono-3-oxobutyrate (**2a-h**) condensation with 2-hydroxy benzoic acid hydrazide (**3**) to gave 1-(2-hydroxybenzoyl)-3-methyl-4-(2- substituted phenyl hydrazono)-1H-pyrazol-5(4H)-one (**4a-h**).

The structures of (**2a-h**) were confirmed by elemental analysis and IR spectra showing an absorption band at 1620-1640 (C=N), 3030-3080 (C-H of Ar.), 2815-2850 (-OCH$_2$), 2950, 1370 (-CH$_3$,CH$_2$) and 1695-1750 cm^{-1} (C=O).

Orbital Elec. J. Chem., Campo Grande, 2(3): 303-310, 2010

305

^{1}H NMR (400MHz , DMSO - d$_{6}$,δ/ppm): 1.25 (t, 3H, CH$_{3}$), 2.35 (s, 3H, COCH$_{3}$), 4.29 (q, 2H, COCH$_{2}$), 11.62 (s, 1H, NH); (**2a**): 6.89-7.37 (s, 5H, ArH); (**2b**): 2.36 (s, 3H, CH$_{3}$) , 6.74-7.19 (s, 4H, ArH); (**2c**): 7.11-7.26 (s, 4H, ArH); (**2d**): 6.56-7.38 (s, 4H, ArH); (**2e**): 7.24-8.08 (s, 4H, ArH); (**2f**): 8.01-8.92 (s, 3H, ArH); (**2g**): 8.04-8.20 (s, 2H, ArH); (**2h**): 7.01-7.08 (s, 2H, ArH).

^{13}C NMR (100MHz,DMSO,δ/ppm): 14.2 (CH$_{3}$), 62.6 (OCH$_{2}$), 27.1 (CH$_{3}$), 163.5-196.4 (-CO), 126.9 (C=N); (**2a**): 114.6-143.7 (Ar-C); (**2b**): 17.9 (CH$_{3}$), 113.4-142.1 (Ar-C); (**2c**): 118.2-130.4 (Ar-C); (**2d**): 116.9-142.5 (Ar-C); (**2e**): 113.7-149.5 (Ar-C); (**2f**): 116.9-139.1 (Ar-C); (**2g**): 125.1-140.8 (Ar-C); (**2h**): 109.8-152.7 (Ar-C).The C, H, N analysis data of all compounds are presented in Table 1.

The IR spectra of (**4a-h**) are 1624-1640 (C=N), 3030-3088 (C-H of Ar.), 2960, 1380 (-CH$_{3}$), 1705-1765 (C=O) and 3450-3550 cm^{-1} (-OH).

^{1}H NMR (400MHz, DMSO-d$_{6}$, δ/ppm): 2.42 (s, 3H, CH$_{3}$), 5.48 (s, 1H, OH), 11.62 (s, 1H, NH); (**4a**): 6.90-8.10 (s, 9H, ArH); (**4b**): 2.24 (s, 3H, CH$_{3}$), 6.84-7.90 (s, 8H, ArH); (**4c**): 7.04-8.06 (s, 8H, ArH); (**4d**): 7.20-8.13 (s, 8H, ArH); (**4e**): 7.24-8.08 (s, 8H, ArH); (**4f**): 7.05-8.92 (s, 7H, ArH); (**4g**): 7.04-8.24 (s, 6H, ArH); (**4h**): 7.01-7.74 (s, 6H, ArH).

^{13}C NMR (100MHz, DMSO, δ/ppm): 11.6 (CH$_{3}$), 163.7-172.4 (-CO), 129.4 (C=N); (**4a**): 114.2-160.7 (Ar-C); (**4b**): 17.5 (CH$_{3}$), 113.3-160.6 (Ar-C); (**4c**): 117.9-160.4 (Ar-C); (**4d**): 116.9-160.5 (Ar-C); (**4e**): 114.4-159.9 (Ar-C); (**4f**): 117.1-161.2 (Ar-C); (**4g**): 118.3-161.8 (Ar-C); (**4h**): 109.7-161.4 (Ar-C). The C, H, N analysis data of all compounds are presented in Table -2.

The examination of data reveals that the elemental contents are consistence with the predicted structure shown in Scheme 1.The IR data also direct for assignment of the predicted structure. The LC-MS of one sample i.e. **4a** shows the peak of M^{+} ion at 346 which is consistent of molecular weight of **4a** i.e. 322. LC-MS data of all compounds are presented in Tables 1 and 2. All these facts confirm the structures **4a-h**.

The examination of antibacterial activity data reveals that the compounds **4c** and **4h** found more active against the gram-positive and gram-negative bacteria. Among them compound **4c** was found more toxic for microbes. Other compounds found to be less or moderate active than tetracycline. Also the compound **4c** and **4h** showed more antifungal activity than other compounds.

Acknowledgements

Orbital Elec. J. Chem*., Campo Grande, 2(3): 303-310, 2010*

306

Table 1. Physical and analytical data of the compounds synthesized **2a-h**

Compound	R	Molecular Formula (Mol.wt.)	LC-MS Data (M$^+$)	M.P.* °C	Yield %	Elemental Analysis					
						C%		H%		N%	
						Found	Calcd.	Found	Calcd.	Found	Calcd.
2a	H	$C_{12}H_{14}N_2O_3$ (228)	245	94-96	72	63.13	63.15	6.12	6.14	12.25	12.28
2b	2-Me	$C_{13}H_{16}N_2O_3$ (242)	260	98-99	80	64.44	64.46	6.60	6.61	11.49	11.57
2c	4-Cl	$C_{12}H_{13}N_2O_3Cl$ (268.5)	281	112-115	76	53.61	53.63	4.81	4.84	10.35	10.42
2d	4-Br	$C_{12}H_{13}N_2O_3Br$ (313)	324	114-117	82	45.97	46.00	4.13	4.15	8.86	8.94
2e	4-NO$_2$	$C_{12}H_{13}N_3O_5$ (279)	297	82-84	65	51.59	51.61	4.63	4.65	14.98	15.05
2f	2,4-Dinitro	$C_{12}H_{12}N_4O_7$ (324)	339	118-120	66	44.42	44.44	3.67	3.70	17.25	17.28
2g	2,4-Dichloro-6-Nitro	$C_{12}H_{11}N_3O_5Cl_2$ (348)	364	126-128	77	41.35	41.37	3.14	3.16	11.95	12.06
2h	2,4,6-Tribromo	$C_{12}H_{11}N_2O_3Br_3$ (471)	492	122-125	84	30.54	30.57	2.31	2.33	5.89	5.94

* Uncorrected

Table 2. Physical and analytical data of the compounds synthesized **4a-h**

Compound	R	Molecular Formula (Mol.wt.)	LC-MS Data	M.P. * °C	Yield %	Elemental Analysis					
						C%		H%		N%	
						Found	Calcd.	Found	Calcd.	Found	Calcd.
4a	H	$C_{17}H_{14}N_4O_3$ (322)	346	186-189	56	63.33	63.35	4.32	4.34	17.37	17.39
4b	2-Me	$C_{18}H_{16}N_4O_3$ (336)	352	194-196	62	64.26	64.28	4.75	4.76	16.65	16.66
4c	4-Cl	$C_{17}H_{13}N_4O_3Cl$ (356.5)	373	204-205	53	57.21	57.22	3.63	3.64	15.68	15.70
4d	4-Br	$C_{17}H_{13}N_4O_3Br$ (401)	423	210-213	58	50.84	50.87	3.20	3.24	13.94	13.96
4e	4-NO$_2$	$C_{17}H_{13}N_5O_5$ (367)	382	188-191	49	55.53	55.58	3.52	3.54	19.03	19.07
4f	2,4-Dinitro	$C_{17}H_{12}N_6O_7$ (412)	438	198-200	55	49.48	49.51	2.89	2.91	20.36	20.38
4g	2,4-Dichloro-6-Nitro	$C_{17}H_{11}N_5O_5Cl_2$ (422)	446	184-167	54	48.31	48.34	2.57	2.60	13.24	13.27
4h	2,4,6-Tribromo	$C_{17}H_{11}N_4O_3Br_3$ (559)	578	216-218	57	36.46	36.49	1.93	1.96	09.98	10.01

* Uncorrected

Table 3. Antibacterial activity of compounds **4a-h**

Compounds	Zone of Inhibition(mm) (Activity Index)[std]				
	Gram +ve		Gram -ve		
	Bacillus subtilis	*Staphylococcus aureus*	*Kllebsiella promioe*	*Salmonella typhl*	*E. coli*
4a	54 (0.68)	46 (0.83)	46 (0.54)	44 (0.60)	63 (0.87)
4b	43 (0.54)	44 (0.80)	57 (0.67)	54 (0.73)	57 (0.79)
4c	71 (0.89)	48 (0.87)	75 (0.89)	66 (0.90)	64 (0.88)
4d	66 (0.83)	46 (0.83)	70 (0.83)	62 (0.84)	60 (0.83)
4e	43 (0.54)	44 (0.80)	67 (0.79)	42 (0.57)	57 (0.79)
4f	64 (0.81)	45 (0.81)	44 (0.52)	63 (0.86)	58 (0.80)
4g	65 (0.82)	43 (0.78)	58 (0.69)	61 (0.83)	56 (0.77)
4h	70 (0.88)	47 (0.85)	71 (0.84)	67 (0.91)	65 (0.90)
Tetracycline	79	55	84	73	72

(Activity Index) [std] = Zone of Inhibition of the sample/ Zone of Inhibition of the standard.

Table 4. Antifungal activity of compounds **4a-h**

Compounds	Zone of Inhibition at 1000 ppm (%)				
	Penicillium expansum	*Botrydepladia thiobromine*	*Nigrosspora sp.*	*Trichothesium sp.*	*Rhizopus nigricuns*
4a	70	62	70	53	49
4b	62	72	64	54	67
4c	71	73	78	79	71
4d	67	69	68	58	63
4e	54	57	62	62	67
4f	51	64	58	73	58
4g	61	71	62	67	51
4h	73	78	74	74	69

References and Notes

[1]   Amir, M.; Agrawal, R. *J. Indian Chem. Soc*. **1997**, *74*, 154.

309

Orbital Elec. J. Chem*., Campo Grande,* 2(3): 303-310, 2010

[2]   Silveria, J. A.; Paulo, L. G.; Miranda, A. L.; Rocha, S. O.; Freitas, A. C.; Barreiro, E. J. *Braz. J. Med. Biol. Res*. **1991**, *24*, 947.

[3]   Jolly, V. S.; Pathak, M.; Jain, R. *Indian J. Chem*. **1993**, *32B*, 505.

[4]   Amir, M.; Khan, S. A.; Drabu, S. J. *Ind. Chem. Soc*. **2002**, *79*, 280.

[5]   Amir, M.; Hasan, S. M.; Wadood, A. *Orient J. Chem*. **2002**, *18*, 351.

[6]   Amir, M.; Siddiqui, A. A.; Rizwan, S. *Oriental J. Chem.* **2003**, *19*, 629.

[7]   Shiradkar, M. R.; Murahari, K. K.; Gangadasu, H. R.; Suresh, T.; Kalyan, C. C.; Panchal, D.; Kaur, R.; Burange, P.; Ghogare, J.; Mokale, V.; Raut, M. *Bioorg. Med. Chem*. **2007**, *15*, 3997.

[8]   Janin, Y. *Bioorg. Med. Chem.* **2007**, *15*, 2479.

[9] Gursoy, E.; Guzeldemirci-Ulusoy, N. *Eur. J. Med. Chem*. **2007**, *42*, 320.

[10] Rao, M. R.; Hart, K.; Devanna, N.; Chandrasekhar, K. B. *Asian J. Chem*. **2008**, *20*, 1402.

[11] Kaymakcioglu, K. B.; Oruc, E. E.; Unsalan, S.; Kandemirli, F.; Shvets, N.; Rollas, S.; Anatholy, D. *Eur. J. Med. Chem*. **2006**, *41*, 1253.

[12] Kalsi, R.; Shrimali, M.; Bhalla, T. N.; Barthwal, J. P. *Indian J. Pharm. Sci*. **2006**, *41*, 353.

[13] Gemma, S.; Kukreja, G.; Fattorusso, C.; Persico, M.; Romano, M.; Altarelli, M.; Savini, L.; Campiani, G.; Fattorusso, E.; Basilico, N. *Bioorg. Med. Chem. Lett*. **2006**, *16*, 5384.

[14] Sriram, D.; Yogeeswari, P.; Madhu, K. *Bioorg. Med. Chem. Lett*. **2005**, *15*, 4502.

[15] Nayyar, A.; Jain, R. *Curr. Med. Chem.* **2005**, *12*, 1873.

[16] Fikry, R. M.; Ismael, N. A.; El-Bahnasawy, A. A.; Sayed El-Ahl, A. A. *Phos. Sulf and Silicon*. **2004**, *179*, 1227.

[17] Walcourt, A.; Loyevsky, M.; Lovejoy, D. B.; Gordeuk, V. R.; Richardson, D. R. *Int. J. Biochem. Cell Biol*. **2004**, *36*, 401.

[18] Mamolo, M. G.; Falagiani, V.; Zampieri, D.; Vio, L.; Banfi, E.; Scialino, G. *Farmaco* **2003**, *58*, 631.

[19] Terzioglu, N.; Gursoy, A. *Eur. J. Med. Chem. 2003*, *38*, 781.

[20] Kucukguzel, S. G.; Oruc, E. E.; Rollas, S.; Sahin, F.; Ozbek, A. *Eur. J. Med. Chem*. **2002**, *37*, 197.

[21] Rollas, S.; Gulerman, N.; Erdeniz, H. *Farmaco* **2002**, *57*, 171.

[22] Al-Mawsawi, L. Q.; Dayam, R.; Taheri, L.; Witvrouw, M.; Debyser, Z.; Neamati, N. *Bioorg. Med. Chem. Lett*. **2007**, 17, 6472.

[23] Plasencia, C.; Daym, R.; Wang, Q.; Pinski, J.; Burke, T. R. Jr.; Quinn, D. I.; Neamati, N. *Mol. Cancer Ther.* **2005**, *4*, 1105.

[24] Zhao, H.; Neamati, N.; Sunder, S.; Hong, H.; Wang, S.; Milne, G. W.; Pommier, Y.; Burke, T. R. Jr. *J. Med. Chem.* **1997**, *40*, 937.

[25] Dexter, M.; Manor, B. US pat. 3110696, 1963.

[26] Barry, A. L. The Antimicrobial Susceptibility Test: Principal and Practices,4th ed., Philadelphia: Illuslea and Feger, 1976, 180.

Orbital Elec. J. Chem*., Campo Grande*, 2(3): 303-310, 2010

310

Short Communication

Synthesis and antifungal activity of 3-aryl-1-(5-phenyl-1*H*-tetrazol-1-yl)prop-2-en-1-One

Popat B.Mohite[a], Vaidhun H. Bhaskar*[b]

[a]Department of Pharmaceutical Chemistry, MES College of Pharmacy, Sonai, Ahmednagar, 414105, India
[b]MP Patel College of Pharmacy, Kapadwanj, Gujrat, 687320, India

ABSTRACT: *5-phenyl 1-acetyl tetrazole were allowed to react separately with different aromatic aldehydes in presence of alkaline medium to yield corresponding 5-phenyl tetrazole 1- substituted chalcones.The compounds were identified by spectral data and screened for in-vitro antifungal activity by using cup and plate method.*

Keywords: *5-phenyl tetrazole; chalcone; antifungal activity*

Tetrazole an heterocyclic compound possess various biological activities like antibacterial [1], antifungal [2], analgesic [3], anti-inflammatory [4] and antitubercular activity [5]. Chalcones are products of condensation of simple or substituted aromatic with simple or substituted acetophenones in presence of alkali. Chalcone constitute an important group of natural products and some of them possess a wide range of biological activities such as antimicrobial [6], anticancer [7], antitubercular [8] and antiviral activity etc. During their chemical studies in the structure of clavicin, it is found that a structural feature which was responsible for antibacterial activity was α,β-unsaturated keto functional group. The diverse properties of chalcones have prompted us to synthesize them in order to study their antimicrobial activity. The present work deals with the reaction of 5-phenyl tetrazole (**1**) with acetic anhydride to yield 5-phenyl 1-acetyl tetrazole (**2**) which on a further reaction with different aromatic aldehydes forms chalcones (**3a-j**).The structures of all the synthesized compounds were assigned on the basis of elemental analysis, IR and ^{1}H NMR spectral data. These compounds were screened for their in-vitro antifungal activity.

* Corresponding author. E-mail: mohitepb@rediffmail.com

The melting points were determined with open capillary and were uncorrected. FTIR spectra were recorded on a Shimadzu FT-IR model 8010 spectrophotometer, ^{1}H NMR spectra were recorded in DMSO on a Varian mercury FT-NMR model YH- 300 instrument using TMS as internal standard.

Synthesis of 5-Phenyl 1-Acetyl Tetrazole: A solution of 5-phenyl tetrazole (12.8g, 0.08 moles) and acetic anhydride (0.08 moles) and 2-3 drops of concentrated sulphuric acid was warmed for 15-20 min. on water bath. Cooled and poured into ice cold water. The product separated was filtered, dried. It was further purified by crystallization from ethanol.

General procedure for the preparation of 3-aryl-1-(5-phenyl-1H-tetrazol-1-yl) prop-2-en-1-one (chalcones) (3a-j): A solution of 5-phenyl 1-acetyl tetrazole (85 g, 0.005 moles) and aromatic aldehydes (0.005 mole) in ethanol (12 mL) was cooled to 5 to 10 °C in an ice bath. The cooled solution was treated with aqueous sodium hydroxide (2.5 mL, 50%) by drop wise addition. The reaction mixture was magnetically stirred for 30 min and then left over night. The resulting dark solution was diluted with ice water and carefully acidified using dilute hydrochloric acid. The tetrazole analogues of chalcones which crystallizes out, were collected by filtration after washing with sodium bicarbonate and water. It was further purified by crystallization from ethanol.

Scheme 1. Synthesis of chalcones

a. $(CH_3CO)_2O/GAA$ **b.** R-CHO/NaOH
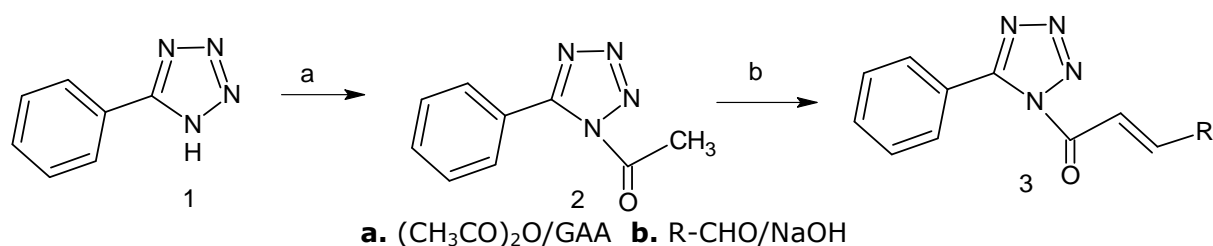
IR (KBr, cm^{-1}) and ^{1}H NMR (DMSO, ppm)

3-phenyl -1-(5-phenyl-1H-tetrazol-1-yl) prop-2-en-1-one (3a): FT-IR:1 285 (N-N=N), 1108 and 1138 (Tetrazole ring), 1735 (C=O), 1630 (C=C), 3054 (Ar-CH). ^{1}H NMR: 6.61 (1H, d, J=12.7 Hz,-CO-CH=), 7.05 (1H, d, J=7.6 Hz, =CH-Ar), 7.14-7.80 (10H, m, Ar-H).

3-(2-chlorophenyl)-1-(5-phenyl-1H-tetrazol-1-yl) prop-2-en-1-one (3b): FT-IR: 1285 (N-N=N-), 1108 and 1138 (Tetrazole ring), 1733 (C=O), 1627 (C=C), 3052 (Ar-CH), 785(C-Cl). ^{1}H NMR: 6.62 (1H, d, J=12.2 Hz, -CO-CH=), 7.06 (1H, d, J=7.8Hz, =CH-Ar), 7.14-7.75 (9H, m, Ar-H).

*3-(4-chlorophenyl) -1-(5-phenyl-1H-tetrazol-1-yl) prop-2-en-1-one (3c):* FT-IR: 1284

312

Orbital Elec. J. Chem*., Campo Grande,* 2(3): 311-315, 2010

(N-N=N-), 1108 and 1138 (Tetrazole ring),1734 (C=O), 1632(C=C), 3050 (Ar-CH), 785(C-Cl). ^{1}H NMR: 6.63 (1H, d, J=12.2Hz. -CO-CH=), 7.06(1H, d, J=7.8Hz, =CH-Ar), 7.14-7.80 (9H, m, Ar-H).

3-(4-bromophenyl) -1-(5-phenyl-1H-tetrazol-1-yl) prop-2-en-1-one (3d): FT-IR: 1283 (N-N=N-), 1108 and 1138 (Tetrazole ring),1735 (C=O), 1630 (C=C), 3055 (Ar-CH), 652 (C-Br). ^{1}H NMR: 6.5 (1H, d, J=12.2Hz,-CO-CH=), 7.03 (1H, d, J=7.8Hz, =CH-Ar), 7.14-7.81 (9H, m, Ar-H).

3-(4-methoxyphenyl) -1-(5-phenyl-1H-tetrazol-1-yl) prop-2-en-1-one (3e): FT-IR: 1285 (N-N=N-), 1108 and 1138 (Tetrazole ring), 1736 (C=O), 1635 (C=C), 3058 (Ar-CH), 1251 (-OCH3). ^{1}H NMR: 6.58 (1H, d, J=12.7Hz, -CO-CH=), 7.02 (1H, d, J=7.64Hz, =CH-Ar), 7.14-7.75 (9H, m, Ar-H).

Table 1. Physical data of compounds

Compound	R	Molecular Formula	MW	% Yield	M.P.^{0}c	Calcd (Found)%		
						C	H	N
3a	C_6H_5	$C_{16}H_{12}N_4O$	276	72	198	69.58 (69.55)	4.40 (4.38)	20.40 (20.38)
3b	$2\text{-Cl-}C_6H_5$	$C_{16}H_{11}ClN_4O$	310	66	222	61.90 (61.84)	3.59 (3.57)	17.99 (18.03)
3c	$4\text{-Cl-}C_6H_5$	$C_{16}H_{11}ClN_4O$	310	66	224	61.90 (61.84)	3.59 (3.57)	17.99 (18.03)
3d	$4\text{- Br -}C_6H_5$	$C_{16}H_{11}BrN_4O$	355	72	248	54.01 (54.10)	3.08 (3.12)	15.75 (15.77)
3e	$4\text{-OCH3-}C_6H_5$	$C_{17}H_{14}N_4O_2$	306	64	235	66.56 (66.66)	4.62 (4.61)	18.30 (18.29)
3f	$2\text{-NO2-}C_6H_5$	$C_{16}H_{11}N_5O_3$	321	59	252	59.91 (59.81)	3.48 (3.45)	21.85 (21.80)
3g	$4\text{-NO2-}C_6H_5$	$C_{16}H_{11}N_5O_3$	321	59	250	59.91 (59.81)	3.48 (3.45)	21.85 (21.80)
3h	$4\text{-(CH3)N-}C_6H_5$	$C_{18}H_{17}N_5O$	319	60	230	67.73 (67.70)	5.30 (5.37)	21.85 (21.80)
3i	$4\text{-CH3-}C_6H_5$	$C_{17}H_{14}N_4O$	290	54	218	70.25 (70.33)	4.80 (4.86)	19.38 (19.30)
3j		$C_{14}H_{10}N_4O_2$	266	70	188	65.10 (65.15)	3.82 (3.79)	21.10 (21.04)

3-(2-nitrophenyl) -1-(5-phenyl-1H-tetrazol-1-yl) prop-2-en-1-one (3f): FT-IR: 1285 (N-N=N-), 1108 and 1138 (Tetrazole ring), 1734 (C=O), 1630(C=C), 3055 (Ar-CH), 1578 (-NO2). ^{1}H NMR: 6.60 (1H, d, J=12.2 Hz, -CO-CH=), 7.01 (1H, d, J=7.8Hz, =CH-Ar), 7.14-7.68 (9H, m, Ar-H).

3-(4-nitrophenyl) -1-(5-phenyl-1H-tetrazol-1-yl) prop-2-en-1-one (3g): FT-IR: 1285 (N-N=N-), 1108 and 1138 (Tetrazole ring), 1735 (C=O), 1630(C=C), 3054 (Ar-CH), 1578(-NO2). ^{1}H NMR: 6.61 (1H, d, J=12.2 Hz, -CO-CH=), 7.01 (1H, d, J=7.8Hz, =CH-Ar), 7.14-7.70 (9H, m, Ar-H).

313

Orbital Elec. J. Chem., Campo Grande, 2(3): 311-315, 2010

*3-(4-dimethylaminophenyl) -1-(5-phenyl-1H-tetrazol-1-yl) prop-2-en-1-one (**3h**):* FT-IR: 1285 (N-N=N-), 1108 and 1138 (Tetrazole ring), 1735 (C=O), 1630 (C=C), 3054 (Ar-CH), 1321(-N(CH3)$_2$). ^{1}H NMR: 2.9 (6H, d, CH$_3$), 6.63 (1H, d, J=12.7Hz, -CO-CH=), 7.03 (1H, d, J=7.8,Hz, =CH-Ar), 7.14-7.50 (9H, m, Ar-H).

*3-(4-methylphenyl) -1-(5-phenyl-1H-tetrazol-1-yl) prop-2-en-1-one (**3i**):* FT-IR: 1285 (N-N=N-), 1108 and 1138 (Tetrazole ring), 1733 (C=O), 1630 (C=C), 3054 (Ar-CH), 1365(CH3). ^{1}H NMR: 3.72 (3H, CH3), 6.62 (1H, d, J=12.7Hz, -CO-CH=), 7.02 (1H, d, J=7.6Hz, =CH-Ar), 7.14-7.50 (9H, m, Ar-H).

*3-(furan-2yl) -1-(5-phenyl-1H-tetrazol-1-yl) prop-2-en-1-one (**3j**):* FT-IR: 1285 (N-N=N), 1108 and 1138 (Tetrazole ring), 1734 (C=O), 1630 (C=C), 3077(Furan). ^{1}H NMR: 6.60 (1H, d, J=12.2Hz, -CO-CH=), 7.01 (1H, d, J=7.7Hz, =CH-Ar), 6.25-7.40 (3H, m, Furyl) .

Antifungal Activity

All the newly synthesized compounds were screened for antifungal activity against *C. albicans* and *A. niger according* to cup and plate method at a concentration 50 μg/mL and 100 μg/mL, respectively. Griseofulvin was used as standard for comparison of antifungal activity. Solvent dimethyl sulphoxide (DMSO) was used as control. The results of screening are given in Table 2.

Table 2- Antifungal data of chalcones

Compound	Mean zone of inhibition in mm			
	Candida albicans		*Aspergillus niger*	
	50 μg/mL	100 μg/mL	50 μg/mL	100 μg/mL
3a	12	15	10	12
3b	17	20	15	16
3c	18	20	13	15
3d	16	18	11	13
3e	19	22	20	22
3f	12	15	08	11
3g	13	15	10	12
3h	15	17	09	11
3i	12	14	11	12
3j	10	13	11	13
Griseofulvin	21	24	21	24

From the results of Table 2 of antifungal screening, it is evident that the compounds **3b**, **3c** and **3e** possess very good activity against fungi *Candida albicans* and *Aspergillus niger* and compound **3d** showed moderate activity all bacteria and fungi tested. Rest of the compounds shows little antifungal activity.

These compounds were synthesized with the objective of developing better

314

Orbital Elec. J. Chem*., Campo Grande*, 2(3): 311-315, 2010

antifungal molecules with maximum yield and optimum antifungal activity. It was observed that halogen substituted aromatic compounds were more active than unsubstituted aromatic compounds and aromatic compounds were more active than alkyl substituted compounds against fungi *Candida albicans* and *Aspergillus niger* at a higher dose of 50 μg/mL and 100 μg/mL, respectively.

Acknowledgements

References and Notes

[1] Mulwad, V. V.; Rupesh, B. P.; Atul, C. C. *J. Korean Chem. Soc.* **2008**, *52*, 249.

[2] Rajasekaran, A.; Murugesan, S.; Rajagopal, K. A. *Archives of Pharmacal Research* **2006**, *29*, 535.

[3] Upadhayaya, R. S.; Jain, S.; Sinha, N.; Kishore, N.; Chandra, R.; Arora, S. K. *Eur. J. Med. Chem.* **2004**, *39*, 579.

[4] Bachar, S. C.; Lahiri, S. C. *Pharmazie* **2004**, *59*, 435.

[5] Ray, S. M.; Lahiri, S. C. *J. Ind. Chem. Soc*. **1990**, *67*, 324.

[6] Adamec, J.; Waisser, K.; Kunes, J.; Kaustova, J. *Arch Pharm*. **2005**, *338*, 385.

[7] Herencia, F.; Ferrandiz, M. L.; Josen, A. U. *Bioorg. Med. Chem. Lett.* **1998**, *8*, 1169.

[8] Shivakumar, P. M.; Geetha, B. S. M.; Mukesh, D. *Chem. Pharm. Bull*. **2005**, *55*, 44.

[9] Ganesh, K. Antibiotic assay laboratory manual in microbiology, New Age publications, **1996**, 75.

[10] Indian Pharmacopoeia; Biological Assay, Govt. of India, **1996**, 2. A-88.

[11] Prasad, Y. R.; Kumar, P. P.; Kumar, P. R. *Eur. J. Chem*. **2008**, *5*, 144.

[12] Shen, J.; ChangTsung, L.; Loti, S.; Ru, W. J.; Horng, H. K. *Eur. J. Med. Chem*. **2005**, *40*, 103.

315

Orbital Elec. J. Chem*., Campo Grande*, 2(3): 311-315, 2010